DISSERTATION

CHARACTERIZATION OF *DJ-1* MUTATION IN MOUSE ASTROCYTES

Submitted by:

Amanda Kathleen Ashley

Graduate Degree Program in Cell and Molecular Biology

In partial fulfillment of the requirements

For the Degree of Doctor of Philosophy

Colorado State University

Fort Collins, Colorado

Spring 2008

COLORADO STATE UNIVERSITY

April 8, 2008

WE HEREBY RECOMMEND THAT THE DISSERTATION
PREPARED UNDER OUR SUPERVISION BY AMANDA KATHLEEN ASHLEY
ENTITLED
CHARACTERIZATION OF *DJ-1* MUTATION IN MOUSE ASTROCYTES
BE ACCEPTED AS FULFILLING IN
PART REQUIREMENTS FOR THE DEGREE OF DOCTOR OF PHILOSOPHY.

Committee on Graduate Work

Ronald B. Tjalkens, Ph.D.

Richard Slayden, Ph.D.

Marie E. Legare

Marie E. Legare, D.V.M, Ph.D., Adviser

William H. Hanneman

William H. Hanneman, Ph.D. Co-Adviser

Norman P.Curthoys, Ph.D., Program Director

ABSTRACT OF DISSERATION

CHARACTERIZATION OF *DJ-1* MUTATION IN MOUSE ASTROCYTES

Mutations in *DJ-1* cause early-onset Parkinson's disease (PD), a progressive, irreversible neurodegenerative condition. Currently, the only known cause of PD is mutation of certain genes including *DJ-1*, however these mutations account for only 5-10% of overall PD cases. The initial studies attempt to discern if expression of *VEGF* and *HIF1α*, factors thought to contribute to both PD as well as carcinogenesis were altered as a result of *DJ-1* mutation. In fact, *VEGF* expression decreased in the brain of *DJ-1*$^{-/-}$ mice, and increased in lung tissue. As PD is a complex, multi-factorial condition, our studies are designed to incorporate mutation of the PD gene *DJ-1* in our target cell type, astrocytes, which are exposed to toxic agents. Overall our results indicate that *DJ-1*$^{-/-}$ astrocytes do not have an exaggerated phenotype compared to *DJ-1*$^{+/+}$ counterparts, however subtle alterations in cell function are observed in mitochondrial membrane potential, expression of proinflammatory mediators, as well as intracellular calcium (Ca^{2+}) dynamics. First, *DJ-1*$^{-/-}$ astrocytes' resting mitochondrial membrane potential is significantly lower than that of *DJ-1*$^{+/+}$ cells. Following treatment with 10μg/mL lipopolysaccharide (LPS), expression of *COX2,* and *NOS2* were similar in both genotypes, however expression of *TNFα* was significantly lower in *DJ-1*$^{-/-}$ astrocytes. Finally, a delay in return to baseline intracellular Ca^{2+} levels following treatment with 1μM ATP was observed in *DJ-1*$^{-/-}$

cells. Interestingly, expression and secretion of TNFα were decreased in our *DJ-1*$^{-/-}$ astrocytes following LPS exposure, while expression of *COX2* and *NOS2* were similar. In conclusion, these changes, though modest, indicate basal dysfunction in astrocyte homeostasis induced by mutation of *DJ-1*. Secretion of TNFα may be the most significant finding, as it may predispose neurons to degeneration due to lack of sufficient protection against early neurotoxic insults that secreted TNFα may provide. These specific indicators are significant because mitochondrial dysfunction, altered neuroinflammation, and reactive gliosis are all implicated in PD. While altering astrocyte cellular function may not be the primary cause of *DJ-1*-linked PD, it is possible that changes in this cell type may contribute the progression of parkinsonism.

Amanda Kathleen Ashley
Graduate Degree Program in Cell and Molecular Biology
Colorado State University
Fort Collins, CO 80523
Spring 2008

ACKNOWLEDGEMENTS

I would like to sincerely thank my graduate committee of Dr. Marie Legare, Dr. William Hanneman, Dr. Ron Tjalkens, and Dr. Rick Slayden for their expertise and encouragement throughout this research project. In particular, I would like to express my gratitude to Dr. Marie Legare and Dr. William Hanneman, who served as my co-advisors for the past four years, guiding and directing my research. Further, they committed to funding and training a fugitive in their laboratory in a time where pecuniary resources are very limited, something I have been quite aware of and quite grateful for throughout my graduate career. Dr. Legare has been an outstanding advisor, and an influential, energetic, and caring mentor. Dr. Hanneman constantly encourages me to keep a proper perspective, and has given me endless advice on all aspects of the project. I have grown so much under their careful mentorship, and I hope to make them proud of the scientist I become. Dr. Ron Tjalkens has always provided me a fresh perspective and expected me to excel, while continuously encouraging my scientific curiosity. Dr. Rick Slayden challenged my ambition, pushing me to rethink my conceived limitations. I thank them for their assistance and guidance.

Within the laboratory, many individuals have aided my success in numerous ways. First, Julie Moreno has been an amazing friend and colleague to me throughout my tenure, helping me with a myriad of laboratory procedures and always lending an ear. I cannot thank Julie enough for her relentless encouragement and camaraderie; she is sincerely a wonderful friend and

confidante with a kind and caring heart. I feel truly blessed to know her. Takeshi Katoh also helped me in many experiments, always with a warm smile, friendly disposition and quite determination. Dr. Dave Carbone has fielded many questions from me, helped me with many experimental designs, and reminded me that science, even at its worst, is fun. Karin Streifel keeps me smiling and is constantly inquisitive, always with a kind attitude and desire to learn. Dr. Greg Dooley brings a unique perspective and down-to-earth approach to everything he does, and has always offered me helpful advice. Chrissy Battaglia and Laura Chubb taught me almost everything when I first began, and remain true friends. Many others have contributed during my Ph.D. work in too many ways to enumerate, including Elizabeth Eikman, Lisa Gerjevic, Brianne Mohl, Ashley Pollack, Carolyn Broccardo, Max Hennessey, Ruth Billings, Kelly Sullivan, Claire Yeomans, Sean McGrath, and especially Courtney Amerin. All of my coworkers have truly contributed to my work, either directly or even just through friendship. I am grateful to have had the opportunity to work with you all.

My parents deserve much acknowledgement for their contributions. They sacrificed much to ensure I received a good, well-rounded education, including their time, their money, and their own desires. My mom, Kathy Clayshulte, has been a constant source of love and encouragement. She has always advocating for her children to reach for their dreams and done all she can to support our success. My dad, John Clayshulte, has also helped each of us to strive for success, always reminding us that the road of life may be full of obstacles, but

with we can overcome anything with perseverance, integrity and determination. Both of my parents have instilled in me the confidence and work ethic necessary to complete this degree, and have supported me through the path I have taken to complete it-thanks, Mom and Dad. My big sister, Kristen Legault is one of my best friends and confidants. Kristen always puts things into perspective for me and I can tell her anything; she has been essential to maintaining my sanity and (usually) happy disposition. Thanks Kris and Mark for always being there. Jake and Natalie Clayshulte, my brother and sister-in-law have been so supportive and encouraging; I truly appreciate both their confidence in me, and constant encouragement of my endeavors. James Clayshulte, my little brother, always supports me, encourages me, and reminds me to keep work in perspective, and to enjoy life. Joseph Clayshulte, my youngest brother, has been my touchstone with my family. I appreciate so much that he calls me and misses me; I cherish the fact that time and distance apart has only made us closer friends. Also, my little sis, Dr. Tiffany Granone, has been a constant encouragement and an amazing example of endurance. I am so blessed that she is part of my life and has always believed in me. My in-laws, Jeff and Ruth Ashley have given me so much love and encouragement. I am so lucky and so happy that I am their daughter-in-law. My brother-in-law, Justin Ashley, has been a great friend, especially in tough times, and really accepted me into his family as his sister. All of my family has been essential in this process, and though there is much more I could say, everything can basically be condensed in my heart-felt thanks for your endless love and support.

My amazing husband, Dr. Ryan Ashley has provided me with so much throughout this project. Ryan taught me many laboratory procedures, provided me with feedback on everything from techniques, to experimental design, to writing. Moreover, he has always supported and encouraged me. When circumstances seemed insurmountable, he helped me muster the courage to persevere. I cannot begin to express how much and in how many ways Ryan has helped, encouraged, and sometimes consoled me. Without Ryan, I would not have completed my Ph.D.

Lastly, I thank God, my Creator, for blessing me with the opportunity to complete this degree, the fortitude to endure, and a wonderful group of people to help me along the way.

TABLE OF CONTENTS

LIST OF TABLES AND FIGURES

CHAPTER 2

Figure 2.5. Time-lapse of varying doses of JC-1 exposed to the mitochondrial uncoupler CCCP. Primary cortical astrocytes were loaded with 1, 3, 5, or 10μM of the ratiometric mitochondrial dye JC-1 for 20 min at 37°C. After baseline sampling (8 min), 5μM carbonyl cyanide 3-chlorophenylhydrazone (CCCP) was added, and the red to green (λ599:λ519) ratio was examined. Immediately following exposure to CCCP, all concentrations of JC-1 exhibited a significant decline in λ599:λ519, indicating a robust depolarization that continued for the duration of sampling (60 min).

Table 2.1. Tukey's multiple comparisons test of DJ-1 and MitoTracker correlation coefficients. ANOVA values reveal statistical differences in astrocytes exposed to 0, 10, 25, or 50 μg/mL LPS for 72 h followed by 24h exposure to 0, 50, 500,

Table 2.2. Tukey's multiple comparisons test of DJ-1 and DAPI correlation coefficients. ANOVA values reveal statistical differences in astrocytes exposed to 0, 10, 25, or 50 μg/mL LPS for 72 h followed by 24h exposure to 0, 50, 500, or 1000nM rotenone, then probed for DJ-1 and mounted in DAPI-containing medium.

Figure 2.6. Resting mitochondrial membrane potential is decreased in *DJ-1*$^{-/-}$ astrocytes. Cells were loaded with 5μM JC-1 for 20 min at 37°C, and the ratio of λ599:λ519 over time (A). After baseline sampling, 0, 50, 500, or 1000nM rotenone was added in (B) *DJ-1*$^{+/+}$ and (C) *DJ-1*$^{-/-}$ astrocytes. (D) Initial membrane polarization in *DJ-1*$^{+/+}$ astrocytes is higher than in *DJ-1*$^{-/-}$ cells (n=48, p=0.02). (E) Final mitochondrial membrane potential was similar in both *DJ-1*$^{+/+}$ and *DJ-1*$^{-/-}$ astrocytes following addition of 0, 50, 500, or 1000nM rotenone (p>0.05, n=12).

Figure 2.7. Bax production is similar in *DJ-1*$^{+/+}$ and *DJ-1*$^{-/-}$ astrocytes. Protein was isolated from primary astrocytes, and production of both Bax and β-actin was detected via Western blotting (A). Densitometry reveals no significant difference in Bax production in cells with mutation of *DJ-1* (B, p=0.62).

Figure 2.8: In brain tissue, expression of *HIF1α* does not change due to mutation of *DJ-1*, however *VEGF* expression significantly declines. RNA isolated from *DJ-1*$^{+/+}$ or *DJ-1*$^{-/-}$ tissues (n=5) were analyzed for expression of *HIF1α* and *VEGF* via real-time PCR. (A) No genotype-specific alterations in *HIF1α* expression occurred. (B) In contrast, expression of *VEGF* significantly decrease in the brain of *DJ-1*$^{-/-}$ animals (p=0.003).

Figure 2.9: In the lung, cells with one or two copies of mutated *DJ-1* have increased *VEGF* expression, and *DJ-1*$^{+/-}$ tissues have decreased HIF1α expression. RNA isolated from *DJ-1*$^{+/+}$ or *DJ-1*$^{-/-}$ tissues (n=5) were analyzed for expression of *HIF1α* and *VEGF* via real-time PCR. (A) Expression of *HIF1α* is

Figure 3.3. Intracellular Ca^{2+} peak in *DJ-1*$^{+/+}$ astrocytes following 24h exposure to rotenone. Astrocytes were exposed to 0, 50, 500, or 1000nM rotenone for 24h. After baseline sampling for 1 min, astrocytes were exposed to 1μM ATP and fluorescence was monitored for 9 additional min. Bars with differing letters significantly differ from one another ($p<0.05$). Peak Ca^{2+} concentration increased in cells exposed to 50 or 500nM rotenone ($p<0.05$). Final intracellular Ca^{2+} levels remained significantly elevated through the duration of sampling, with rotenone-treated samples more elevated than control ($n\geq274$, $p<0.05$).

Figure 3.4. Intracellular Ca^{2+} peak in *DJ-1*$^{-/-}$ astrocytes following 24h exposure to rotenone. Astrocytes were exposed to 0, 50, 500, or 1000nM rotenone for 24h. After baseline sampling for 1 min, astrocytes were exposed to 1μM ATP and fluorescence was monitored for 9 additional min. Bars with differing letters significantly differ from one another ($p<0.05$). Peak Ca^{2+} concentration was similar at all rotenone doses. Final intracellular Ca^{2+} levels remained elevated at all levels or rotenone exposure, though 50nM rotenone was significantly lower than all other doses ($n\geq111$, $p<0.05$).

Figure 3.5. DACT increases and delays peak intracellular Ca^{2+} concentrations in *DJ-1*$^{+/-}$, *DJ-1*$^{-/-}$ but not *DJ-1*$^{+/+}$ primary cortical astrocytes. Astrocytes were exposed to 300μM DACT or DMSO for 24h, then the ATP-induced increase in intracellular Ca^{2+} was examined. Following baseline sampling, 1μM ATP was added. A, B: DACT significantly decreased peak intracellular Ca^{2+} concentrations ($p<0.001$, $n\geq351$) in *DJ-1*$^{+/-}$ cells and tended to delay time to peak Ca^{2+} levels. C, D, E. DACT significantly increased peak Ca^{2+} concentration in *DJ-1*$^{-/-}$ astrocytes ($p<0.01$). Although final Ca^{2+} levels were significantly lower in DACT-treated *DJ-1*$^{+/+}$ astrocytes, intracellular levels remained elevated through the duration of imaging in all *DJ-1*$^{-/-}$ astrocytes, with DACT-treated cells having highest final Ca^{2+} levels ($p<0.001$, $n\geq401$).

CHAPTER 4

Figure 4.1. LPS-induced relative expression of *COX2* decreases with inhibition of p38 but not MEK or JNK. Astrocytes were exposed to DMSO, U0126 (MEK inhibitor, 10μM), JNK inhibitor II (10μM), or SB203580 (p38 inhibitor, 30μM) for 2h, then PBS or 10μg/mL LPS for 24h, and RNA was isolated. Expression of *COX2* was determined via real-time PCR, and values are expressed relative to *DJ-1*$^{+/+}$ cells exposed to DMSO and PBS. Bars with differing letters significantly differ from one another ($p<0.05$). LPS significantly increased expression of *COX2* in all exposed samples (A,B,C, $p<0.001$). No genotype-specific alterations occurred, but inhibition of p38 (C) decreased *COX2* relative expression in both genotypes ($p<0.05$).

Figure 4.2. LPS-induced relative expression of *NOS2* tends to decrease with inhibition of p38 but not MEK or JNK. Astrocytes were exposed to DMSO, U0126 (MEK inhibitor, 10μM), JNK inhibitor II (10μM), or SB203580 (p38 inhibitor, 30μM) for 2h, then PBS or 10μg/mL LPS for 24h, and RNA was isolated. Expression of *NOS2* was determined via real-time PCR, and values are expressed relative to *DJ-1*$^{+/+}$ cells exposed to DMSO and LPS, as all expression levels in PBS-treated samples were too low to detect. Bars with differing letters significantly differ from one another ($p<0.05$). *NOS2* expression was similar in all groups (A,B,C $p>0.05$), though p38 inhibition tended to decrease expression (C, *DJ-1*$^{+/+}$ $p=0.11$, *DJ-1*$^{-/-}$ $p=0.07$).

Figure 4.3. LPS-induced relative expression of *TNFα* is lower in *DJ-1*$^{-/-}$ astrocytes, and does not decrease following inhibition of MEK, JNK, or p38. Astrocytes were exposed to DMSO, U0126 (MEK inhibitor, 10μM), JNK inhibitor II (10μM), or SB203580 (p38 inhibitor, 30μM) for 2h, then PBS or 10μg/mL LPS for 24h, and RNA was isolated. Expression of *TNFα* was determined via real-time PCR, and values are expressed relative to *DJ-1*$^{+/+}$ cells exposed to DMSO and PBS. Bars with differing letters significantly differ from one another ($p<0.05$). *TNFα* expression was significantly lower in all *DJ-1*$^{-/-}$ cells regardless of exposure to inhibitor ($p<0.01$). No inhibitor altered expression of *TNFα*.

Figure 4.4. Mutation of *DJ-1*$^{-/-}$ decreases secretion of TNFα from astrocytes exposed to LPS. Astrocytes were exposed to DMSO, U0126 (MEK inhibitor, 10μM), JNK inhibitor II (JNKi II,10μM), or SB203580 (p38 inhibitor, 30μM) for 2h, then PBS or 10μg/mL LPS for 24h, and culture media was collected. Secretion of TNFα into culture media was determined via ELISA (eBiosciences). Bars with differing letters significantly differ from one another ($p<0.05$). Levels of TNFα in all PBS-treated samples were below the assay detection limit (8pg/mL). Without exposure to inhibitors, LPS-induced secretion of TNFα was lower in *DJ-1*$^{-/-}$ compared to *DJ-1*$^{+/+}$ ($p<0.001$). Inhibition of JNK decreased levels of TNFα in *DJ-1*$^{+/+}$ media ($p<0.01$). Inhibition of p38 decreased secretion of TNFα from both *DJ-1*$^{+/+}$ and *DJ-1*$^{-/-}$ astrocytes ($p<0.05$).

Figure 4.5. NOS2 production increases with coexposure to manganese and LPS. Primary astrocytes were exposed to 50μM manganese (Mn), cytokines (1ng/mL tumor necrosis factor α and 10pg/mL interferon γ), 10μg/mL LPS, or manganese in combination with cytokines or LPS for 24h. NOS2 was detected via immunofluorescence, and expressed per number of cells assessed. Bars with differing letters significantly differ ($p<0.05$).

Figure 4.6. LPS induces rapid phosphorylation of MAPK proteins. Astrocytes were serum-starved for 24h, and then exposed to 10μg/mL LPS for 0, 5, 15, 30, 60, 90, or 120 min. Protein was isolated and levels of phospho-ERK, phospho-JNK, phospho-p38, or phospho-AKT (ser 473) were analyzed. Phospho-ERK increased at 5 and 15 min, and by 120 min at below baseline

values. Phospho-JNK (46kDa) increased also at 5 and 15 min, and stayed elevated until 120 min, although the 54kDa form was not detected. Phospho-p38 increased at 5 and 15 min, and subsequent times were similar to time 0 values. P-Akt (Ser 473) increased at 5 and 15 min as well, and then quickly returns to baseline levels.

Figure 4.7. LPS induces binding of NFκB to the NOS2 promoter. The chromatin immunoprecipitation assay was employed to analyze astrocytes exposed to 10μg/mL LPS for 0, 1, 6, or 8h with an anti-p65 antibody and primers designed to flank the proximal κB response elements of the NOS2 promoter. Following 1h of exposure, NFκB binding was detected at the NOS2 promoter region. Input controls unexposed to antibody were sampled to assure that a lack PCR product following exposure to antibody was not due to degradation of DNA.

CHAPTER 1

LITERATURE REVIEW

PARKINSON'S DISEASE

Parkinson's disease (PD) is a chronic, progressive, neurodegenerative disease resulting primarily from loss of dopaminergic neurons in the substantia nigra pars compacta, with an ultimate consequence of striatal dopamine deficiency. Furthermore, PD is characterized by gliosis and the formation of intracytoplasmic, proteinacious inclusions known as Lewy bodies in surviving neurons. The mean age of onset of PD is 55, with incidence increasing dramatically with age (Dauer and Przedborski, 2003). Clinical symptoms of PD include resting tremor, rigidity, bradykinesia, hypokinesia, akinesia, masked faces, and alterations in stride length. Further, cognitive impairments often occur, such as alterations in personality, depression, and dementia. All current PD medications treat the clinical symptoms, but none are able to retard degeneration of the dopaminergic neurons.

Approximately 90-95% of PD are considered "sporadic," referring to a lack of apparent genetic linkage, and only 5-10% of diagnosed PD are known to be associated with genetic mutations (Thomas and Beal, 2007). Mutations in the following genes have been shown to be associated with the development of PD: *Parkin* (Kitada *et al.*, 1998), *α-synuclein* (Polymeropoulos *et al.*, 1997), *PINK1* (Valente *et al.*, 2004), *UCHL1* (Leroy *et al.*, 1998), *LRRK2* (Paisan-Ruiz *et al.*, 2004), and *DJ-1* (Bonifati *et al.*, 2003b), with *Parkin* mutations accounting for approximately 50% of genetically-linked PD cases known to date. Aside from genetic mutations, other environmental factors may contribute to development of

or protection against PD. A number of epidemiological studies demonstrate a strong correlation between pesticide exposure and/or rural living with an increased incidence of PD (Gorell *et al.*, 1998; Ritz and Yu, 2000; Priyadarshi *et al.*, 2001; Vanacore *et al.*, 2002), though this remains controversial. Interestingly, although the mechanism(s) of protection remain unclear, coffee consumption and smoking cigarettes are habits inversely related with development of PD (Hernan *et al.*, 2002). Clearly, PD is a multifaceted, complex disease with many contributing factors complicated by the possibility of genetic predispositions. Over the next three decades, the proportion of the world's population age 65 and older is expected to dramatically increase, approximately doubling the number of individuals with PD (Kontakos and Stokes, 1999), highlighting the eminent need for elucidating the etiology of this disease.

ASTROGLIA AND NEURODEGENERATION

An essential element in unraveling the pathogenesis of PD is defining how astroglial dysfunction is involved in the progression of neuronal injury. Astrocytes vastly outnumber neurons, are present throughout all regions of the brain, and are increasingly recognized to play critical and integral roles in maintaining normal neuronal physiological functions (Vernadakis, 1996). Astrocytes supply neurons with neurotrophic factors such as nerve growth factor, neurotrophin-3, brain-derived growth factor (Barde *et al.*, 1982), fibroblast growth factor (Chadi *et al.*, 1993), metabolic substrates such as lactate (Pellerin *et al.*, 1998; Bouzier-Sore *et al.*, 2003a; Bouzier-Sore *et al.*, 2003b), and antioxidants including

glutathione precursors (Sagara *et al.*, 1993) which promote neuronal function and viability. Furthermore, astrocytes also take up glutamate (Schousboe *et al.*, 1979), potassium (Newman, 1996), and calcium (Duffy and MacVicar, 1996), thus maintaining the extracellular environment shared with local neurons and preventing neuronal excitotoxicity. Defects in astrocyte functions have been linked to childhood neurodegenerative diseases such as vanishing white matter leukodystrophy (Francalanci *et al.*, 2001) and Alexander disease (Borrett and Becker, 1985). However, the mechanisms by which astrocytes mediate neurodegeneration are not well understood.

During inflammation, astrocytes undergo a state of "gliosis" in response to stress, and release cytokines (Benveniste, 1998), and when this condition is sustained, excess cytokines are ultimately deleterious to neurons (Viviani *et al.*, 2004). Reactive gliosis and concomitant inflammatory processes are implicated in the pathogenesis and progression of PD, however modulation of these processes by specific endogenous and xenobiotic compounds is not understood. Glial cell activation has been reported in sporadic PD (Hunot *et al.*, 1999; Wszolek *et al.*, 2002b; Wu du *et al.*, 2002), neurodegeneration induced by 1-methyl-4-phenyl-1,2,3,6-tetrahydropyrindine (MPTP) (Kohutnicka *et al.*, 1998), rotenone (Sherer *et al.*, 2003c), manganese (Tomas-Camardiel *et al.*, 2002) and in mutant α-synuclein mice (Gomez-Isla *et al.*, 2003). Collectively, studies have suggested that compromising astrocytic function could be a significant mechanism in neurodegeneration. It has been postulated that subtle alterations in astroglial

mitochondrial function may serve as predisposing factors in the pathogenesis of neurodegenerative disorders (Krieger and Duchen, 2002). Preferential vulnerability of astrocytes to environmental toxin exposure indicate astrocytes, rather than neurons, may be the primary targets of specific neurotoxicants (Jayakumar *et al.*, 2004). Theories behind this selective vulnerability include induction of free radicals, mitochondrial inner membrane depolarization and dissipation of mitochondrial integrity, all of which are implicated in PD (Bai *et al.*, 2001; Bai and Cederbaum, 2001).

DJ-1 BACKGROUND

GENERAL INFORMATION

Initially, DJ-1 was identified as a protein able to transform NIH3T3 cells in conjunction with Ras (Nagakubo *et al.*, 1997). DJ-1 is currently classified as an oncogene (Nagakubo *et al.*, 1997; MacKeigan *et al.*, 2003; Kim *et al.*, 2005a) where overexpression and/or secretion may be associated with a variety of cancers, discussed in detail below. Mutations in *DJ-1* were first associated with autosomal recessive early-onset PD (EOPD) via genetic mapping in two consanguineous European families (Bonifati *et al.*, 2003b). Bonifati and colleagues describe the human *DJ-1* gene as containing 8 exons distributed over 24 kb, with the first two non-coding exons (1^A and 1^B) splicing alternatively in *DJ-1* mRNA, and encoding a 189 amino acid protein (Bonifati *et al.*, 2003b). Further, protein distribution is ubiquitous in humans, found in both neuronal and non-neuronal tissues. Recent genetic studies have uncovered 11 distinct

homozygous mutations in DJ-1 as well as one compound heterozygous mutation inducing EOPD (Abou-Sleiman *et al.*, 2003; Hague *et al.*, 2003a). Furthermore, mutations in DJ-1 occur in approximately 1-2% of EOPD patients, placing mutations in DJ-1 as the second most common mutation in EOPD after Parkin mutations (Abou-Sleiman *et al.*, 2003; Hague *et al.*, 2003b). Positron emission tomography (PET) scans of individuals with *DJ-1*-linked parkinsonism have revealed dopaminergic terminal dysfunction in the striatum that is more uniform than classical PD and greater than expected based upon clinical presentation (Dekker *et al.*, 2004). Because tissue from *DJ-1*-linked PD patients is not yet available, it is unclear if this mutation induces hallmark parkinsonian Lewy bodies, or if any other remarkable pathological abnormalities exist due to this specific mutation. Individuals harboring *DJ-1* mutations have an average age of onset in the early thirties. Interestingly, psychiatric disturbances, including severe anxiety, have been reported in many individuals with *DJ-1* mutations. Similar disturbances are reported in individuals with other genetic mutations and in sporadic PD, so whether this is related to mutation of *DJ-1* gene specifically remains to be elucidated. Interestingly, plasma levels of DJ-1 increase in both sporadic PD and dementia with Lewy bodies, with circulating DJ-1 positively correlating to the severity of disease onset of PD (Waragai *et al.*, 2007).

DISTRIBUTION

Bandopadhyay and coworkers (2004) demonstrated DJ-1 is abundant in the frontal cortex of individuals without PD, with idiopathic PD, and with phenotypic

PD having the non-pathogenic R98Q DJ-1 polymorphism. Furthermore, in normal human brain, DJ-1 immunoreactivity was faint in neuronal cells, but more prominent in astrocytes and astrocytic processes (Bandopadhyay *et al.*, 2004). Shang and colleagues (2004) described the distribution of *DJ-1* mRNA in the mouse brain. In contrast to the human, cells highly expressing *DJ-1* mRNA in mice were those with neuronal morphology, though *DJ-1* expression between neuronal cells may have been glial. Interestingly, high expression of DJ-1 was noted in structures involved in regulation of motor activity, namely the motor cortex, caudate putamen, substantia nigra, and red nucleus (Shang *et al.*, 2004). Other areas of high protein production include the cerebellum (especially neurons of the granule cell layers, deep cerebellar nuclei, and Purkinje cells), globus pallidus, hippocampus, piriform cortex, and reticular nucleus of the thalamus (Shang *et al.*, 2004). Via *in situ* hybridization and immunohistochemistry, Bader and colleagues characterized *DJ-1* expression in the adult mouse CNS (Bader *et al.*, 2005). This study demonstrated *DJ-1* mRNA is expressed throughout the brain and spinal cord, but specifically enriched in grey matter regions, thus primarily in neurons. However, DJ-1 was found in all cell types of the CNS, primarily localized to the cytoplasm, soma and proximal regions of cellular processes, but was excluded from the nucleus. DJ-1 was localized to tyrosine hydroxylase-, GAD-, and serotonin-immunopositive cells. Cholinergic neuronal staining failed, however, localization of DJ-1 to the ventral horn in the spinal cord is indicative that these neurons likely also actively express *DJ-1*. Astrocytes, microglia and oligodendrocytes all expressed DJ-1.

Significantly, confinement was not noted within either a single functional system or a specific anatomical area (Bader *et al.*, 2005), in contrast to other reports (Bonifati *et al.*, 2003b; Shang *et al.*, 2004). Immunohistochemical analysis of DJ-1 in α-synucleinopathies revealed weak neuronal and neuropil staining, (Neumann *et al.*, 2004). Notably, reactive astrocytes consistently have high expression of DJ-1 in a number of pathological conditions, suggesting DJ-1 has a significant role in gliosis or is elevated resultant to the gliosis (Bandopadhyay *et al.*, 2004; Neumann *et al.*, 2004; Rizzu *et al.*, 2004; Meulener *et al.*, 2005).

In vitro studies have shown that DJ-1 is localized to the cytoplasm, nucleus, and mitochondria, though debate remains about its *in vivo* localization to the nucleus (Neumann *et al.*, 2004; Zhang *et al.*, 2005). DJ-1 mitochondrial localization is poorly understood, however DJ-1 seems to be significant in mitochondrial function (Zhang *et al.*, 2005). In response to exposure to a number of toxins, including those inducing oxidative stress, DJ-1 will localize to the mitochondria (Canet-Aviles *et al.*, 2004; Blackinton *et al.*, 2005; Li *et al.*, 2005; Zhang *et al.*, 2005; Betarbet *et al.*, 2006b). Interestingly, many of the pathogenic DJ-1 mutants have higher mitochondrial localization, though this remains controversial in the literature (Xu *et al.*, 2005). Specifically, DJ-1 has been shown to be a constituent of the inner membrane space and mitochondrial matrix, which are the aqueous or hydrophilic regions of the mitochondria, but not within the membranes themselves (Zhang *et al.*, 2005). While the mechanism of this translocation remains to be elucidated, the association of DJ-1 with chaperones is enhanced

by exposure to oxidative stress, and it is hypothesized this mechanism results in DJ-1 translocation to the mitochondria (Li *et al.*, 2005). Although nuclear localization of DJ-1 is also poorly understood, its interactions with certain proteins specifically in the nucleus, discussed in detail below, are very significant to its physiological role in the cell.

DJ-1 PROTEIN

The crystal structure of DJ-1 suggests that it functions as a dimer (Honbou *et al.*, 2003; Huai *et al.*, 2003; Tao and Tong, 2003; Wilson *et al.*, 2003) with structural similarity to bacterial cysteine proteases as well as heat shock protein 31 (Lee *et al.*, 2003; Quigley *et al.*, 2003). The pathogenic L166P mutant form of DJ-1 does not participate in dimerization due to disruption of an α helix, and this is thought to cause the dysfunction of L166P DJ-1 (Cookson, 2003; Honbou *et al.*, 2003; Wilson *et al.*, 2003; Gorner *et al.*, 2004; Olzmann *et al.*, 2004). Further, L166P mutant DJ-1 tends to be unstable and will rapidly degrade, suggesting DJ-1 mutations inducing the EOPD phenotype are loss-of-function rather than overexpression, as is the case with other parkinsonian genes. DJ-1 regulation at the transcriptional level remains largely unknown, however approximately 100bp upstream from the transcription start site is a Specificity Protein 1 site, thought to control most of the promoter activity (Taira *et al.*, 2001).

ANTIOXIDANT PROPERTIES

DJ-1 has been identified as a potential antioxidant (Mitsumoto and Nakagawa, 2001; Mitsumoto *et al.*, 2001). Mitsumoto and colleagues found DJ-1 scavenged hydrogen peroxide or paraquat, resulting in a conversion of the protein to a variant with a lowered pI, i.e., 6.2 to ~5.8, though interestingly DJ-1 did not respond to nitric oxide (Mitsumoto and Nakagawa, 2001; Mitsumoto *et al.*, 2001). Further, the acidic form of DJ-1 accumulates in brains of PD patients (Bandopadhyay *et al.*, 2004). *In vitro* studies have confirmed that DJ-1 is capable of eliminating hydrogen peroxide (H_2O_2) by oxidizing itself (Taira *et al.*, 2004c). Formation of cysteine-sulfonic and cysteine-sulfinic acids, putatively responsible for pI change, have been identified in oxidized DJ-1 (Kinumi *et al.*, 2004). Of all cysteine residues, cysteine-106 of DJ-1 is, by far, the most sensitive to H_2O_2 mediated oxidation *in vivo*, forming a cysteine-sulfonic acid, and oxidation of this residue is thought to regulate DJ-1 function, though other cysteine residues also undergo oxidative modifications (Kinumi *et al.*, 2004). In support, Canet-Avilés and colleagues, found DJ-1 localized to mitochondria of neuroblastoma cells following exposure to paraquat, and this localization could be blocked by a C106A mutation but not C53A or C46A mutations (Canet-Avilés *et al.*, 2004). Knocking down *DJ-1* or expression of pathogenic or dimer-disrupting mutants decreased cellular viability of SH-SY5Y neuroblastoma cells following exposure to hydrogen peroxide, 1-methyl-4-phenylpyridinium (MPP+), or 6-hydroxydopamine, further indicating DJ-1 has an important role in prevention of oxidative stress (Taira *et al.*, 2004c). Yokota and coworkers report that a

partial knockdown regulation of DJ-1 in Neuro2A cells did not affect cell death. However, following treatment with H_2O_2, a significant increase in apoptotic cell death was observed. This phenotype could be rescued via overexpression of DJ-1, but not in a L166P mutant (Yokota *et al.*, 2003). Some have suggested that DJ-1 is an atypical peroxiredoxin-like peroxidase, capable of scavenging reactive oxygen species (Andres-Mateos *et al.*, 2007). Overall, the literature suggests mutation of DJ-1 will likely decrease cellular resistance to oxidative injury, promoting cellular susceptibility to both endogenous and exogenous oxidative stress. However, as DJ-1 has only a modest ability to scavenge reactive oxygen species (Junn *et al.*, 2005), whether the shift in pI is a cytoprotective event itself or serves as a method of sensing the redox environment remains to be seen. Moreover, through a yet unknown mechanism, DJ-1 stabilizes Nrf2, a master regulator of antioxidant response genes (Clements *et al.*, 2006), which likely contributes to its cytoprotective effects following oxidative stress.

DJ-1 ~ PROTEIN INTERACTIONS

DJ-1 may interact with a number of intracellular proteins each with a variety of roles, highlighting the diverse pathways that may be affected by DJ-1. Xu and colleagues found that DJ-1 protects against neuronal apoptosis via functioning as a transcription co-activator. In the nucleus, pyrimidine-tract binding protein-associated factor (PSF) functions as a transcriptional silencer, promoting apoptosis through its interactions with p54nrb. DJ-1, but not its pathogenic mutants, block the interaction of PSF with p54nrb through an unknown

mechanism mediated at the protein level, preventing apoptosis (Xu *et al.*, 2005). DJ-1 has also been demonstrated to bind the proapoptotic protein Daxx, sequestering it to the nucleus. Upon proapoptotic stimuli, Daxx normally translocates to the cytosol where it activates ASK-1, allowing its oligomerization and promotion of Fas-mediated apoptosis. DJ-1 but not L166P prevents the interaction of these proteins (Junn *et al.*, 2005). Other reports suggest that DJ-1 binds homeodomain-interacting protein kinase 1 (HIPK1), an enzyme which has been suggested to be involved in the Daxx-ASK1 pathway (Sekito *et al.*, 2006). DJ-1 negatively regulates the tumor-suppressor PTEN, causing hyperphosphorylation of PKB/Akt and promoting cell survival (Kim *et al.*, 2005a). DJ-1 has also been identified as a subunit of an RNA-binding protein (Hod *et al.*, 1999). DJ-1 binds to a family of SUMO-1 ligases, PIAS proteins, which modulate the activity of a variety of transcription factors, and is sumoylated itself at lysine 130 (Takahashi *et al.*, 2001; Kotaja *et al.*, 2002; Junn *et al.*, 2005). DJ-1 may also modulate p53, and some studies have suggested DJ-1 may actually bind this protein to alter its transcriptional activity, though the physiological consequences thereof remain poorly understood (Shinbo *et al.*, 2005; Bretaud *et al.*, 2007; Fan *et al.*, 2008). DJ-1 is structurally related to a heat shock protein, Hsp31, and has been suggested to function as a redox-dependent chaperone capable of interacting with α-synuclein to promote its proper folding (Lee *et al.*, 2003; Shendelman *et al.*, 2004; Zhou *et al.*, 2006).

OTHER NEUROLOGICAL DISORDERS

Aside from PD, other endogenous and experimentally-induced neurological disorders have concomitant alterations in DJ-1, including Alzheimer's disease (Choi *et al.*, 2006), multiple system atrophy, Pick's disease, (Neumann *et al.*, 2004), mutant huntingtin cells (Goswami *et al.*, 2006), ischemia/reperfusion (Aleyasin *et al.*, 2007; Yanagisawa *et al.*, 2007) and experimental autoimmune encephalomyelitis (Lev *et al.*, 2006) emphasizing that DJ-1 may play a significant role in maintaining CNS homeostasis. In Alzheimer's disease as well as PD, oxidative damage of DJ-1, specifically cysteine and methionine oxidation, as well as carbonylation has been observed. The same study revealed that overall DJ-1 protein levels increase in the brains of individuals with PD and Alzheimer's disease (Choi *et al.*, 2006). Neumann and colleagues observed DJ-1 immunoreactivity in neuronal tau inclusions in Pick's disease, corticobasal degeneration, progressive supranuclear palsy, and Alzheimer's disease. Additionally, in both sporadic PD and α-synuclein transgenic mice, similar pathology to Pick's disease were found including DJ-1 immunoreactivity in glial inclusions and corticobasal degeneration, progressive supranuclear palsy, and multiple system atrophy, though Lewy bodies were negative (Neumann *et al.*, 2004). Kumaran and coworkers also report DJ-1 immunoreactivity in a subset of neurofibrillary tangles, neuropil threads and neuritis in extracellular plaques of patients with Alzheimer's. However, in corticobasal degeneration, DJ-1 was only observed in astrocytic plaques (Kumaran *et al.*, 2007). In cells expressing mutant huntingtin (polyglutamine-expanded truncated N-terminal huntingtin), increases in

DJ-1 protein have been observed (Goswami *et al.*, 2006) and the possible contribution of DJ-1 to this disease warrants further investigation. In another study, cerebral ischemia was induced in rats via middle cerebral artery occlusion and an intrastriatal injection of recombinant glutathione *S*-transferase-tagged DJ-1 was administered. In rats receiving the tagged DJ-1, infarct size, behavioral dysfunction, and nitrotyrosine formation were significantly inhibited, demonstrating that DJ-1 may have a protective role in prevention of ischemia/reperfusion injury (Yanagisawa *et al.*, 2007). Finally, DJ-1 expression increases in animal models of multiple sclerosis, experimental autoimmune encephalomyelitis, and these increases correlate to disease severity (Lev *et al.*, 2006). While the research related to DJ-1 in these various disorders is in its infancy, results unequivocally suggest that DJ-1 potentially contributes to disease pathogenesis in a number of neurological conditions.

NON-NEURONAL TISSUES

DJ-1 was first described in non-neuronal tissues as a novel oncogene in NIH3T3 cells, serving to transform the cells in cooperation with Ras, with three times the transforming activity of Ras/Myc combination (Nagakubo *et al.*, 1997). Interestingly, these researchers also noted that DJ-1 translocated to the nucleus during S phase, suggesting it is a mitogen-dependent oncogene (Nagakubo *et al.*, 1997). DJ-1 is also thought to regulate RNA-protein interactions (Hod *et al.*, 1999). In thyroid tissue, DJ-1 expression is altered in cancerous versus non-cancerous states, though the change was not sufficient to aid in differentiating

neoplastic from non-neoplastic conditions (Srisomsap *et al.*, 2002). In non-small cell lung carcinomas, overexpression of DJ-1 significantly reduced taxol-induced apoptosis, suggesting DJ-1 may function as an oncogene (MacKeigan *et al.*, 2003). DJ-1 has also been implicated in the pathogenesis of prostate cancer (Hod, 2004; Pitkanen-Arsiola *et al.*, 2006; Hudson *et al.*, 2007; Tillman *et al.*, 2007). During the progression of prostate cancer from androgen-dependent to androgen-independent, a period when patients are treated with antiandrogens, DJ-1 has been identified as a protein whose production increases, thus implicating that DJ-1 may be involved in this transition (Pitkanen-Arsiola *et al.*, 2006). Furthermore, following exposure of primary human prostate epithelial cells to either androgens or antiandrogens, DJ-1 stability increases with a resultant increase in overall protein levels, and this is attributed to DJ-1 binding to the androgen receptor (Pitkanen-Arsiola *et al.*, 2006). Further evidence also supports the idea that DJ-1 may directly bind the androgen receptor, and this mechanism may dictate its role in progression of prostate cancer to an androgen-independent carcinoma (Tillman *et al.*, 2007). In breast cancer, DJ-1 has been identified as a circulating tumor antigen, readily detected in ~37% of newly diagnosed cancer patients (Le Naour *et al.*, 2001), whose production correlates negatively with expression of the tumor suppressor PTEN (Kim *et al.*, 2005a).

DJ-1 IN REPRODUCTION

DJ-1 may also modulate reproductive functions, especially in males, through interactions with the androgen receptor (Takahashi *et al.*, 2001; Niki *et al.*, 2003;

Yoshida *et al.*, 2003; Taira *et al.*, 2004a; Pitkanen-Arsiola *et al.*, 2006). DJ-1 is also known as sperm protein 22 or SP-22 as well as contraception-associated protein 1 or CAP1 in the rat, named due to its localization to spermatozoa (Wagenfeld *et al.*, 1998; Welch *et al.*, 1998; Klinefelter *et al.*, 2002). DJ-1 has an important though poorly delineated role in fertilization, as preincubation with isolated sperm with an anti-DJ-1 antibody results in a decrease in fertilization both *in vitro* and *in vivo* (Okada *et al.*, 2002). Furthermore, through its interactions with PIAS$\chi\alpha$ and DJ-1 binding protein (DJBP), DJ-1 alleviates their inhibition of the androgen receptor (Takahashi *et al.*, 2001; Niki *et al.*, 2003). Although much research remains to elucidate how DJ-1 may modulate reproduction, it is noteworthy that all *DJ-1*$^{-/-}$ mice reported to date breed normally (see below for further description of these mice). However, further investigations into DJ-1 in sperm, especially in toxin-challenged conditions, could prove fruitful.

DJ-1 KNOCKOUT MICE

Although in humans *DJ-1* mutation induces parkinsonism, *DJ-1* knockout mice fail to consistently recapitulate the hallmarks of PD which include loss of dopaminergic neurons, decrease in dopamine, formation of Lewy bodies, and locomotor dysfunction (Chen *et al.*, 2005; Goldberg *et al.*, 2005; Kim *et al.*, 2005c; Yamaguchi and Shen, 2007). Kim and colleagues found increased sensitivity of *DJ-1*$^{-/-}$ neurons to hydrogen peroxide and rotenone, and increased sensitivity of the mutant mouse to MPTP and amphetamines (Kim *et al.*, 2005c). Chen and coworkers noted locomotor impairment in their male mutant mice at 5

and 11 months of age, though other parkinsonian hallmarks were not observed (Chen *et al.*, 2005). Goldberg *et al.* described decreased locomotor activity in another *DJ-1*$^{-/-}$ mouse, though again, no other parkinsonian characteristics were observed (Goldberg *et al.*, 2005). Finally, Yamaguchi and Shen characterized an additional *DJ-1* mutant mouse and this mouse also failed to acquire any protypical PD phenotypes (Yamaguchi and Shen, 2007). Because PD is primarily a disease of age, and mice have a much shorter lifespan, it is not surprising that they fail to mimic PD. Further, unlike their human counterparts, mice lack neuromelanin in their dopaminergic neurons, and whether or not this compound itself contributes to the development of parkinsonism remains controversial. Therefore, mutation of *DJ-1* alone is likely not sufficient to induce parkinsonism in the mouse, however these mice provide an excellent platform for investigating PD as a multi-factorial disease and the cellular and molecular effects of DJ-1 in neural cells.

LIPOPOLYSACCHARIDES

Lipopolysaccharides (LPS) is a component of the outer membrane of Gram-negative bacteria, and may potently activate mammalian cells (Ulevitch and Tobias, 1995; Chow *et al.*, 1999) through its interactions with Toll-like Receptor-4 via the NF-κB pathway, causing production of proinflammatory cytokines (Chow *et al.*, 1999). In PD, elevated levels of cytokines are observed in the brains of patients (Boka *et al.*, 1994; Mogi *et al.*, 2000), as well as concomitant oxidative stress, which is thought to be significant in disease development. Furthermore,

LPS increases microglial activation in the substantia nigra which may further potentiate cytokine production in this area of the brain (Ling *et al.*, 2002). *In utero* exposure to LPS leads to increases in fetal proinflammatory cytokines, decreases in dopaminergic neurons and possibly other CNS impairments in offspring (Ling *et al.*, 2002). Maternal bacterial vaginosis may therefore be a risk factor for PD, likely due to increased susceptibility of the offspring to environmental insults later in life. Interestingly, DJ-1 protein increases following exposure to LPS (Ejima *et al.*, 2000; Mitsumoto and Nakagawa, 2001). Therefore, DJ-1 may play an important role in preventing or alleviating LPS-induced toxicity.

ROTENONE

A number of epidemiological studies demonstrate a strong correlation between pesticide exposure and an increased incidence of PD (Gorell *et al.*, 1998; Ritz and Yu, 2000; Priyadarshi *et al.*, 2001; Vanacore *et al.*, 2002). Chronic exposure to the herbicide rotenone recapitulates parkinsonism in rodents (Betarbet *et al.*, 2000). The mechanism of action for rotenone has been shown to be inhibition of mitochondrial complex I (Schuler and Casida, 2001a), however it may also deleteriously alter interactions between microglia and dopaminergic neurons (Gao *et al.*, 2002) and increase oxidative stress. Because rotenone is lipophilic, it can readily cross the blood brain barrier and inhibit complex I throughout the central nervous system. Interestingly, it preferentially destroys dopaminergic neurons in rats, suggesting an increased susceptibility of these neurons to

complex I inhibition (Betarbet *et al.*, 2000). Increases in thiobarbituric acid reactive substances, indicators of lipid peroxidation, as well as nitric oxide are noted in rats chronically exposed to rotenone (Bashkatova *et al.*, 2004). Further, chronic rotenone exposure may also lead to formation of cytoplasmic inclusions containing α-synuclein and ubiquitin, similar to the PD pathological hallmark, Lewy bodies (Betarbet *et al.*, 2000). When treated *in vivo* with rotenone, *DJ-1*$^{-/-}$ neurons had significantly decreased survival compared to *DJ-1*$^{+/+}$ neurons (Kim *et al.*, 2005b). Additionally, chronic rotenone exposure in rats induces oxidative modification of DJ-1 and redistribution of DJ-1 to the mitochondria (Betarbet *et al.*, 2006a). Because the DJ-1 protein may function in maintaining a homeostatic cellular redox environment and may modulate mitochondrial response to oxidative stress, it may indeed affect rotenone-induced toxicity. Due to rotenone's ability to inhibit mitochondrial complex I, its induction of oxidative stress, its efficaciousness in inducing parkinsonism in rodents, and the fact that it is a pesticide, rotenone exposure is a good experimental model for chemically-induced PD.

SUMMARY

PD is a complicated, multi-faceted disease with numerous potential contributing factors. Clearly, the most significant risk factor for PD is age, which allows accumulation of oxidative stress and decreases in innate antioxidant defenses, not to mention normal degeneration of the nigrostriatal pathway. Furthermore, because dopamine itself can undergo quinone cycling, the substantia nigra is an

inherently oxidative environment. However, as mutations in a number of genes contribute to a small, yet significant portion of PD cases, the influence of genetic mutations and/or polymorphism is also important to understanding and unraveling the etiology of this disease. Therefore, using a mouse with a genetic mutation known to cause PD in humans coupled with exposure to the proinflammatory stimulus, LPS, or the prototypical mitochondrial complex I inhibitor, rotenone, incorporates many suspected aspects of PD development, and may assist in further explicating this complicated and crippling condition.

CHAPTER 2

MUTATION OF *DJ-1* INDUCES ALTERATIONS IN BASAL VEGF EXPRESSION IN CEREBRAL AND LUNG TISSUE IN THE MOUSE

ABSTRACT

DJ-1 mutation induces early-onset Parkinson's disease, and conversely over-expression of DJ-1 is associated with cancer in numerous tissues. A gene-trap screening library conducted in embryonic stem cells was utilized for generation of a *DJ-1* mutant mouse. Real-time PCR and immunoblotting confirmed functional mutation of the *DJ-1* gene with lack of expression in the homozygous mutant. DJ-1 protein production in normal adult mouse tissue was characterized and demonstrates high production in brain tissue with wide systemic distribution. Primary astrocytes isolated from *DJ-1*$^{-/-}$ mice reveal an increased localization of DJ-1 protein to the mitochondria in response to rotenone, with a concomitant decrease in nuclear localization. Resting mitochondrial membrane potential was significantly lower in *DJ-1*$^{-/-}$ astrocytes. Bax protein production was similar in *DJ-1*$^{+/+}$ astrocytes compared to *DJ-1*$^{-/-}$ cells. In *DJ-1*$^{-/-}$ tissues, *VEGF* expression was significantly increased in lung and decreased in brain, compared to *DJ-1*$^{+/+}$, though no changes were observed in other tissues. Expression of *HIF1*α was lower in *DJ-1*$^{+/-}$ lung tissue compared to *DJ-1*$^{+/+}$. Preliminary *in vivo* studies do not demonstrate differential response of *DJ-1*$^{-/-}$ mice to MPTP. These findings demonstrate that the *DJ-1*$^{-/-}$ mouse may have basal alterations in their physiology, possibly predisposing them to further insults later in life. Thus this mouse model provides an exciting tool for exploring the molecular and physiological roles of DJ-1 to further explicate its functions in neurodegeneration and carcinogenesis.

INTRODUCTION

Mutations in *DJ-1* are associated with the development of early-onset Parkinson's disease (PD) (Bonifati *et al.*, 2003a), though it is ubiquitously expressed throughout the central nervous system and other organ systems in mammals (Bandopadhyay *et al.*, 2004; Bader *et al.*, 2005). Aside from PD, other endogenous and experimentally-induced neurological disorders have alterations in DJ-1, including Alzheimer's disease (Choi *et al.*, 2006), multiple system atrophy (Neumann *et al.*, 2004), mutant huntingtin cells (Goswami *et al.*, 2006), ischemia/stroke (Aleyasin *et al.*, 2007; Yanagisawa *et al.*, 2007) and experimental encephalomyelitis (Lev *et al.*, 2006), demonstrating that DJ-1 may play a significant role in maintaining CNS homeostasis. Additionally, DJ-1 is classified as a putative oncogene (Nagakubo *et al.*, 1997), where overexpression and/or secretion is associated with a variety of cancers, including breast (Kim *et al.*, 2005a), non-small cell lung carcinoma (MacKeigan *et al.*, 2003), pancreatic (Melle *et al.*, 2007), thyroid (Srisomsap *et al.*, 2002), prostate (Grzmil *et al.*, 2004; Hod, 2004), uveal melanoma (Pardo *et al.*, 2006) and ovarian carcinoma (Davidson *et al.*, 2008). DJ-1 may also modulate reproductive functions, especially in males, through interactions with the androgen receptor (Takahashi *et al.*, 2001; Niki *et al.*, 2003; Yoshida *et al.*, 2003; Taira *et al.*, 2004a; Pitkanen-Arsiola *et al.*, 2006).

Numerous cellular functions have been proposed for DJ-1, including responding to the cellular redox environment (Yokota *et al.*, 2003; Martinat *et al.*, 2004; Taira

et al., 2004b; Takahashi-Niki *et al.*, 2004; Kim *et al.*, 2005c; Moore *et al.*, 2005), a variety of protein-protein interactions (Takahashi *et al.*, 2001; Macedo *et al.*, 2003; Meulener *et al.*, 2005; Sekito *et al.*, 2005; Xu *et al.*, 2005; Bretaud *et al.*, 2007; Fan *et al.*, 2007), and plausible chaperone activity (Martinat *et al.*, 2004; Shendelman *et al.*, 2004). However, the precise role DJ-1 plays in cellular homeostasis and how its dysregulation contributes to PD and carcinogenesis has not been ascertained.

Although in humans *DJ-1* mutation induces parkinsonism, *DJ-1* knockout mice fail to consistently recapitulate the hallmarks of PD which include the loss of dopaminergic neurons, decrease in dopamine, formation of Lewy bodies, and locomotor dysfunction (Chen *et al.*, 2005; Goldberg *et al.*, 2005; Kim *et al.*, 2005c; Yamaguchi and Shen, 2007). However, Kim and colleagues found increased sensitivity of *DJ-1*$^{-/-}$ neurons to hydrogen peroxide and rotenone, and increased sensitivity of the mutant mouse to MPTP and amphetamines (Kim *et al.*, 2005c). Chen and coworkers noted locomotor impairment in their mutant male mice at 5 and 11 months of age, though other parkinsonian hallmarks were not observed (Chen *et al.*, 2005). Goldberg et al described decreased locomotor activity in another *DJ-1*$^{-/-}$ mouse, though again, no other characteristics of PD were observed (Goldberg *et al.*, 2005). Finally, Yamaguchi and Shen characterized an additional DJ-1 mutant mouse and this mouse also failed to acquire any protypical PD phenotypes (Yamaguchi and Shen, 2007). Therefore, mutation of *DJ-1* alone is likely not sufficient to induce parkinsonism in the

mouse, however these mice provide an excellent platform for investigating Parkinson's as a multi-factorial disease.

An essential element in unraveling the pathogenesis of PD is defining how astroglial dysregulation is involved in the progression of neuronal degeneration. Astrocytes vastly outnumber neurons, are present throughout all regions of the brain, and are increasingly recognized to play critical and integral roles in maintaining normal neuronal physiological functions (Vernadakis, 1996). Astrocytes supply neurons with neurotrophic factors such as nerve growth factor, neurotrophin-3, brain-derived growth factor (Barde *et al.*, 1982), and fibroblast growth factor (Chadi *et al.*, 1993), metabolic substrates such as lactate (Pellerin *et al.*, 1998; Bouzier-Sore *et al.*, 2003a; Bouzier-Sore *et al.*, 2003b), and antioxidants including glutathione precursors (Sagara *et al.*, 1993) to promote neuronal function and viability. Furthermore, astrocytes also take up glutamate (Schousboe *et al.*, 1979), potassium (Newman, 1996), and calcium (Duffy and MacVicar, 1996), thus maintaining the extracellular space shared with local neurons. In response to stress, astrocytes undergo a state of gliosis, and release cytokines (Benveniste *et al.*, 1998) that, in excess, are ultimately deleterious to neurons. Reactive gliosis and concomitant inflammatory processes are implicated in the pathogenesis and progression of PD, but modulation of these processes by specific endogenous and xenobiotic compounds remains poorly understood. Glial cell activation is reported in sporadic PD (Hunot *et al.*, 1999; Wszolek *et al.*, 2002a; Wu *et al.*, 2002), and in toxicant-induced

neurodegeneration induced by MPTP (1-methyl-4-phenyl-1,2,3,6-tetrahydropyrindine) (Kohutnicka *et al.*, 1998), rotenone (Sherer *et al.*, 2003a), manganese (Tomas-Camardiel *et al.*, 2002) and in mutant α-synuclein mice (Gomez-Isla *et al.*, 2003). Collectively, studies have suggested that compromising astrocytic function could be a significant mechanism in neurodegeneration.

Lipopolysaccharide (LPS) is a component of the outer membrane of Gram-negative bacteria, and may potently activate mammalian cells (Ulevitch and Tobias, 1995; Chow *et al.*, 1999) through its interactions with Toll-like Receptor-4 via the NF-κB pathway, causing production of proinflammatory cytokines (Chow *et al.*, 1999). In PD, elevated levels of cytokines are observed in the brains of patients (Boka *et al.*, 1994; Mogi *et al.*, 2000), as well as concomitant oxidative stress, which is thought to be significant in disease development. Furthermore, LPS increases microglial activation, inducing putative pathogenic alterations in the substantia nigra, which may in turn further potentiate cytokine production (Ling *et al.*, 2002).

Epidemiological studies demonstrate a correlation between pesticide exposure and increased incidence of PD (Gorell *et al.*, 1998; Ritz and Yu, 2000; Priyadarshi *et al.*, 2001; Vanacore *et al.*, 2002). The pesticide rotenone, for instance, has been shown to induce parkinsonism in rats (Betarbet *et al.*, 2000). The mechanism of action for rotenone is inhibition of mitochondrial complex I (Schuler and Casida, 2001b), however it may also deleteriously alter interactions

between microglia and dopaminergic neurons (Gao *et al.*, 2002) and increase oxidative stress. In support of this theory, reduced complex I activity in the mitochondria of sporadic PD patients has been observed (Mizuno *et al.*, 1989; Schapira *et al.*, 1989; Haas *et al.*, 1995). Because rotenone is lipophilic, it can readily cross the blood brain barrier and inhibit complex I throughout the central nervous system. Interestingly, it preferentially destroys dopaminergic neurons, suggesting an increased susceptibility of these neurons to complex I inhibition (Betarbet *et al.*, 2000). Chronic rotenone exposure may also lead to formation of cytoplasmic inclusions reminiscent of PD Lewy bodies, containing α-synuclein and ubiquitin, (Betarbet *et al.*, 2000). When treated *in vivo* with rotenone, *DJ-1*$^{-/-}$ neurons had significantly decreased survival compared to *DJ-1*$^{+/+}$ neurons (Kim *et al.*, 2005c). Additionally, chronic rotenone exposure induces oxidative modification of DJ-1 and redistribution of DJ-1 to the mitochondria (Betarbet *et al.*, 2006b). Because DJ-1 may function in maintaining a homeostatic cellular redox environment and modulate mitochondrial response to oxidative stress, it also may indeed affect rotenone-induced toxicity.

MPTP is the gold-standard chemical inducer of parkinsonism in mice and primates. In the mid 1980s, heroin addicts accidentally injected the meperidine derivative, MPTP, resulting in irreversible neurodegeneration of the substantia nigra pars compacta and striatum that produced neurological symptoms closely resembling PD (Langston *et al.*, 1983). MPTP toxicity produces loss of dopaminergic neurons in a similar distribution to the pathology of PD, although

unlike PD, no Lewy body pathology is present. MPTP itself is converted to its toxic metabolite, 1-methyl-4-phenyl-pyridinium ion (MPP^+), by monoamine oxidase B via astrocytes in the brain (Langston *et al.*, 1983). Due to its structural similarity to dopamine, MPP^+ is selectively taken up into neurons via dopamine transporter (Javitch and Snyder, 1984). Within neurons, MPP^+ enters mitochondria and inhibits complex I of mitochondrial respirator chain (Heikkila *et al.*, 1984; Mizuno *et al.*, 1987). Inhibition of complex I by MPP+ prevents function of electron transport chain, leading to a decline in energy production as well as generation of free radicals, resulting in dopaminergic neuronal death.

To investigate the physiological consequences of *DJ-1* mutation, we acquired chimeric mice from BayGenomics. As mentioned, DJ-1 likely contributes to carcinogenesis in a number of tissues. Therefore, delineating how *DJ-1* mutation affects regulation of other proteins in various tissues may contribute to elucidating its role in normal cell homeostasis as well as disease states. As DJ-1 is implicated in pathogenesis of both neurodegeneration and carcinogenesis, expression of *VEGF*, common to both disease processes, was investigated in numerous tissues. Taking into consideration the complex etiology of PD, and the fact that DJ-1 knockout mice fail to recapitulate the hallmarks of PD, our experimentation primarily focused on coupling *DJ-1* mutation with relevant chemical exposure. Specifically, mutation of *DJ-1* in astrocytes with concomitant exposure to rotenone or LPS was investigated, focusing upon a possible mitochondrial phenotype, including Bax dysregulation. Our hypothesis is that

mutation in *DJ-1* induces dysregulation of cellular homeostasis, thus causing alterations in expression of *VEGF* and mitochondrial dysfunction.

MATERIALS AND METHODS

DJ-1 KNOCKOUT MOUSE: In order to study the role of *DJ-1* mutation *in vivo*, a gene-trap screening library conducted in embryonic stem cells was used; the *DJ-1* gene was mutated and chimeric mice were generated by BayGenomics (San Francisco). The gene-trapping vector sequence itself contains two reporter constructs, neomycin resistance and β-galactosidase, whose expression is under control of the endogenous *DJ-1* promoter (Figure 2.1B). Via 5' rapid amplification of cDNA ends (5' RACE), the vector insertion point was localized to the sixth intron of *DJ-1*. However in the mouse, this intron is large (approximately 3.5kb), so in order to ascertain the correct genotype of the mice, determining the precise insertion point of the vector was warranted. Forward primers were designed within the sixth intron and reverse primers were designed within the vector itself. Using PCR, we amplified DNA between these primers and determined the molecular weight by electrophoresis on a 1% agarose gel. Target bands were excised, DNA was extracted and ligated into the pGEM®-T vector (Promega) which was used to transform C max (α) competent cells (BioRad). Clones positive for pGEM®-T (i.e., those expressing β-galactosidase) were selected, DNA extracted, and two sets of restriction enzymes, *Nco I* and *Nde I* as well as *Spe I* and *Sph I* were used to screen for insertion into pGEM®-T . Positive DNA samples were sequenced, and analyses revealed the precise insertion site within

the sixth intron (Figure 2.1A). Genotyping was accomplished via amplifying a sequence of neomycin resistance gene within the inserted gene trap vector (*Neo* primers, 5'-CTT GGG TGG AGA GGC TAT TC-3', 5'-GTG AGA TGA CAG GAG ATC-3') combined with amplification of a sequence of DNA spanning the region of the gene trap vector insertion (*DJ-1* primers, 5'-ACC CTT GCA GTC ACT TTA CC-3', 5'-TAG CTG GCA GGA GCT TGG-3). Heterozygous mice were mated, and the newborn mice were utilized for primary culture of cortical astrocytes. Astrocytes were isolated as previously described (Allen *et al.*, 2000a), and maintained at 37°C and 5% CO_2 in minimal essential medium with Earl's balanced salts solution and L-glutamine (Hyclone) supplemented with 10% fetal bovine serum and 1% penicillin/streptomycin/neomycin (Invitrogen).

REAGENTS: Unless otherwise specified, all reagents were purchased from Sigma Aldrich.

REAL TIME PCR: RNA was isolated from snap frozen tissue samples using the Qiagen RNeasy kit, subjected to DNase I treatment, then reverse-transcribed via iScript kit (BioRad). cDNA was analyzed via real-time PCR by assessing SYBR green (BioRad) incorporation over time on a BioRad iCycler. Expression of *DJ-1* (5'-ATC TGA GTC GCC TAT GGT GAA G-3', 5'-ACC TAC TTC GTG AGC CAA CAG-3') or *VEGF* (5' - AGG CTG CTG TAA CGA TGA AG - 3', 5' - TTC TGG CTT TGT TCT GTC TTT C - 3' was normalized to *β-actin* (5'-GAC AGG ATG CAG AAG GAG ATT ACT G-3', 5'-GCT GAT CCA CAT CTG CTG GAA-3') via

the delta-delta C_T method (Livak and Schmittgen, 2001). Samples without reverse transcriptase were also analyzed to assure no DNA contamination was present.

MORPHOMETRIC ANALYSIS: Immunofluorescence was utilized for morphometric analysis of primary mouse cortical astrocytes (Fig 2C). Astrocytes were exposed to PBS, 10μM MPTP or 50μM manganese chloride for 24h. Cells were fixed in 100% methanol then permeabilized with 0.01% Triton X-100 in PBS. Glial fibrillary acidic protein (GFAP) was detected with a primary monoclonal antibody (Sigma, G-3893) conjugated to a secondary fluorescent antibody (Alexa Fluor 568; excitation λ578, emission λ603 Molecular Probes). Cells were mounted in media containing 4,6-diamidino-2-phenylindole (DAPI; Vector Laboratories), allowing for identification of nuclei. Images were obtained using a Zeiss Axiovert 200M microscope equipped with a Hammatsu ORCA-ER cooled charge-coupled device camera. Single cell parameters were established by outlining individual cells using SlideBook software.

No genotype-specific changes were observed in GFAP fluorescence nor mean cell perimeter (data not shown), however, mean cell area was significantly lower in *DJ-1*$^{-/-}$ astrocytes versus *DJ-1*$^{+/+}$ cells with or without exposure to MPTP (Figure 2.2C). Furthermore, as mean cell area is shown to increase by 44% in *DJ-1*$^{-/-}$ cells versus a 36% increase in *DJ-1*$^{+/+}$, astrocytes harboring the *DJ-1* mutation may react more dramatically to toxic insult.

MITOCHONDRIAL MEMBRANE POTENTIAL: To assess mitochondrial membrane potential, the ratiometric dye JC-1 (5,5',6,6'-tetrachloro-1,1',3,3'-tetraethylbenzimidazolylcarbocyanine iodide, Invitrogen) was employed. A decrease in the ratio of λ568:λ488 indicates formation of fewer J-aggregates, or decreased mitochondrial polarization. Differing concentrations of JC-1 were monitored for sensitivity to the uncoupling agent CCCP (carbonyl cyanide 3-chlorophenyl-hydrazone). Based upon a robust depolarization following CCCP administration, 5μM JC-1 was selected for monitoring alterations in mitochondrial membrane potential. Astrocytes were loaded with 5μM JC-1 for 20 min, washed once with MEM without phenol red supplemented with 25mM HEPES, and images were collected every 2 min. After 4 images were collected (8 min), 0, 50, 500 or 1000nM rotenone or was added, and images were collected for 52 additional min for a total of 1 h sampling. Fluorescence intensity at λ568 and λ488 was measured using SlideBook software.

COLOCALIZATION: For analysis of subcellular localization of DJ-1, astrocytes were treated with 0, 10, 25, or 50 μg/mL LPS for 72h, treatments were then removed and cells were washed with PBS. New media was added containing 0, 50, 500, or 1000nM rotenone, and cells were exposed for 24h. Following treatment, cells were loaded for 30 min at 37°C with 500nM MitoTracker Red (Invitrogen, excitation at λ579, emission at λ599), fixed in 4% paraformaldehyde, permeabilized with 0.01% triton X-100, and DJ-1 primary antibody was applied

(1:2000, Neuromics). Alexa Fluor 488-conjugated secondary antibody (Invitrogen, excitation at λ495, emission at λ519) was added, and cells were mounted in DAPI-containing mounting media for visualization of nuclei (Vector Laboratories, excitation at λ360, emission at λ460). Images were obtained the Zeiss microscope mentioned above. Pearson's correlation coefficients, used to assess colocalization of Alexa Fluor 488-conjugated DJ-1 with either the nucleus or the MitoTracker-labeled mitochondria, were calculated using SlideBook Software.

WESTERN BLOTTING: Tissues were snap frozen immediately after harvest to assure protein integrity. Protein was isolated by homogenizing tissue in lysis buffer (50mM Tris, 150mM NaCl, 0.1% SDS, 1% nonidet P-40, 0.5% Na deoxycholate, 2mM Na orthovanadate) supplemented with complete mini protease cocktail inhibitors (Roche). Samples were sonicated for 10 sec at 30% output, placed on ice for 20 min, then centrifuged at 14,000 rpm for 10 min at 4°C. Protein from primary astrocyte cultures was harvested in lysis buffer (see above), placed on ice for 5 min, and then centrifuged as above. Protein content of the supernatant was determined by BCA protein assay (Pierce). Protein was subjected to SDS-PAGE, electrotransferred onto PVDF (VWR) and probed with anti-Bax antibody (Cell Signaling, 1:1000), anti-DJ-1 antibody (Neuromics, 1:2000) alone or with β-actin (Sigma, 1:1000). Protein was detected via chemiluminescence.

ANIMAL STUDIES: Eight-week old mice were treated s.c. with two doses of either sterile saline or 20mg/kg MPTP (free base) in saline 6 h apart. MPTP was stored on ice between injections, and injected volumes were 10mL/kg. MPTP mice were caged separately from saline-exposed mice. One day prior to treatment and 7 days following treatment, open-field locomotor activity was assessed using VersaMax infrared beam activity chambers (Accuscan Instruments), and animal weight was recorded. Locomotor data was analyzed using VersaDat software (Accuscan Instruments). Seven days after saline or MPTP injection, animals were deeply anesthetized with isoflurane, then perfused intracardially with 4% paraformaldehyde in 0.1M $NaKPO_4$ buffer (pH 7.4). The brains were collected and kept in cold 4% paraformaldehyde overnight and stored in 0.1M $NaKPO_4$ buffer at 4°C.

NEURAL TISSUE PATHOLOGY: Coronal 10μm serial sections were assessed using a standard hematoxylin/eosin (H&E) stain, immunohistochemistry (IHC) for tyrosine hydroxylase (TH), or fluorojade including the substantia nigra and striatal regions of the brain. H&E staining was performed according to standard procedures. Prior to IHC or fluorojade staining, slides were incubated xylene followed by a series of ethanols to deparaffinize and rehydrate samples. IHC was performed with an initial antigen retrieval using 0.01M sodium citrate, followed by quenching of endoperoxidases with 0.3% H_2O_2 for 30 min. All washes were carried out in Tris-buffered saline (TBS) and the primary antibody for TH was used at a 1:400 dilution. Sections were developed using a horseradish

peroxidase–conjugated secondary antibody and diaminobenzidine reagents (Vectastain ABC kit, Vector Labs). To enhance visibility of TH immunoreactivity, slides were immersed in hematoxylin for 3 min, and then removed and the stain was allowed developed for 5 min in tap water. Slides were destained in acidified ethanol, and then cleared in diH_2O. After staining, slides were dehydrated through a series of ethanols and xylene, and then mounted in ClearMount media (American Mastertech). Fluorojade was detected via first incubating slides in 0.06% potassium permanganate for 15 min, then washing with diH_2O. Slides were incubated for 30 min in 0.001 % fluorojade (HistoChem) dissolved in 0.1% acetic acid, then dried and mounted in ClearMount media. All images were collected using the microscope detailed above.

STATISTICAL ANALYSES: All statistical analyses were performed using GraphPad Prism software. Figures with three or more means were analyzed using ANOVA, and when means significantly differed ($p<0.05$), Tukey's *post hoc* test was employed. Figures containing two means were analyzed with two-tailed t-tests; when variances significantly differed, Welch's correction was applied to correct for unequal variances.

RESULTS

Based upon 5' rapid amplification of cDNA ends provided by BayGenomics, the exonic sequences upstream of the mutation-inducing gene-trap vector were identified. To facilitate genotyping, the precise location of the gene-trap vector

insertion was determined (Figure 2.1A), and genotyping primers spanning the insertion site were created to assay for the normal *DJ-1* genomic sequence (Figure 2.1B). Additional genotyping primers specific to the neomycin-resistance gene were utilized to detect the inserted exogenous DNA, and allowed differentiation between all three genotypes. Functional mutation of the *DJ-1* gene via insertion of the gene-trap vector was assessed in $DJ\text{-}1^{+/+}$, $DJ\text{-}1^{+/-}$, and $DJ\text{-}1^{-/-}$ brain tissue (Figure 2.1). Real-time PCR of whole brain demonstrated that RNA expression of *DJ-1* was greatly diminished in the $DJ\text{-}1^{-/-}$ tissue compared to both $DJ\text{-}1^{+/-}$ and $DJ\text{-}1^{+/+}$ ($p<0.001$, Figure 2.1C). As the primers utilized in real-time PCR are located in sequences upstream of the gene-trap insert, the minimal transcription observed in the $DJ\text{-}1^{-/-}$ is biologically feasible. Production of the DJ-1 protein is completely lost in the $DJ\text{-}1^{-/-}$ but maintained in both the $DJ\text{-}1^{+/+}$ and the $DJ\text{-}1^{+/-}$ (Figure 2.1D), therefore our mutant mouse model represents a functional knockout of DJ-1.

Real-time PCR and Western blot analysis were utilized to determine relative production of DJ-1 in numerous $DJ\text{-}1^{+/+}$ tissues in the mouse (Figure 2.2). RNA expression was normalized to β-actin, as discussed above, and revealed high *DJ-1* expression in the kidney and the liver (Figure 2.2A). However, to assure this was representative of protein production, Western blot analysis, coupled with densitometry was used. Relative to β-actin, brain tissue had the highest DJ-1 protein production followed by liver, though DJ-1 was detected in all tissues assayed. While production of β-actin can vary dramatically in differing tissue

samples, standardizing DJ-1 protein to this housekeeping protein allows a relative quantitation of tissue distribution. Figure 2.2B depicts DJ-1 in 25μg of protein from each tissue, and follows the overall pattern of distribution presented in Figure 2.2C. Interestingly, DJ-1 in all duodenal samples assayed (n=9) appeared at a lower molecular weight (approximately 19 kDa) than the protein in all other tissues. Curiously, the theoretical molecular weight of DJ-1 due to its 189 amino acid structure is 20kDa, closer to the value observed in the duodenum than in the rest of the body. Therefore, it is feasible that modification(s) of non-gastrointestinal DJ-1 protein (i.e., glycosylation), result in a slightly higher molecular weight, while these are cleaved in the highly acidic gastrointestinal environment. Regardless, this lower molecular weight band is consistently present only in the duodenal samples, and thus is unlikely to be a non-specific band. Notably, DJ-1 is widely and systemically distributed, implicating DJ-1 may play a critical role in cell homeostasis.

Morphometric analysis was done on individual astrocytes from *DJ-1*$^{+/+}$ and *DJ-1*$^{-/-}$ mice to determine whether these cells differentially respond to toxic insult. Primary cortical astrocytes were exposed to 50μM manganese or 10μM MPTP for 24h, and then immunochemically probed for GFAP. Relative production of GFAP in astrocytes increased only in *DJ-1*$^{+/+}$ cells exposed to MPTP ($p<0.05$, $n \geq 47$, Figure 2.3A). Mean cell area increased in all cells exposed to MPTP, but not manganese (Figure 2.3B). Interestingly, *DJ-1*$^{-/-}$ astrocytes were smaller than *DJ-1*$^{+/+}$ cells ($p<0.05$), regardless of treatment, however mean cell area increased

more dramatically (44%) in *DJ-1*$^{-/-}$ cells versus *DJ-1*$^{+/+}$ astrocytes (36%), which may indicate a more exaggerated response to MPTP treatment (Figure 2.3B).

Subcellular localization of DJ-1 in primary astrocytes was analyzed. DJ-1 is normally present in three subcellular pools, the cytosol, mitochondria, and nucleus. Therefore, to assess its localization following chemical exposure, mitochondria were labeled with MitoTracker Red, the nucleus with DAPI, and DJ-1 with AlexaFluor 488. All DJ-1 not localized to the mitochondria or nucleus was considered to be in the cytoplasmic pool, as DJ-1 has not been demonstrated to localize to other subcellular organelles. Astrocytes were treated with a proinflammatory mediator, LPS (10, 25 or 50 μg/mL) in DMSO, rotenone (50, 500, 1000nM) in PBS, combinations of LPS and rotenone, or with PBS + DMSO (controls) after which subcellular localization to the nucleus and mitochondria was analyzed. Interestingly, treatment with 1000nM rotenone induced a significant increase in mitochondrial localization ($p<0.001$, Figure 2.4B), whereas 10μg/mL LPS treatment did not alter mitochondrial localization. Interestingly, decreases in nuclear localization were observed in both 1000nM rotenone and 10μg/mL LPS stimulated cells ($p<0.001$, Figure 2.4C). Possibly, the nuclear pool of DJ-1 translocates to the mitochondria under rotenone-induced complex I inhibition, but not neuroinflammatory stress induced by LPS. Instead, LPS may induce an increase of DJ-1 in the cytosol with a concomitant decrease in nuclear localization, though the cytsolic fraction was not directly assessed. All statistical information for Figures 2.4D and 2.4E are summarized in Table 2.1 and 2.2,

respectively. Generally, nuclear localization of DJ-1 tended to decrease with increasing LPS concentrations, regardless of coexposure to rotenone (Figure 2.4E). Mitochondrial localization of DJ-1 remained fairly similar amongst all treatments with rotenone ± LPS, though overall variability increased as LPS concentrations increased (Figure 2.4D). As a surrogate for cellular viability, percent cells counted per treatment group tended to decrease as the concentration of LPS increased, and this was exacerbated by coexposure to rotenone, presumably due to increased toxicity (Figure 2.4F).

Because DJ-1 may respond to mitochondrial stress, we analyzed mitochondrial membrane potential in *DJ-1*$^{+/+}$ and *DJ-1*$^{-/-}$ astrocytes, and in astrocytes exposed to rotenone using the ratiometric dye JC-1. In a preliminary experiment, differing concentrations of JC-1 were monitored for sensitivity to the uncoupling agent CCCP (carbonyl cyanide 3-chlorophenylhydrazone). Based upon a robust depolarization following CCCP administration, 5μM JC-1 was selected for monitoring alterations in mitochondrial membrane potential (Figure 2.5). Following 8 min initial baseline sampling, 0, 50, 500, or 1000nM rotenone was added and JC-1 fluorescence was measured for an additional 52 min (Figure 2.6B and 2.6C). Interestingly, basal mitochondrial membrane potential was decreased (p<0.03) in *DJ-1*$^{-/-}$ cells compared to *DJ-1*$^{+/+}$ during the first 8 min of imaging (Figure 2.6D). However, following exposure of up to 1000nM rotenone, neither *DJ-1*$^{+/+}$ nor *DJ-1*$^{-/-}$ cells had a significant decrease in mitochondrial

membrane potential, and were no longer significantly different from one another (Figure 2.6E).

Bax is implicated in neurodegeneration and cancer, propagates mitochondrial-mediated apoptosis, and has been implicated in DJ-1 mediated cellular protection in neuroblastomas (Fan *et al.*, 2007). Therefore, we analyzed production of Bax protein in our primary cortical astrocytes. *DJ-1*$^{-/-}$ astrocytes had no basal alterations in Bax compared to *DJ-1*$^{+/+}$ controls (Figure 2.7A and 2.7B), nor were significant alterations noted in cells exposed to 10μg/mL LPS for 24h (data not shown).

As vascular function may be affected in carcinogenesis and neurodegeneration, expression of the proangiogenic factor, *HIF1α,* was assessed along with *VEGF.* In *DJ-1*$^{-/-}$ and *DJ-1*$^{+/-}$ mice, basal *VEGF* expression decreased significantly in brain tissue as compared to *DJ-1*$^{+/+}$ (Figure 2.8B, $p<0.05$). Interestingly, *VEGF* tended to be higher in the lung tissue of *DJ-1*$^{+/-}$ and *DJ-1*$^{-/-}$, though only *DJ-1*$^{+/-}$ was significant increased (Figure 2.9, $p<0.05$ and $p=0.07$, respectively). In contrast to *VEGF, DJ-1*$^{-/-}$ brain tissue had similar expression levels of *HIF1α* (Figure 2.8A) as compared to *DJ-1*$^{+/+}$. However, in the lung, both *DJ-1*$^{+/-}$ and *DJ-1*$^{-/-}$ tissue had decreased levels of HIF1α compared to *DJ-1*$^{-/-}$ (Figure 2.9). No alterations in *VEGF* or *HIF1α* were detected in the other tissues assayed, including heart (Figure 2.10), kidney (Figure 2.11), liver (Figure 2.12), or spleen

(Figure 2.13), though heart expression of *VEGF* tended to be higher in the *DJ-1*$^{+/+}$ mice versus *DJ-1*$^{-/-}$ (p=0.09).

H&E staining was done to detect the presence of eosinophilic Lewy body pathology, a hallmark of PD (Figure 2.14). However, as has been reported with other *DJ-1* mutant mice, no aberrant protein aggregations, typical of Lewy bodies, are observed in either *DJ-1*$^{+/+}$ or *DJ-1*$^{-/-}$ brain tissue. Because MPTP does not induce Lewy body formation, the lack of eosinophilic inclusions in treated animals was anticipated. Although no quantitative assessment has been conducted, it appears that *DJ-1*$^{+/+}$ striatum tend to have an increase in cell number per unit area compared to *DJ-1*$^{-/-}$ tissue. Fluorojade staining in the striatum reveals a tendency for increased reactivity of the perivascular endothelial cells rather than neurons, as might be anticipated in MPTP-treated mice (Figure 2.14H&K, white arrows). This staining pattern is similarly observed in animals treated with manganese, and may point to alterations in capillaries due to toxin exposure, but has yet to be elucidated. Again, no differences were observed between *DJ-1*$^{+/+}$ and *DJ-1*$^{-/-}$ mice. TH staining in the substantia nigra was rather peculiar (Figure 2.14). Following MPTP treatment, TH immunoreactivity should decrease, however in *DJ-1*$^{+/+}$ sections particularly, this was not observed (Figure 2.14 C&F).

Alterations in total distance traveled, vertical activity, and velocity were assessed in animals prior to MPTP or saline administration (Day 0) and one week following treatment (Day 7, Figure 2.15). No significant alterations in locomotor activity was

observed in any of the three criteria assessed, therefore neither genotype nor MPTP treatment affected the overall locomotor activity of the mice.

CONCLUSIONS

DJ-1 was initially identified as an oncogene (Nagakubo *et al.*, 1997), and then gained additional distinction as a gene involved in PD (Bonifati *et al.*, 2003b), however the precise role(s) of DJ-1 remain elusive and ever expanding. The DJ-1 distribution data presented here complements data published elsewhere (Olzmann *et al.*, 2004; Zhang *et al.*, 2005), suggesting DJ-1 is very widely and systemically distributed.

Due to the propensity of mitochondrial dysfunction contributing to neurodegeneration and the localization of DJ-1 to this organelle, increased localization of DJ-1 to the mitochondria following exposure to rotenone is expected. Bertabet and colleagues report increased DJ-1 localization to the mitochondria following chronic (4 week) exposure to 5nM rotenone in SK-N-MC neuroblastoma cells, and our data are in agreement with these (Betarbet *et al.*, 2006b). However, this study is the first to report quantitative analysis on altered localization to either the mitochondria or the nucleus due to rotenone treatment, as well as LPS-induced decline in nuclear localization. While DJ-1 in the nucleus likely translocates to the mitochondria to protect against rotenone-induced toxicity, it is unknown why DJ-1 nuclear localization declines in response to LPS. Other reports suggest DJ-1 protein production increases in placenta following

exposure to LPS (Ejima *et al.*, 2000; Mitsumoto and Nakagawa, 2001), so it is likely DJ-1 may function in a protective manner to combat LPS-induced toxicity, and altering its subcellular location may be critical to this role. Additionally, a decrease in resting mitochondrial membrane potential in *DJ-1*$^{-/-}$ astrocytes compared to *DJ-1*$^{+/+}$ controls suggests DJ-1 may modulate mitochondrial energy dynamics, dysfunction of which is thought to contribute to PD pathogenesis. In support of this concept, *DJ-1*$^{-/-}$ neurons are reportedly more vulnerable to alterations in energy metabolism due to impaired Na+/K+ ATPase function (Pisani *et al.*, 2006).

Interestingly, loss of DJ-1 leads to a converse expression of *VEGF* in lung versus brain tissue, suggesting the mechanism by which DJ-1 modulates VEGF in each tissue may differ. As VEGF is implicated both in neurodegenerative disease and carcinogenesis, especially non-small cell lung carcinoma, DJ-1-mediated regulation of VEGF warrants further investigation. An elegant study by Fan and colleagues in a neuroblastoma line demonstrates an increase in Bax in *DJ-1* knockdown, though we observed no alterations in Bax production in our *DJ-1*$^{-/-}$ astrocytes, even following exposure to LPS (2007). The mechanisms regulating DJ-1-mediated alterations of Bax production have not yet been investigated in astrocytes, so comparison of our data with this study is problematic. However, we present differential *VEGF* expression in our *DJ-1*$^{-/-}$ compared to *DJ-1*$^{+/+}$, increased in lung and decreased in the brain, respectively (Figure 2.6). Therefore the notion that DJ-1 differentially regulates protein production in different tissues

is quite feasible, and may explain differences observed in our data and that of Fan and coworkers.

Regulation of *VEGF* and *HIF1α* in our mice is of interest. Classically, HIF1α is induced by hypoxic insult, and it in turn upregulates VEGF. Upregulation of VEGF in our system is not likely due to increased *HIF1α* expression. However, as hypoxia results in the stabilization of HIF1α, preventing its degradation by the proteosome, it is possible that an aberration of this regulation occurs in our *DJ-1*$^{-/-}$ mouse, leading to decreased *VEGF* expression in the brain. However, as *HIF1α* expression in the lung of *DJ-1*$^{-/-}$ mice actually declines compared to the *DJ-1*$^{+/+}$ mouse, whereas *VEGF* express increases in the *DJ-1*$^{-/-}$, decreased *HIF1α* stabilization coupled with decreased expression should not lead to increases in expression of *VEGF*. Therefore, it is unlikely that the alterations in expression of *VEGF* are due to the observed changes in *HIF1α*, but rather due to another factor. In the mouse, other transcription factors, such as Sp3 (Schwarzenbach *et al.*, 2004), Jun and NFκB (Fujita *et al.*, 2005) amongst others may regulate VEGF expression. Therefore, DJ-1 may be interacting with one or more of these other factors, or somewhere upstream to affect expression of *VEGF* and *HIF1α*. Regardless, our data is the first to demonstrate differential regulation of these genes, involved in angiogenesis and hypoxia, in *DJ-1*$^{-/-}$ mice. As evidence of DJ-1's involvement in not only PD but also ischemia/reperfusion injury and carcinogenesis mounts, exploring this venue of research will likely provide further insight into DJ-1's biological function.

The experiments described herein attempt to determine the function of DJ-1 in normal mouse tissue as well as primary cortical astrocytes. First, alterations in certain genes associated with both neurodegeneration and carcinogenesis were investigated, as DJ-1 may contribute to both. Further, as mutation of *DJ-1* induces parkinsonism in humans and astrocytic support is essential for neuronal vitality, we attempted to discern how this mutation might alter the phenotype of astrocytes, thus rendering the cells either incapable or less efficacious in their neuroprotective role. Incorporating various elements of parkinsonism, astrocytes were profiled for sensitivity to toxic insult, especially exposure to LPS and rotenone to determine if *DJ-1* mutation altered the astrocytic response.

Because the further staining and quantitative assessment remains to be done on the *in vivo* exposure of our *DJ-1*$^{-/-}$ mouse to MPTP, it would be remiss to draw too many conclusions at present. However, based upon our initial pathological assessments, it appears that no overt phenotype is present in our *DJ-1*$^{-/-}$ compared to *DJ-1*$^{+/+}$ mice. Both tended to have fluorojade reactivity at the perivascular area, specifically in cells thought to be endothelial based on location and morphology. Why fluorojade reactivity is not observed in neurons remains enigmatic, as it is a widely accepted marker of dying neurons, which we would anticipate observing following MPTP exposure. However, the finding that the endothelial cells, which maintain the glial-vascular interface, are affected might yield interesting results upon further investigation. No decrease in TH

immunoreactivity in the substantia nigra of our mice is problematic. However, the images depicted may belie the actual number of TH positive neurons present. In fact, it is postulated that the section stained for TH in *DJ-1*$^{+/+}$ mice treated with saline is not ideally cut through the substantia nigra, accounting for the particularly low immunoreactivity in this image. Therefore, further experiments ensuring more consistent sectioning through brain regions of interest are needed to compare not only MPTP- to saline-treated animals, but also any altered responsiveness due to mutation of *DJ-1*.

The locomotor data presented is difficult to interpret. First, no observed changes in any parameter assessed following exposure to MPTP is surprising. In a preliminary study, we followed the suggested MPTP dosing regime for C57Bl6 mice, administering 4x20mg/kg at 2-h intervals. In this study, the mortality rate for MPTP-treated mice was 100%. Therefore, we decreased our dosage to 2x20mg/kg at 6-h intervals and preformed another preliminary experiment. In this case, MPTP-treated animals were lethargic and disheveled by the second dosing, but all remained viable, indicating our mice tolerated this dose well. Furthermore, members of a neighboring laboratory successfully utilized 2x15mg/kg at 12-h intervals and were able to observe a parkinsonian phenotype in their animals. However, at 6 h following the initial injection (i.e., the second dose), the MPTP-treated animals did not appear affected by the injection. Specifically, based upon our experience, MPTP-treated mice tend to be somewhat lethargic and have a rather disheveled coat for the first 24 h after

exposure. However, these mice appeared normal at both 6 and 24 h following injection. To assure we actually had dissolved MPTP in our dosing vial, an aliquot was assessed via analytical chemical analysis, and MPTP was indeed present, although based upon our method of analysis, the concentration could not be determined. Therefore, the reason for the lack of locomotor decline in our MPTP-treated animals is unclear. One possibility is that our n value is too low to detect minute alterations. In some treatments, we only have three animals, and as normal individual variations will exist, it is possible we cannot detect any changes. Another possibility is that we received a vial of MPTP that was, for an unknown reason, non-reactive. For whatever reason, our animals did not respond with alterations in total distance traveled, vertical activity, or velocity.

Although many questions remain regarding the role of DJ-1 in physiology, a protein production so ubiquitously and involved neurological disorders, reproduction and carcinogenesis requires further investigation. In neurodegenerative research, most studies to date have focused on DJ-1 in neurons, however its role in astrocytes remains largely unknown. As astrocytes are critical in maintaining neuronal viability, especially through maintenance of the extracellular space shared with neurons, supplying antioxidants and nutrients, so compromised astrocyte function could deleteriously affect neuronal function and/or survival. Further, pathological reactive astrocytosis is shared by all neurological disorders listed above that DJ-1 is implicated in currently. Thus, elucidating the role of DJ-1 in astrocytes under normal conditions and during

gliosis is vitally important to understanding these diseases, and may provide new targets for therapeutic interdiction. Mutant DJ-1 mice are a useful means for elucidating the role(s) of this protein in a myriad of diseases as well as normal cellular homeostasis.

CHAPTER 2

TABLES AND FIGURES

MUTATION OF *DJ-1*

A

TCAGTGCAGTGCAGTCAGGGGCGGCAAGCCTCGGCTGANGACTCCCTGGCCTCCAGANA
AGTAGATCCCGGCNCTCTTACCAANGGCAAACCCAAAAGGGTCTTTGANCANCAGAGGA
CAGTCAGGAATTCACGGAAATGTGAATACTCNTACTCTTCGGGTACTGTGGGGACGANG
GTAAAGTGACTGCAAGGGTG

Underlined: Exogenous vector sequences
Boxed: Endogenous *DJ-1* sequence, intron 6

B

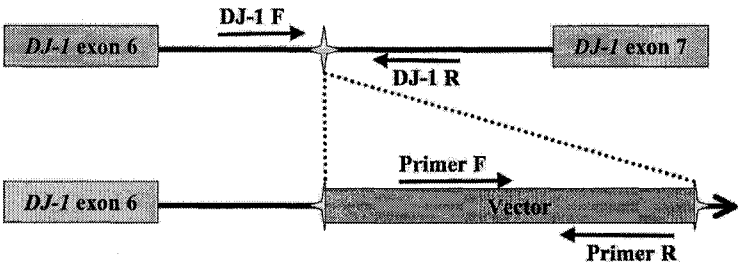

C

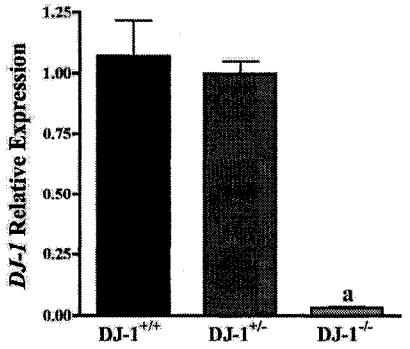

D

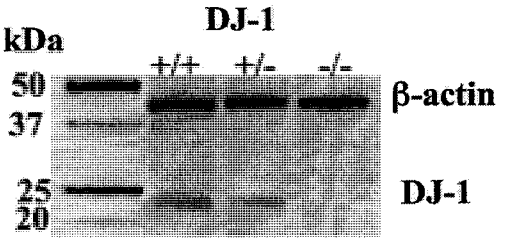

Figure 2.1. Insertion of a gene-trap vector induces a mutation in *DJ-1*. (A) Sequence data demonstrating the location of the gene-trap vector. The underlined sequence corresponds with the gene-trap vector, the boxed sequence aligns with sequence from *DJ-1* intron 6, and font in plain text is intermediate sequence not aligning with either the vector or *DJ-1*. (B) Graphical representation of the gene-trap vector and genotyping primers. (C) Real-time PCR demonstrates virtual elimination of *DJ-1* expression in brain tissue of *DJ-1*$^{-/-}$ mice. (D) Western blot analysis of brain protein reveals no DJ-1 is produced in *DJ-1*$^{-/-}$ brain tissue.

DJ-1 TISSUE DISTRIBUTION

A

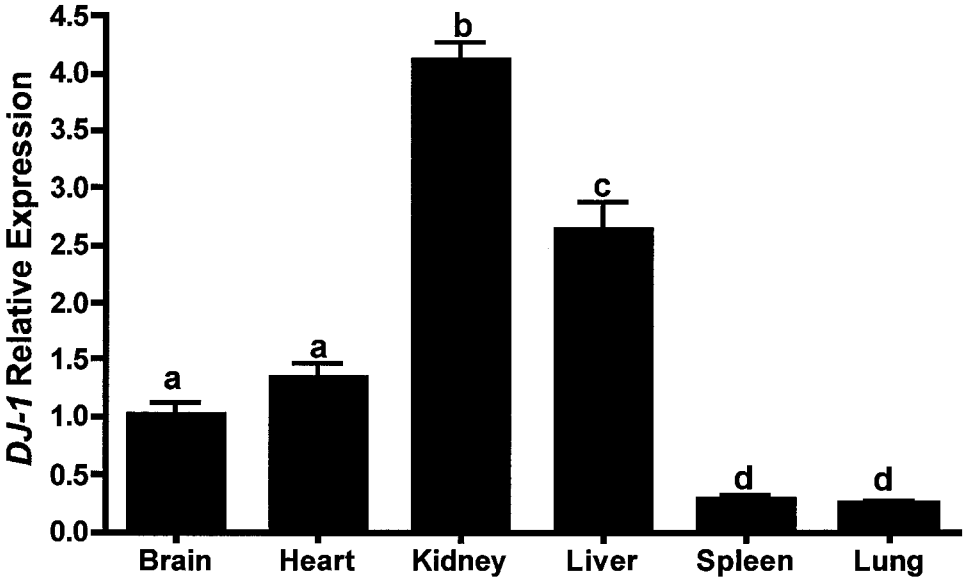

B

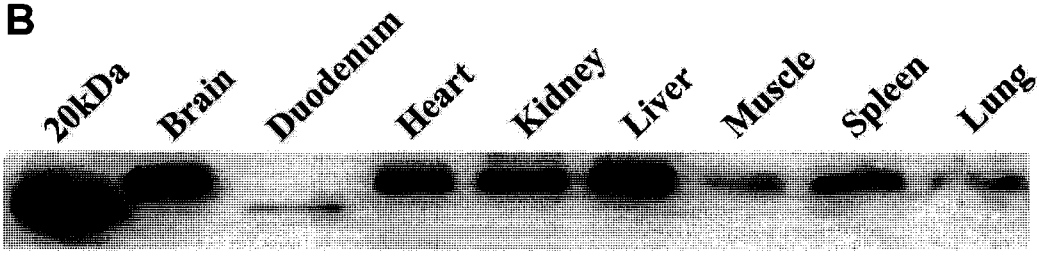

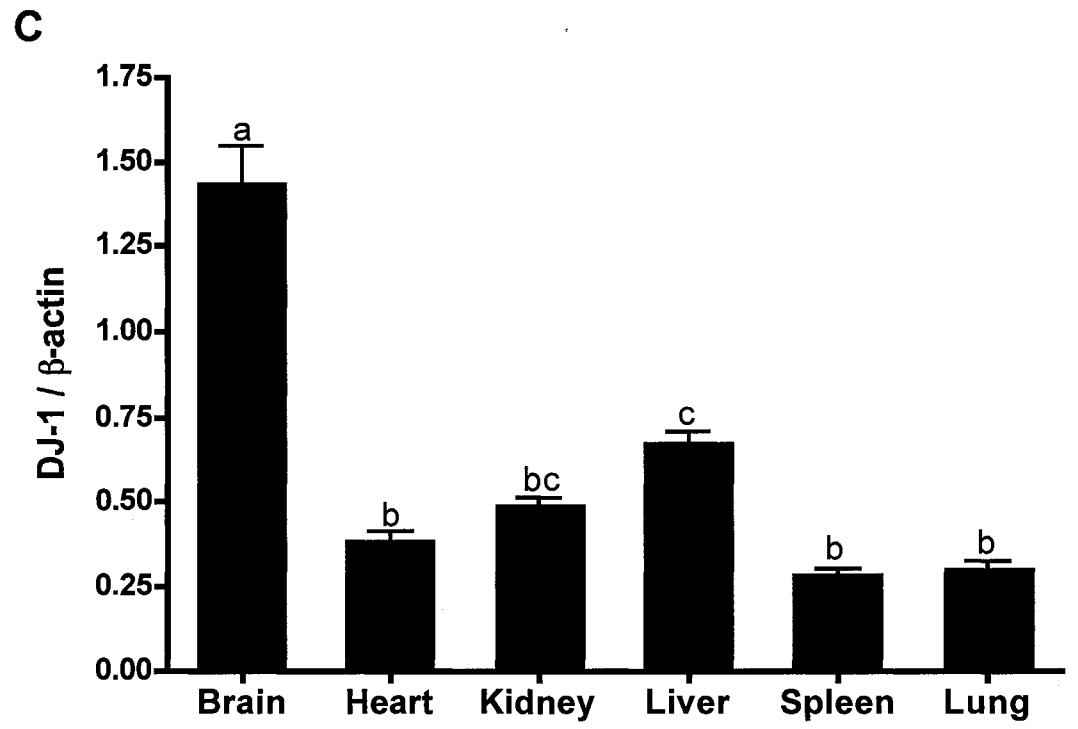

Figure 2.2. DJ-1 protein is widely distribution in the mouse. (A) Real-time PCR analysis of *DJ-1* in various tissues normalized to expression of *β-actin* reveals wide tissue expression, especially in the kidney and liver (n=5, $p<0.05$) (B) A representative blot depicts relative expression of DJ-1 in 25 μg of protein from each respective tissue. (C) DJ-1 protein levels were assayed and are expressed relative to β-actin in each tissue ($n \geq 4$), and demonstrate high production in brain tissue. Bars with differing letters are significantly different from one another ($p < 0.05$).

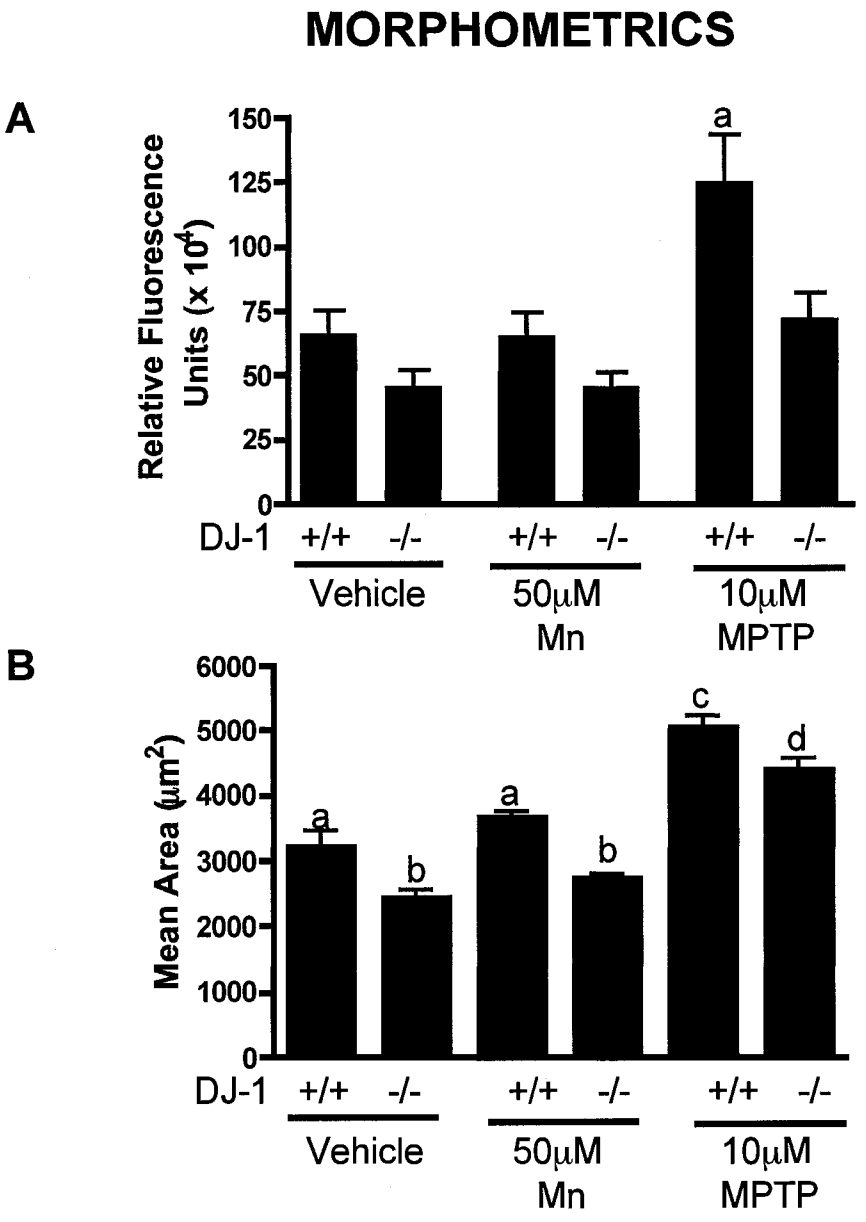

Figure 2.3. Morphometric analysis of *DJ-1*$^{+/+}$ and *DJ-1*$^{-/-}$ astrocytes. Primary cortical astrocytes were exposed to 50μM manganese or 10μM MPTP for 24h, and then immunochemically probed for expression of GFAP. Individual cell morphometric analysis was accomplished using SlideBook. (A). Relative expression of GFAP in astrocytes increases only in *DJ-1*$^{+/+}$ cells exposed to MPTP ($p<0.05$, $n\geq47$). (B). Mean cell area increases in all cells exposed to MPTP, but not manganese. *DJ-1*$^{-/-}$ astrocytes were smaller than *DJ-1*$^{+/+}$ cells ($p<0.05$, $n\geq47$), regardless of treatment, however mean cell area increased more dramatically (44%) in *DJ-1*$^{-/-}$ cells versus *DJ-1*$^{+/+}$ astrocytes (36%).

MITOCHONDRIAL LOCALIZATION

A

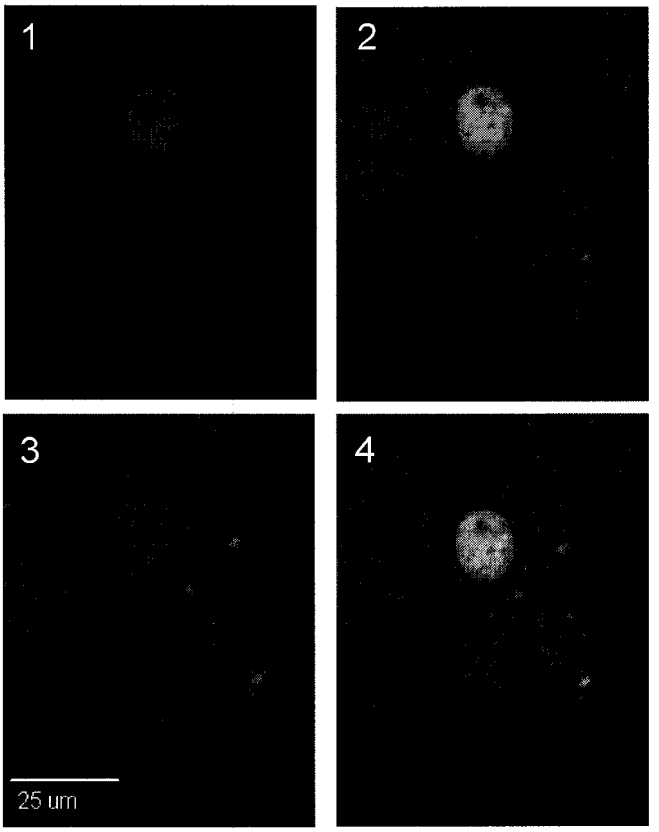

B: DJ-1 Localization to the Mitochondria

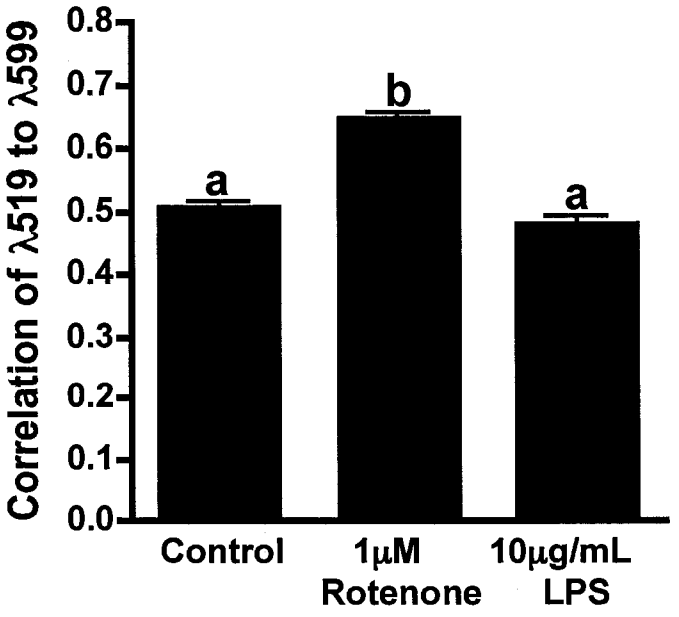

C: Localization of DJ-1 to the Nucleus

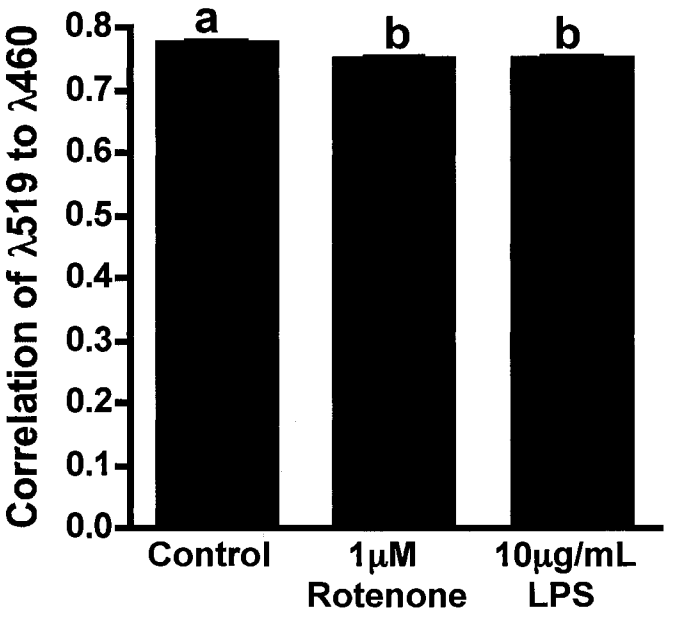

D: DJ-1 Localization to Mitochondria

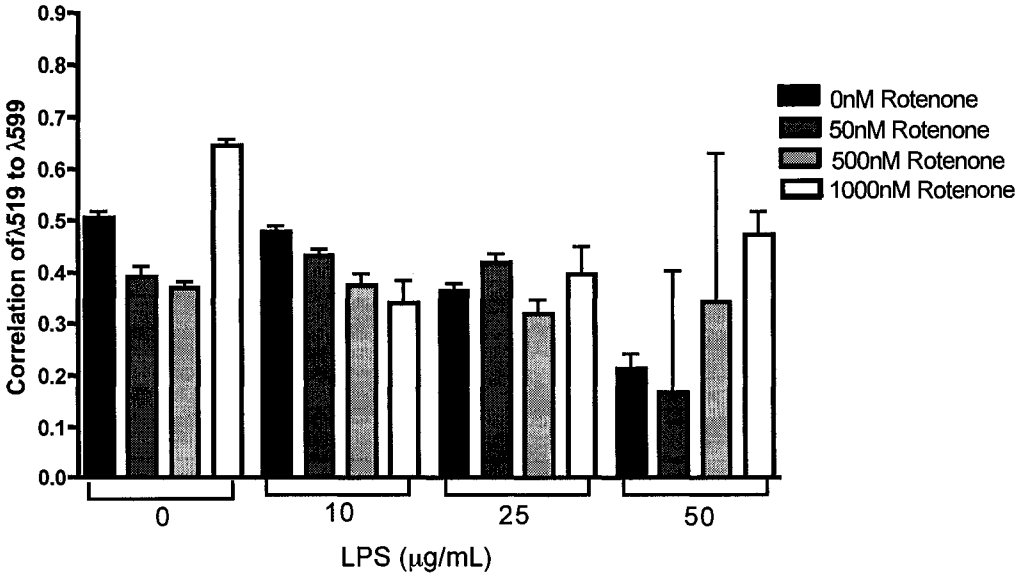

E: DJ-1 Localization to Nuclei

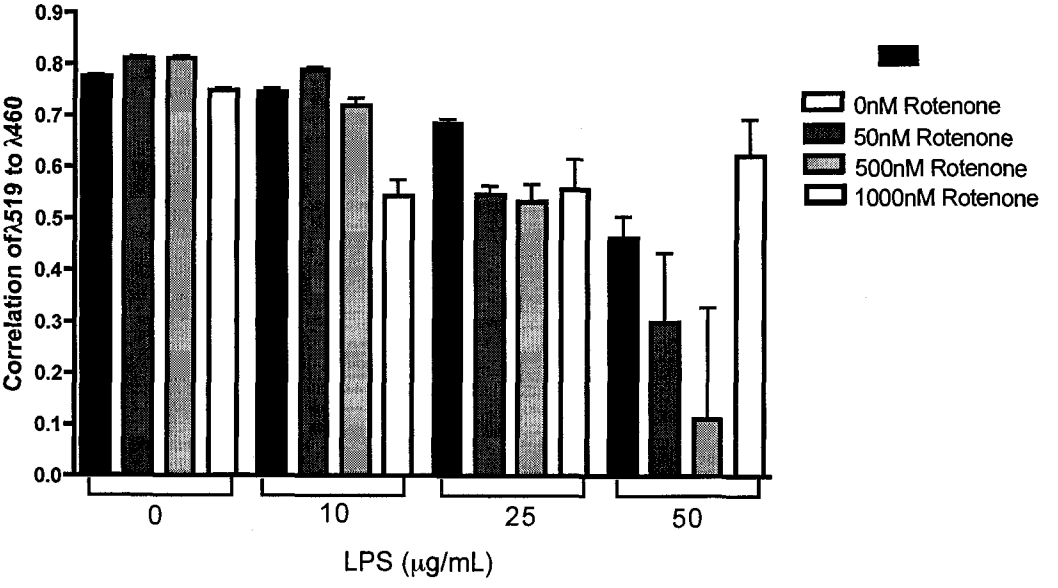

F: Percent cells counted

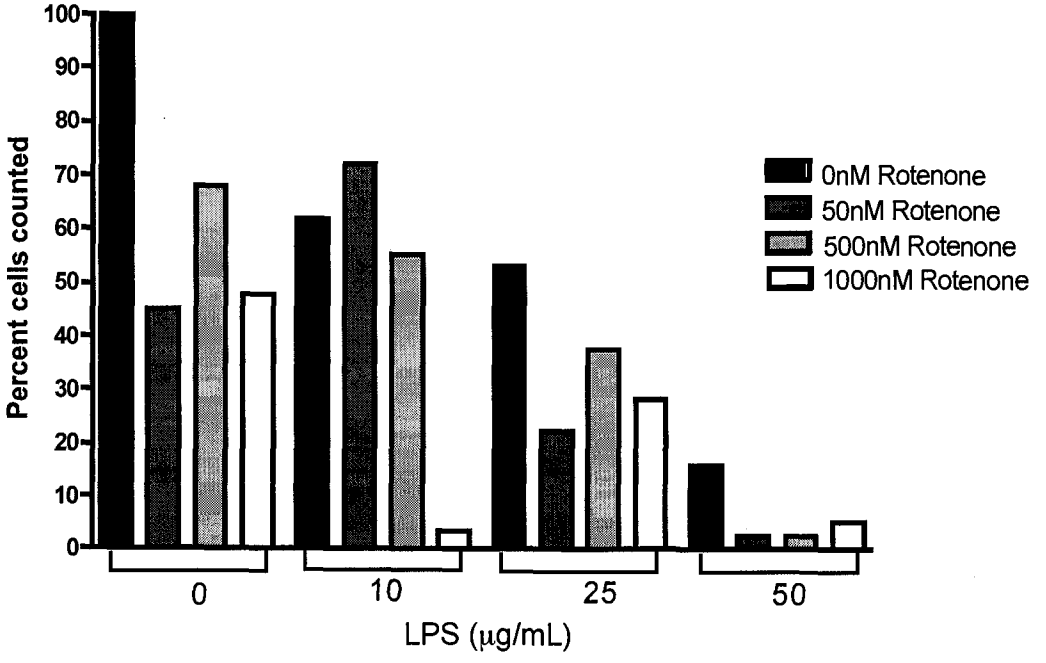

Figure 2.4. DJ-1 localization to the mitochondria or nucleus in primary cortical astrocytes following exposure to LPS for 72h, then exposed for 24h to rotenone. Astrocytes were treated with 0, 10, 25, or 50 μg/mL LPS for 72h, then treatments were removed and cells were washed with PBS. New media was added containing 0, 50, 500, or 1000nM rotenone, and cells were exposed for 24h. DJ-1 was detected via immunofluorescence in MitoTracker-loaded cells. Mounting media contains a DAPI-stain to detect nuclei. Pearson's correlation coefficients were calculated using SlideBook software image analysis. (A) Representative images of (A1) DAPI staining, (A2) DJ-1 immunofluorescence, (A3) MitoTracker, and (A4) merged image of all 3. (B, D) Correlation of DJ-1 to MitoTracker, (C, E) correlation of DJ-1 to DAPI, and (F) percent cells analyzed compared to control values.

Table 2.1. Tukey's multiple comparisons test of DJ-1 and MitoTracker correlation coefficients. ANOVA values reveal statistical differences in astrocytes exposed to 0, 10, 25, or 50 μg/mL LPS for 72 h followed by 24h exposure to 0, 50, 500, or 1000nM rotenone, then probed for DJ-1 in MitoTracker-loaded cells.

Trt		Trt	P value		Trt		Trt	P value
0 LPS 0 R	vs.	0 LPS 50 R	P < 0.001		10 LPS 50 R	vs.	10 LPS 500 R	P > 0.05
		0 LPS 500 R	P < 0.001				10 LPS 1000 R	P > 0.05
		0 LPS 1000 R	P < 0.001				25 LPS 0 R	P > 0.05
		10 LPS 0 R	P > 0.05				25 LPS 50 R	P > 0.05
		10 LPS 50 R	P < 0.05				25 LPS 500 R	P < 0.01
		10 LPS 500 R	P < 0.001				25 LPS 1000 R	P > 0.05
		10 LPS 1000 R	P > 0.05				50 LPS 0 R	P < 0.001
		25 LPS 0 R	P < 0.001				50 LPS 50 R	P > 0.05
		25 LPS 50 R	P > 0.05				50 LPS 500 R	P > 0.05
		25 LPS 500 R	P < 0.001				50 LPS 1000 R	P > 0.05
		25 LPS 1000 R	P < 0.05		10 LPS 500 R	vs.	10 LPS 1000 R	P > 0.05
		50 LPS 0 R	P < 0.001				25 LPS 0 R	P > 0.05
		50 LPS 50 R	P < 0.01				25 LPS 50 R	P > 0.05
		50 LPS 500 R	P > 0.05				25 LPS 500 R	P > 0.05
		50 LPS 1000 R	P > 0.05				25 LPS 1000 R	P > 0.05
0 LPS 50 R	vs.	0 LPS 500 R	P > 0.05				50 LPS 0 R	P < 0.01
		0 LPS 1000 R	P < 0.001				50 LPS 50 R	P > 0.05
		10 LPS 0 R	P > 0.05				50 LPS 500 R	P > 0.05
		10 LPS 50 R	P > 0.05				50 LPS 1000 R	P > 0.05
		10 LPS 500 R	P > 0.05		10 LPS 1000 R	vs.	25 LPS 0 R	P > 0.05
		10 LPS 1000 R	P > 0.05				25 LPS 50 R	P > 0.05
		25 LPS 0 R	P > 0.05				25 LPS 500 R	P > 0.05
		25 LPS 50 R	P > 0.05				25 LPS 1000 R	P > 0.05
		25 LPS 500 R	P > 0.05				50 LPS 0 R	P > 0.05
		25 LPS 1000 R	P > 0.05				50 LPS 50 R	P > 0.05
		50 LPS 0 R	P < 0.01				50 LPS 500 R	P > 0.05
		50 LPS 50 R	P > 0.05				50 LPS 1000 R	P > 0.05
		50 LPS 500 R	P > 0.05		25 LPS 0 R	vs.	25 LPS 50 R	P > 0.05
		50 LPS 1000 R	P > 0.05				25 LPS 500 R	P > 0.05
0 LPS 500 R	vs.	0 LPS 1000 R	P < 0.001				25 LPS 1000 R	P > 0.05
		10 LPS 0 R	P < 0.001				50 LPS 0 R	P < 0.05

Trt		Trt	P value		Trt		Trt	P value
0 LPS 500 R	vs.	10 LPS 50 R	P > 0.05		25 LPS 0 R	vs.	50 LPS 50 R	P > 0.05
		10 LPS 500 R	P > 0.05				50 LPS 500 R	P > 0.05
		10 LPS 1000 R	P > 0.05				50 LPS 1000 R	P > 0.05
		25 LPS 0 R	P > 0.05		25 LPS 50 R	vs.	25 LPS 500 R	P > 0.05
		25 LPS 50 R	P > 0.05				25 LPS 1000 R	P > 0.05
		25 LPS 500 R	P > 0.05				50 LPS 0 R	P < 0.001
		25 LPS 1000 R	P > 0.05				50 LPS 50 R	P > 0.05
		50 LPS 0 R	P < 0.01				50 LPS 500 R	P > 0.05
		50 LPS 50 R	P > 0.05				50 LPS 1000 R	P > 0.05
		50 LPS 500 R	P > 0.05		25 LPS 500 R	vs.	25 LPS 1000 R	P > 0.05
		50 LPS 1000 R	P > 0.05				50 LPS 0 R	P > 0.05
0 LPS 1000 R	vs.	10 LPS 0 R	P < 0.001				50 LPS 50 R	P > 0.05
		10 LPS 50 R	P < 0.001				50 LPS 500 R	P > 0.05
		10 LPS 500 R	P < 0.001				50 LPS 1000 R	P > 0.05
		10 LPS 1000 R	P < 0.05		25 LPS 1000 R	vs.	50 LPS 0 R	P < 0.01
		25 LPS 0 R	P < 0.001				50 LPS 50 R	P > 0.05
		25 LPS 50 R	P < 0.001				50 LPS 500 R	P > 0.05
		25 LPS 500 R	P < 0.001				50 LPS 1000 R	P > 0.05
		25 LPS 1000 R	P < 0.001		50 LPS 0 R	vs.	50 LPS 50 R	P > 0.05
		50 LPS 0 R	P < 0.001				50 LPS 500 R	P > 0.05
		50 LPS 50 R	P < 0.001				50 LPS 1000 R	P < 0.05
		50 LPS 500 R	P < 0.05		50 LPS 50 R	vs.	50 LPS 500 R	P > 0.05
		50 LPS 1000 R	P > 0.05				50 LPS 1000 R	P > 0.05
10 LPS 0 R	vs.	10 LPS 50 Ro	P > 0.05		50 LPS 500 R	vs.	50 LPS 1000 R	P > 0.05
		10 LPS 500 R	P < 0.01					
		10 LPS 1000 R	P > 0.05					
		25 LPS 0 R	P < 0.01					
		25 LPS 50 R	P > 0.05					
		25 LPS 500 R	P < 0.001					
		25 LPS 1000 R	P > 0.05					
		50 LPS 0 R	P < 0.001					
		50 LPS 50 R	P < 0.05					
		50 LPS 500 R	P > 0.05					
		50 LPS 1000 R	P > 0.05					

Table 2.2. Tukey's multiple comparisons test of DJ-1 and DAPI correlation coefficients. ANOVA values reveal statistical differences in astrocytes exposed to 0, 10, 25, or 50 μg/mL LPS for 72 h followed by 24h exposure to 0, 50, 500, or 1000nM rotenone, then probed for DJ-1 and mounted in DAPI-containing medium.

Trt		Trt	P value		Trt		Trt	P value
0 LPS 0 R	vs.	0 LPS 50 R	P > 0.05		10 LPS 50 R	vs.	10 LPS 500 R	P > 0.05
		0 LPS 500 R	P > 0.05				10 LPS 1000 R	P > 0.05
		0 LPS 1000 R	P > 0.05				25 LPS 0 R	P < 0.01
		10 LPS 0 R	P > 0.05				25 LPS 50 R	P < 0.001
		10 LPS 50 R	P > 0.05				25 LPS 500 R	P < 0.001
		10 LPS 500 R	P > 0.05				25 LPS 1000 R	P < 0.001
		10 LPS 1000 R	P > 0.05				50 LPS 0 R	P < 0.001
		25 LPS 0 R	P < 0.05				50 LPS 50 R	P < 0.001
		25 LPS 50 R	P < 0.001				50 LPS 500 R	P < 0.001
		25 LPS 500 R	P < 0.001				50 LPS 1000 R	P > 0.05
		25 LPS 1000 R	P < 0.001		10 LPS 500 R	vs.	10 LPS 1000 R	P > 0.05
		50 LPS 0 R	P < 0.001				25 LPS 0 R	P > 0.05
		50 LPS 50 R	P < 0.001				25 LPS 50 R	P < 0.001
		50 LPS 500 R	P < 0.001				25 LPS 500 R	P < 0.001
		50 LPS 1000 R	P > 0.05				25 LPS 1000 R	P < 0.001
0 LPS 50 R	vs.	0 LPS 500 R	P > 0.05				50 LPS 0 R	P < 0.001
		0 LPS 1000 R	P > 0.05				50 LPS 50 R	P < 0.001
		10 LPS 0 R	P > 0.05				50 LPS 500 R	P < 0.001
		10 LPS 50 R	P > 0.05				50 LPS 1000 R	P > 0.05
		10 LPS 500 R	P > 0.05		10 LPS 1000 R	vs.	25 LPS 0 R	P > 0.05
		10 LPS 1000 R	P > 0.05				25 LPS 50 R	P > 0.05
		25 LPS 0 R	P < 0.01				25 LPS 500 R	P > 0.05
		25 LPS 50 R	P < 0.001				25 LPS 1000 R	P > 0.05
		25 LPS 500 R	P < 0.001				50 LPS 0 R	P > 0.05
		25 LPS 1000 R	P < 0.001				50 LPS 50 R	P > 0.05
		50 LPS 0 R	P < 0.001				50 LPS 500 R	P < 0.05
		50 LPS 50 R	P < 0.001				50 LPS 1000 R	P > 0.05
		50 LPS 500 R	P < 0.001		25 LPS 0 R	vs.	25 LPS 50 R	P < 0.05
		50 LPS 1000 R	P > 0.05				25 LPS 500 R	P < 0.001
0 LPS 500 R	vs.	0 LPS 1000 R	P > 0.05				25 LPS 1000 R	P < 0.05
		10 LPS 0 R	P > 0.05				50 LPS 0 R	P < 0.001
		10 LPS 50 R	P > 0.05				50 LPS 50 R	P < 0.01

Trt		Trt	P value		Trt		Trt	P value
0 LPS 500 R	vs.	10 LPS 500 R	P < 0.05		25 LPS 0 R	vs.	50 LPS 500 R	P < 0.001
		10 LPS 1000 R	P > 0.05				50 LPS 1000 R	P > 0.05
		25 LPS 0 R	P < 0.001		25 LPS 50 R	vs.	25 LPS 500 R	P > 0.05
		25 LPS 50 R	P < 0.001				25 LPS 1000 R	P > 0.05
		25 LPS 500 R	P < 0.001				50 LPS 0 R	P > 0.05
		25 LPS 1000 R	P < 0.001				50 LPS 50 R	P > 0.05
		50 LPS 0 R	P < 0.001				50 LPS 500 R	P < 0.001
		50 LPS 50 R	P < 0.001				50 LPS 1000 R	P > 0.05
		50 LPS 500 R	P < 0.001		25 LPS 500 R	vs.	25 LPS 1000 R	P > 0.05
		50 LPS 1000 R	P > 0.05				50 LPS 0 R	P > 0.05
0 LPS 1000 R	vs.	10 LPS 0 R	P > 0.05				50 LPS 50 R	P > 0.05
		10 LPS 50 R	P > 0.05				50 LPS 500 R	P < 0.001
		10 LPS 500 R	P > 0.05				50 LPS 1000 R	P > 0.05
		10 LPS 1000 R	P > 0.05		25 LPS 1000 R	vs.	50 LPS 0 R	P > 0.05
		25 LPS 0 R	P > 0.05				50 LPS 50 R	P > 0.05
		25 LPS 50 R	P < 0.001				50 LPS 500 R	P < 0.001
		25 LPS 500 R	P < 0.001				50 LPS 1000 R	P > 0.05
		25 LPS 1000 R	P < 0.001		50 LPS 0 R	vs.	50 LPS 50 R	P > 0.05
		50 LPS 0 R	P < 0.001				50 LPS 500 R	P < 0.05
		50 LPS 50 R	P < 0.001				50 LPS 1000 R	P > 0.05
		50 LPS 500 R	P < 0.001		50 LPS 50 R	vs.	50 LPS 500 R	P > 0.05
		50 LPS 1000 R	P > 0.05				50 LPS 1000 R	P > 0.05
10 LPS 0 R	vs.	10 LPS 50 Ro	P > 0.05		50 LPS 500 R	vs.	50 LPS 1000 R	P < 0.001
		10 LPS 500 R	P > 0.05					
		10 LPS 1000 R	P > 0.05					
		25 LPS 0 R	P > 0.05					
		25 LPS 50 R	P < 0.001					
		25 LPS 500 R	P < 0.001					
		25 LPS 1000 R	P < 0.001					
		50 LPS 0 R	P < 0.001					
		50 LPS 50 R	P < 0.001					
		50 LPS 500 R	P < 0.001					
		50 LPS 1000 R	P > 0.05					

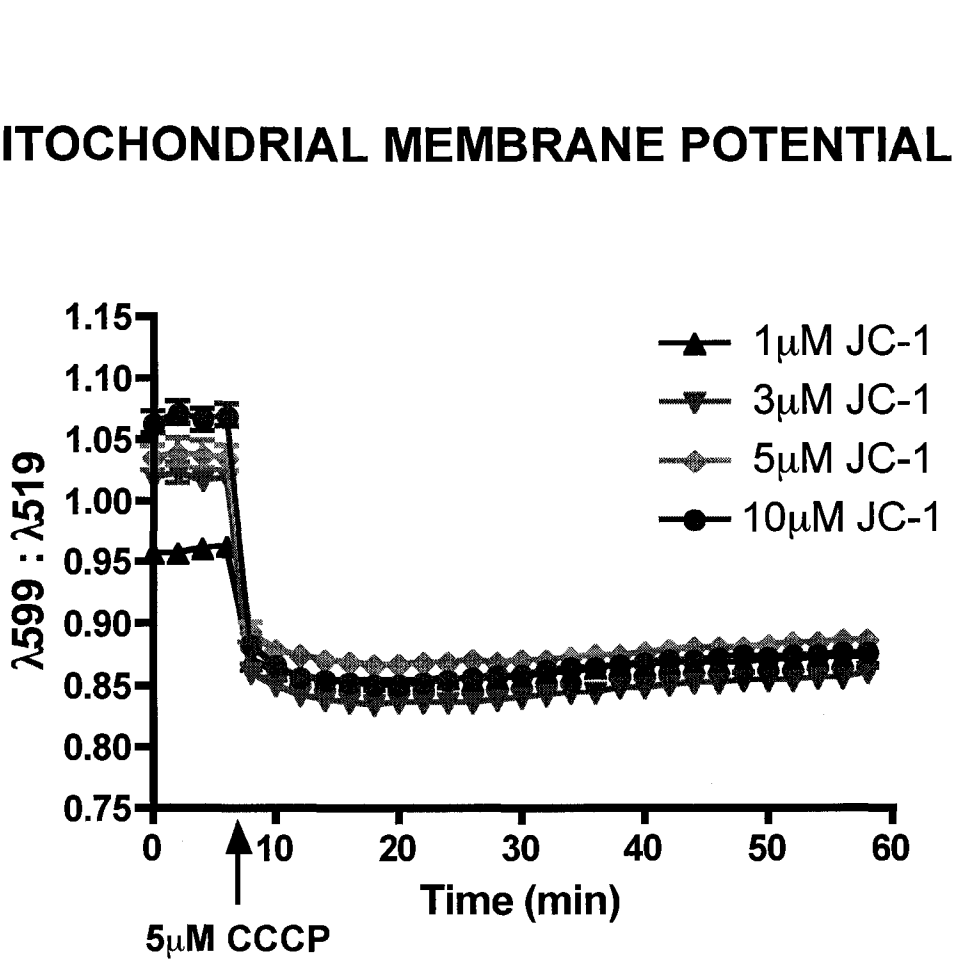

Figure 2.5. Time-lapse of varying doses of JC-1 exposed to the mitochondrial uncoupler CCCP. Primary cortical astrocytes were loaded with 1, 3, 5, or 10μM of the ratiometric mitochondrial dye JC-1 for 20 min at 37°C. After baseline sampling (8 min), 5μM carbonyl cyanide 3-chlorophenylhydrazone (CCCP) was added, and the red to green (λ599:λ519) ratio was examined. Immediately following exposure to CCCP, all concentrations of JC-1 exhibited a significant decline in λ599:λ519, indicating a robust depolarization that continued for the duration of sampling (60 min).

A


1
2
3

B

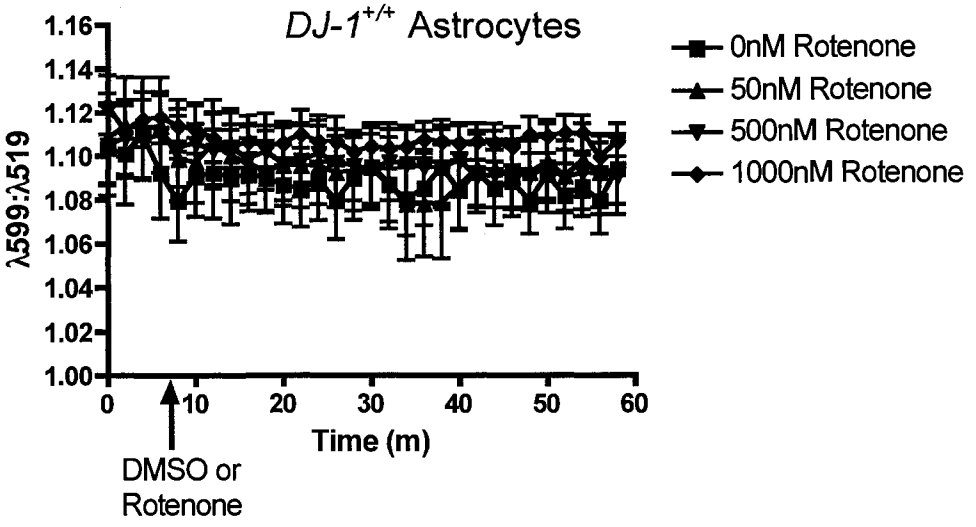
DJ-1+/+ Astrocytes
0nM Rotenone
50nM Rotenone
500nM Rotenone
1000nM Rotenone
λ599:λ519
1.16
1.14
1.12
1.10
1.08
1.06
1.04
1.02
1.00
0
10
20
30
40
50
60
Time (m)
DMSO or
Rotenone

C

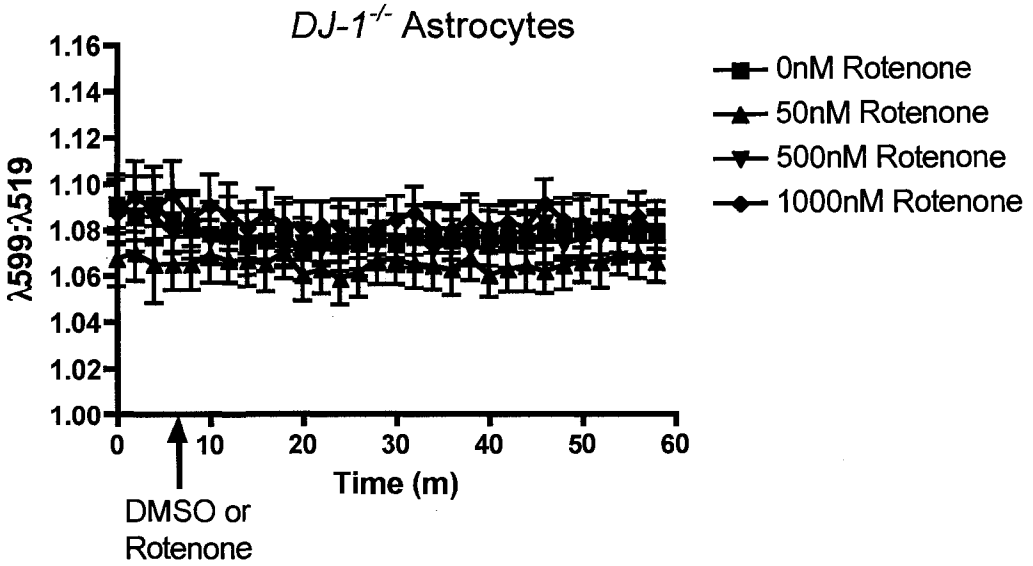
DJ-1-/- Astrocytes
0nM Rotenone
50nM Rotenone
500nM Rotenone
1000nM Rotenone
λ599:λ519
1.16
1.14
1.12
1.10
1.08
1.06
1.04
1.02
1.00
0
10
20
30
40
50
60
Time (m)
DMSO or
Rotenone

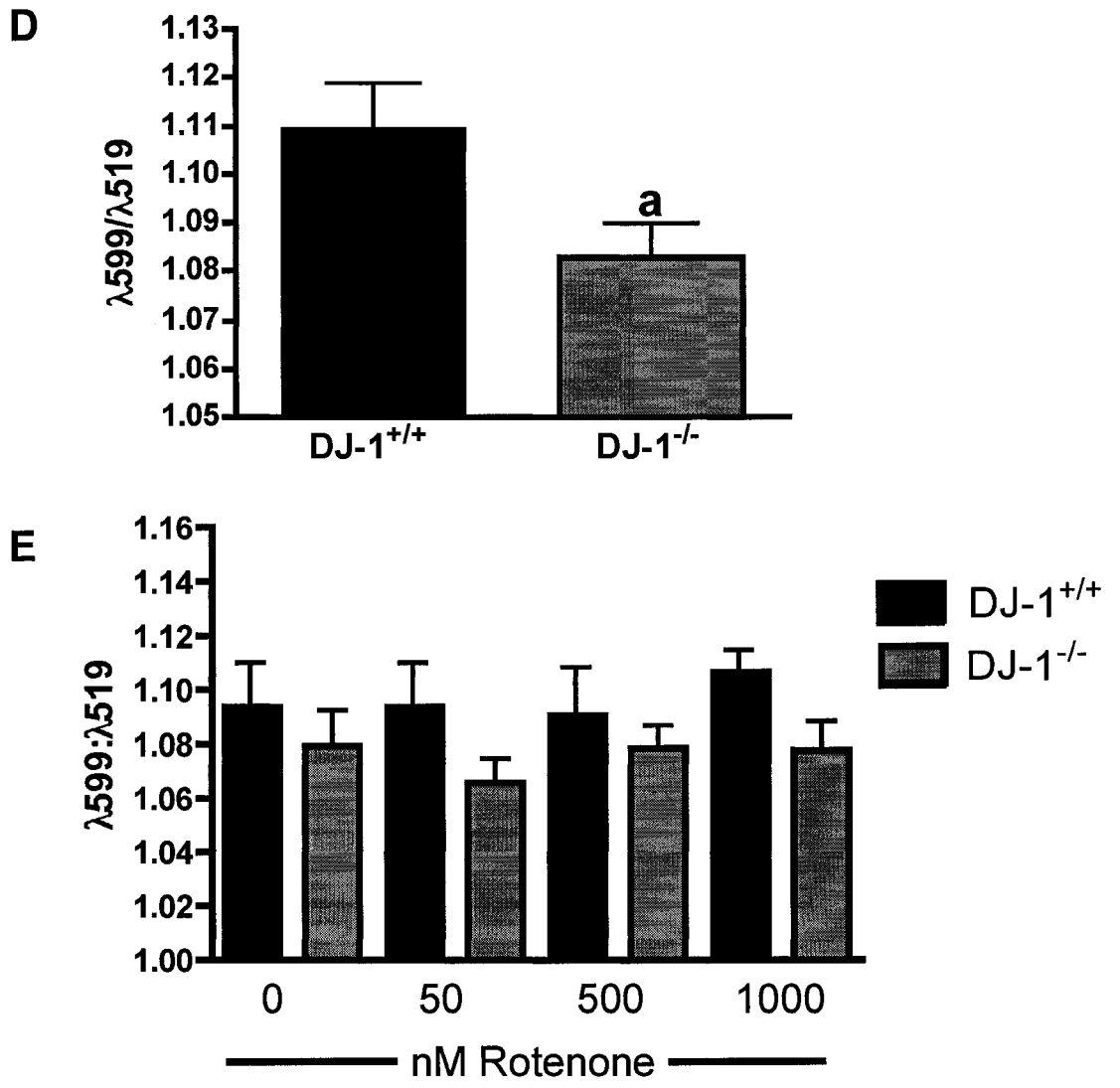

Figure 2.6. Resting mitochondrial membrane potential is decreased in *DJ-1*$^{-/-}$ astrocytes. Cells were loaded with 5μM JC-1 for 20 min at 37°C, and the ratio of λ599:λ519 over time (A). After baseline sampling, 0, 50, 500, or 1000nM rotenone was added in (B) *DJ-1*$^{+/+}$ and (C) *DJ-1*$^{-/-}$ astrocytes. (D) Initial membrane polarization in *DJ-1*$^{+/+}$ astrocytes is higher than in *DJ-1*$^{-/-}$ cells (n=48, p=0.02). (E) Final mitochondrial membrane potential was similar in both *DJ-1*$^{+/+}$ and *DJ-1*$^{-/-}$ astrocytes following addition of 0, 50, 500, or 1000nM rotenone (p>0.05, n=12).

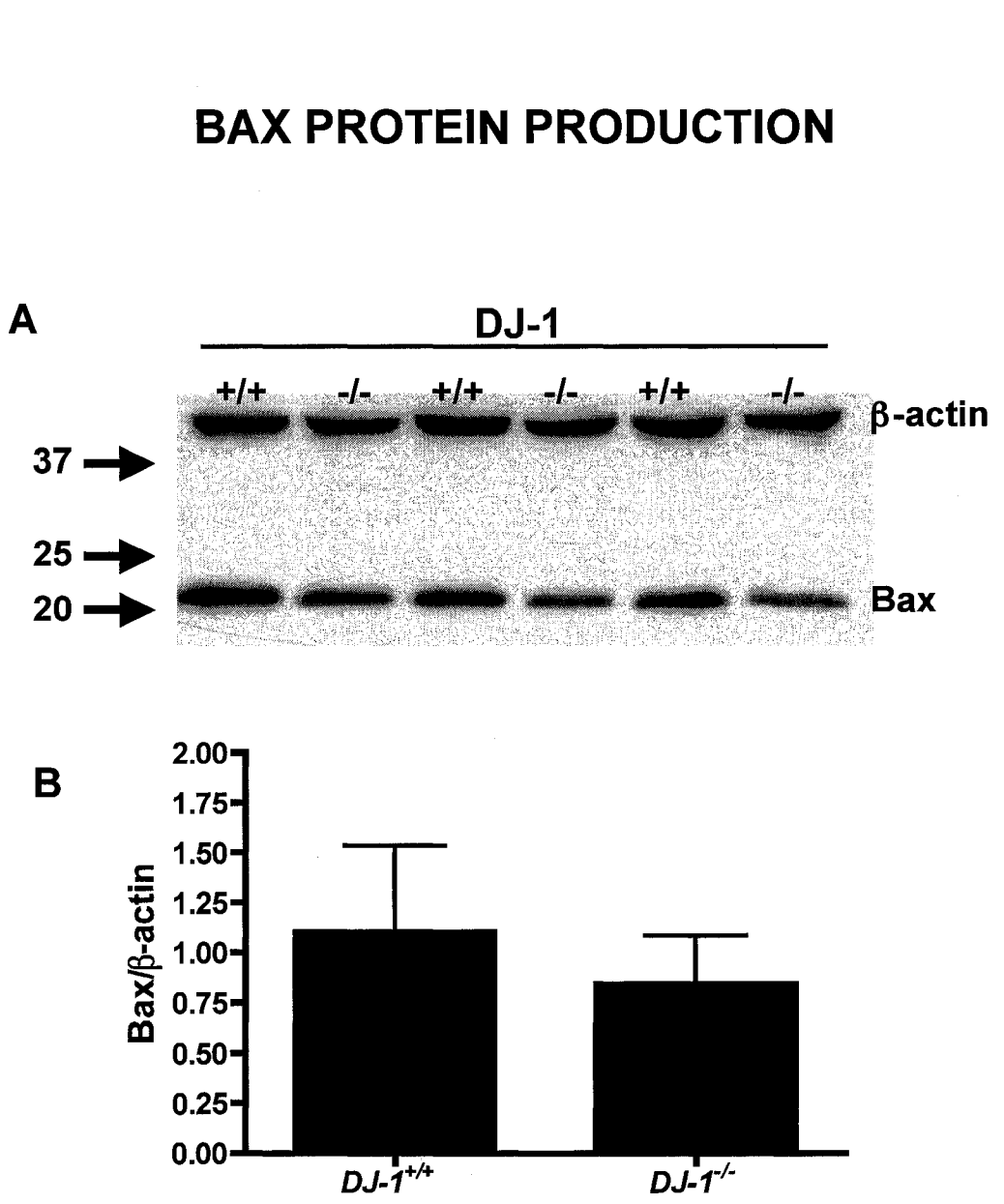

Figure 2.7. Bax production is similar in *DJ-1*$^{+/+}$ and *DJ-1*$^{-/-}$ astrocytes. Protein was isolated from primary astrocytes, and production of both Bax and β-actin was detected via Western blotting (A). Densitometry reveals no significant difference in Bax production in cells with mutation of *DJ-1* (B, p=0.62).

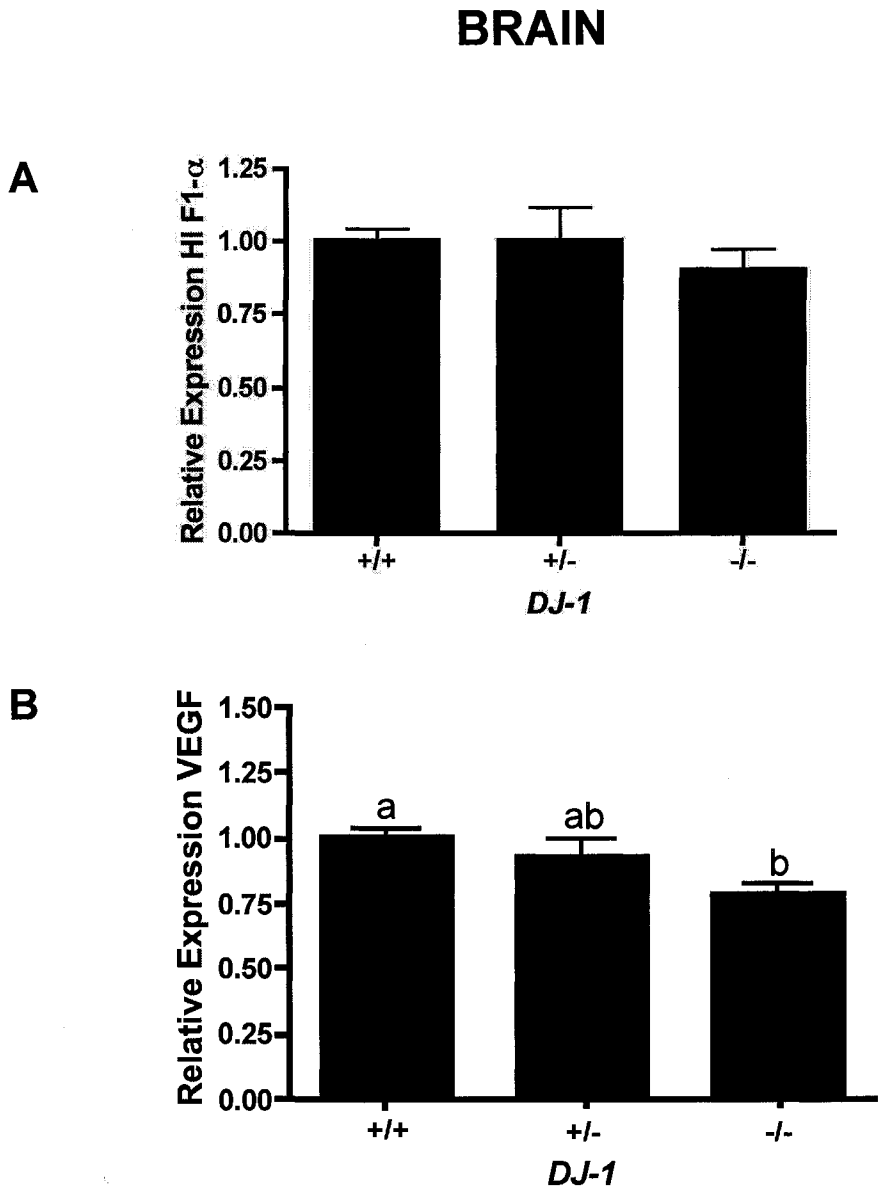

Figure 2.8. In brain tissue, expression of *HIF1α* does not change due to mutation of *DJ-1*, however *VEGF* expression significantly declines. RNA isolated from *DJ-1*$^{+/+}$ or *DJ-1*$^{-/-}$ tissues (n=5) were analyzed for expression of *HIF1α* and *VEGF* via real-time PCR. (A) No genotype-specific alterations in *HIF1α* expression occurred. (B) In contrast, expression of *VEGF* significantly decrease in the brain of *DJ-1*$^{-/-}$ animals (p=0.003).

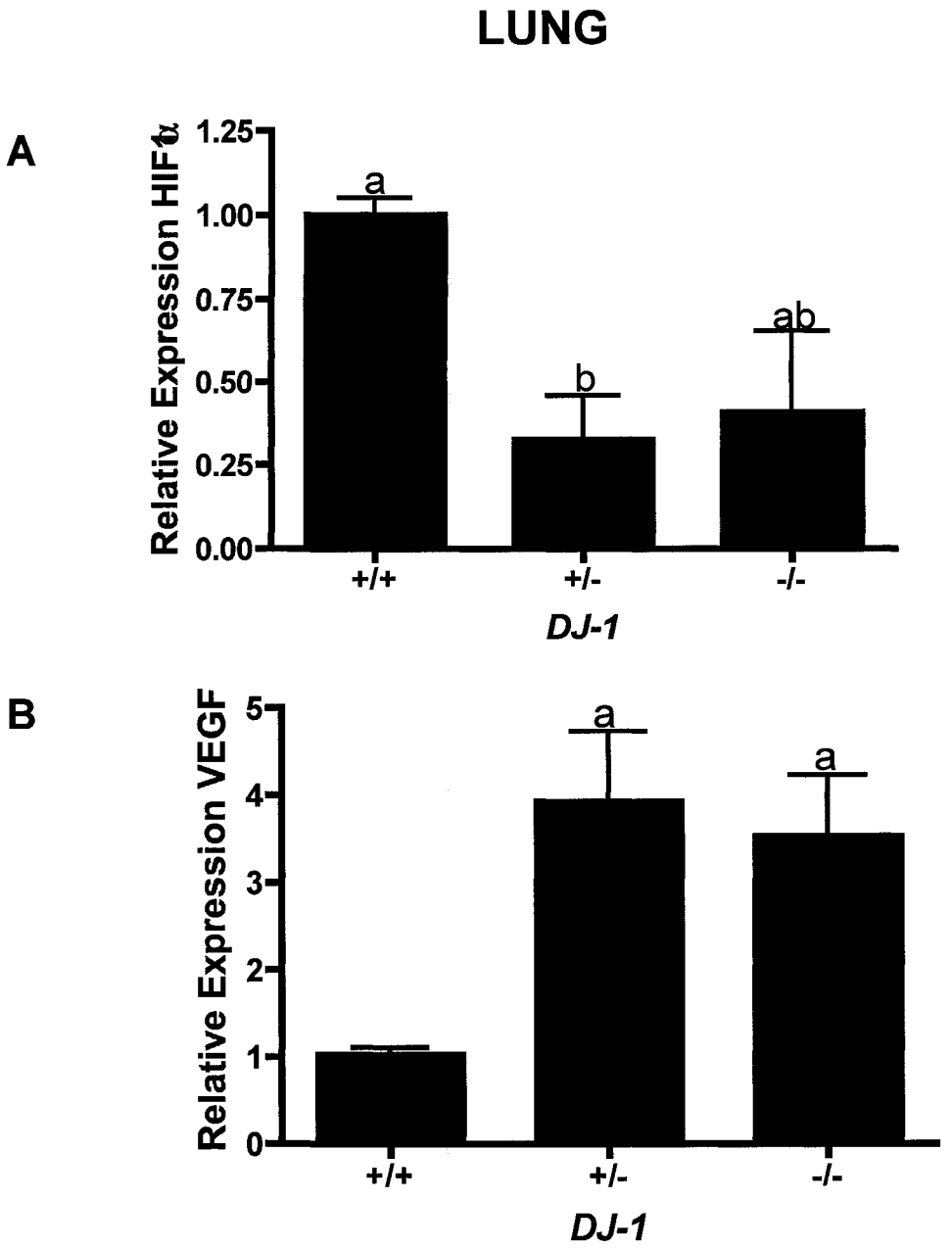

Figure 2.9. In the lung, cells with one or two copies of mutated *DJ-1* have increased VEGF expression, and *DJ-1*$^{+/-}$ tissues have decreased HIF1α expression. RNA isolated from *DJ-1*$^{+/+}$ or *DJ-1*$^{-/-}$ tissues (n=5) were analyzed for expression of *HIF1α* and *VEGF* via real-time PCR. (A) Expression of HIF1α is significantly lower in *DJ-1*$^{+/-}$ lung tissue compared to *DJ-1*$^{+/+}$(p<0.05), and tended to be lower in *DJ-1*$^{-/-}$ tissue (p=0.07). (B) Expression of VEGF is significantly higher in *DJ-1*$^{+/-}$ and *DJ-1*$^{-/-}$ lung tissue (p<0.05).

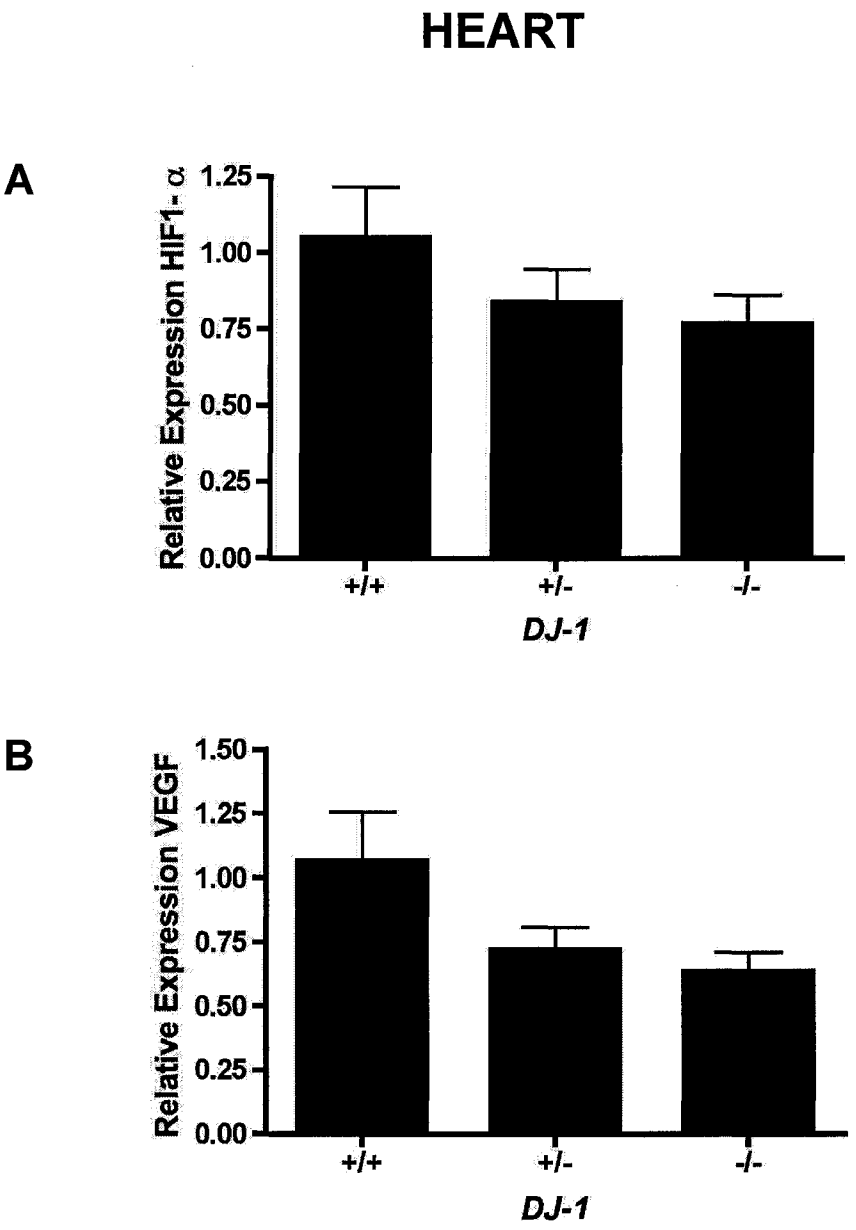

Figure 2.10. In heart tissue, neither *HIF1α* nor *VEGF* expression changed due to mutation of *DJ-1*. RNA isolated from *DJ-1*$^{+/+}$ or *DJ-1*$^{-/-}$ tissues (n=5) were analyzed for expression of *HIF1α* and *VEGF* via real-time PCR. (A) No genotype-specific alterations in *HIF1α* expression, or (B) *VEGF* expression occurred, though *DJ-1*$^{+/+}$ tissue tends to be higher than *DJ-1*$^{-/-}$ heart tissue (p=0.09).

KIDNEY

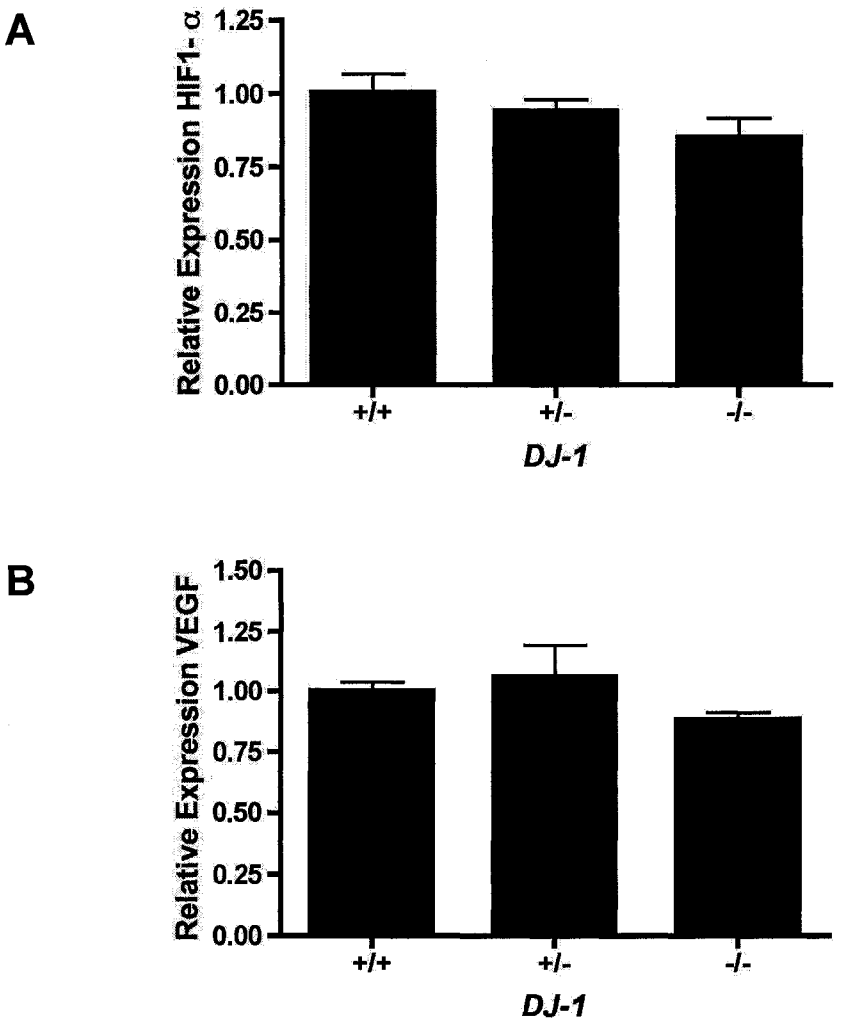

Figure 2.11. In the kidney, neither *HIF1α* nor *VEGF* expression changed due to mutation of *DJ-1*. RNA isolated from *DJ-1*$^{+/+}$ or *DJ-1*$^{-/-}$ tissues (n=5) were analyzed for expression of *HIF1α* and *VEGF* via real-time PCR. (A) No genotype-specific alterations in *HIF1α* expression, or (B) *VEGF* expression occurred.

LIVER

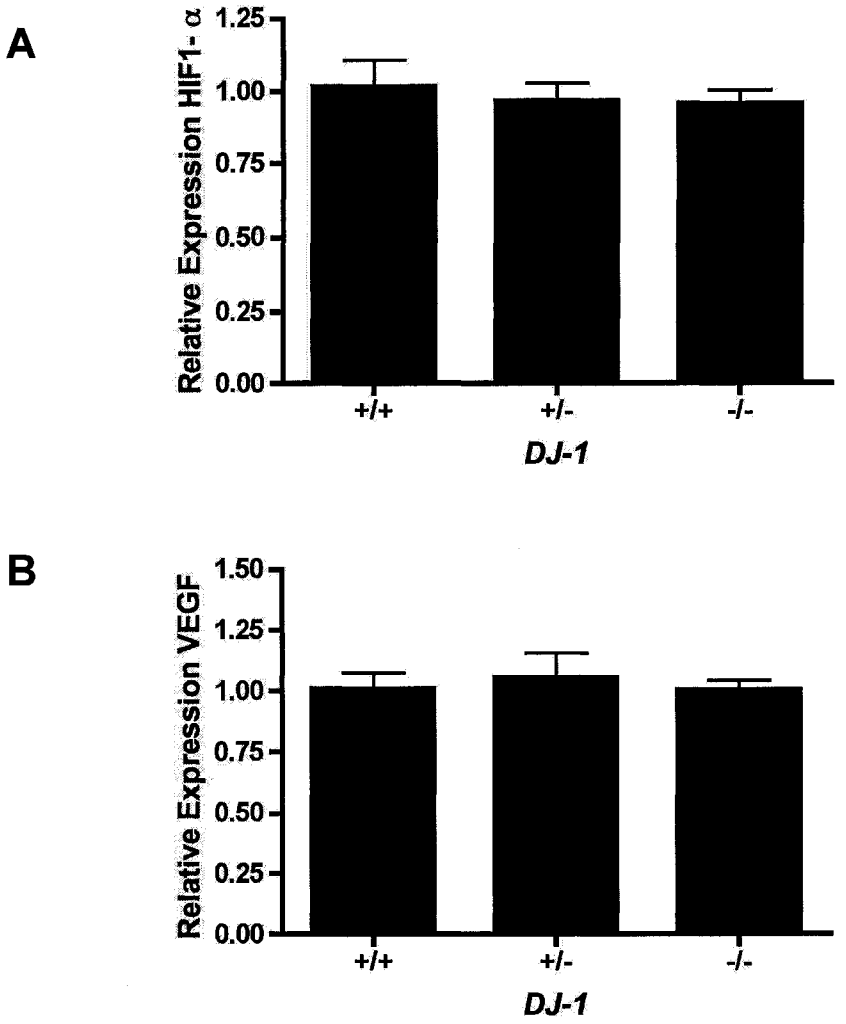

Figure 2.12. In liver samples, neither *HIF1α* nor *VEGF* expression changed due to mutation of *DJ-1*. RNA isolated from *DJ-1*$^{+/+}$ or *DJ-1*$^{-/-}$ tissues (n=5) were analyzed for expression of *HIF1α* and *VEGF* via real-time PCR. (A) No genotype-specific alterations in *HIF1α* expression, or (B) *VEGF* expression occurred.

SPLEEN

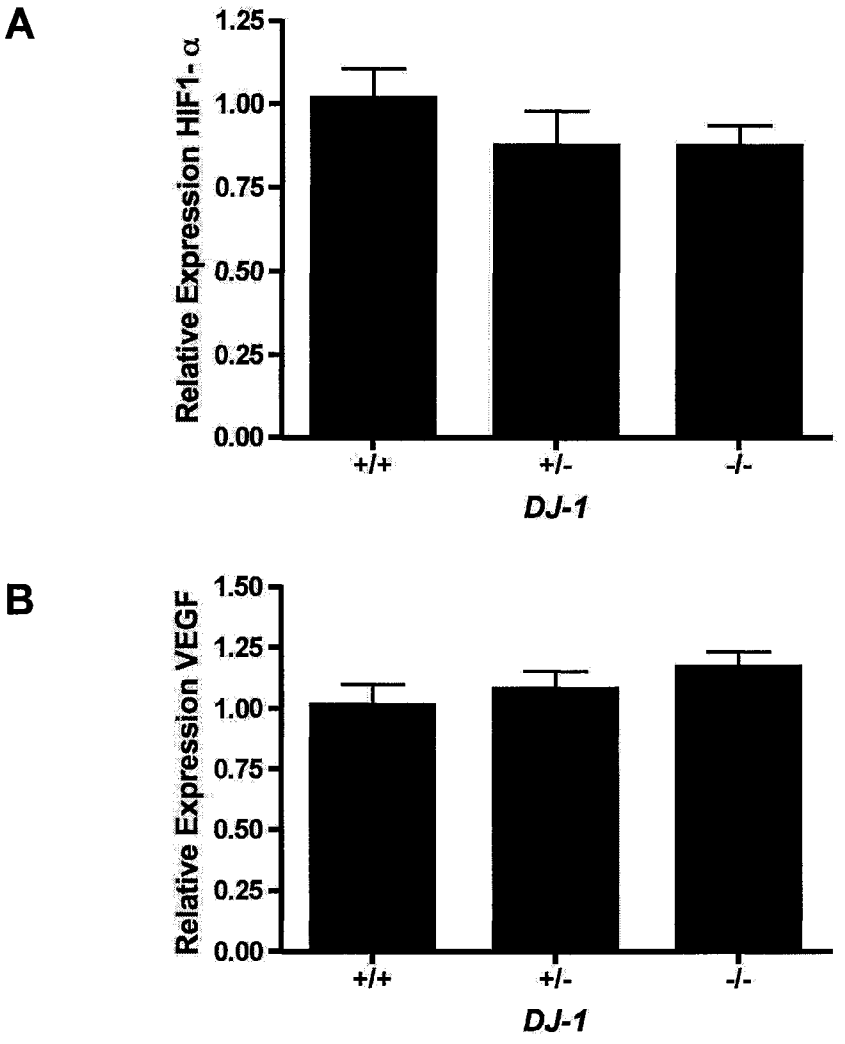

Figure 2.13. Neither *HIF1α* nor *VEGF* expression changed due to mutation of *DJ-1* in the spleen. RNA isolated from *DJ-1*$^{+/+}$ or *DJ-1*$^{-/-}$ tissues (n=5) were analyzed for expression of *HIF1α* and *VEGF* via real-time PCR. (A) No genotype-specific alterations in *HIF1α* expression, or (B) *VEGF* expression occurred.

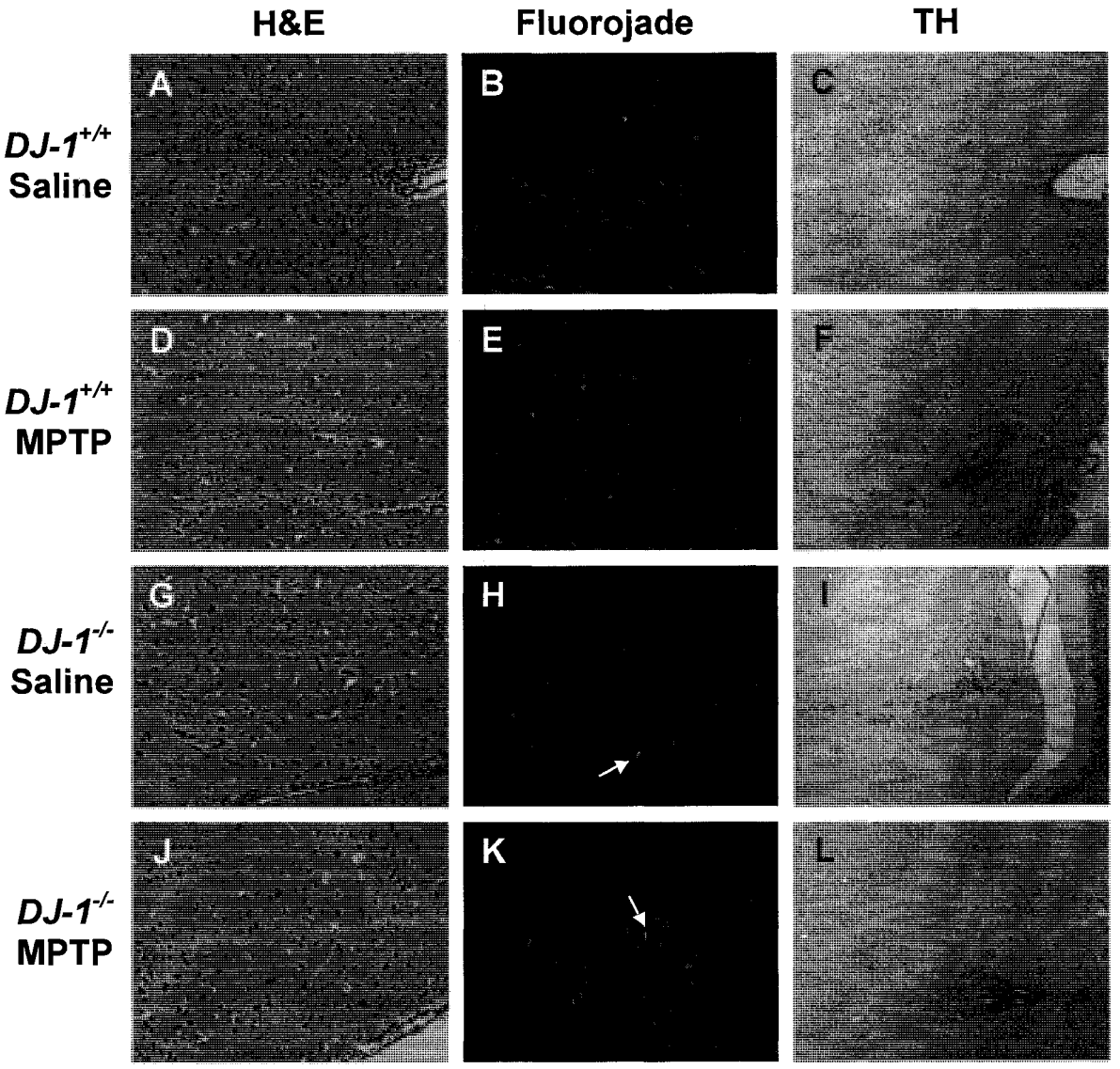

Figure 2.14. Pathology of MPTP- or saline-treated *DJ-1*$^{+/+}$ or *DJ-1*$^{-/-}$ mice. Mice were exposed to saline or 2x20mg/kg MPTP at 6-h intervals, the lesions were allowed 1 week to develop, then brain tissue was fixed for pathological assessment. A, D, G, J: hemotoxylin/esoin staining was done by Colorado HistoPrep. B, E, H, K: Fluorojade reactivity for dying cells; white arrows depict reactive endothelial cells. C, F, I, J: Tyrosine hydroxylase (TH) immunohistochemistry. No changes are seen between any saline (A, B, C and G, H, I) and MPTP (D, E, F and J, K, L) tissues, regardless of genotype.

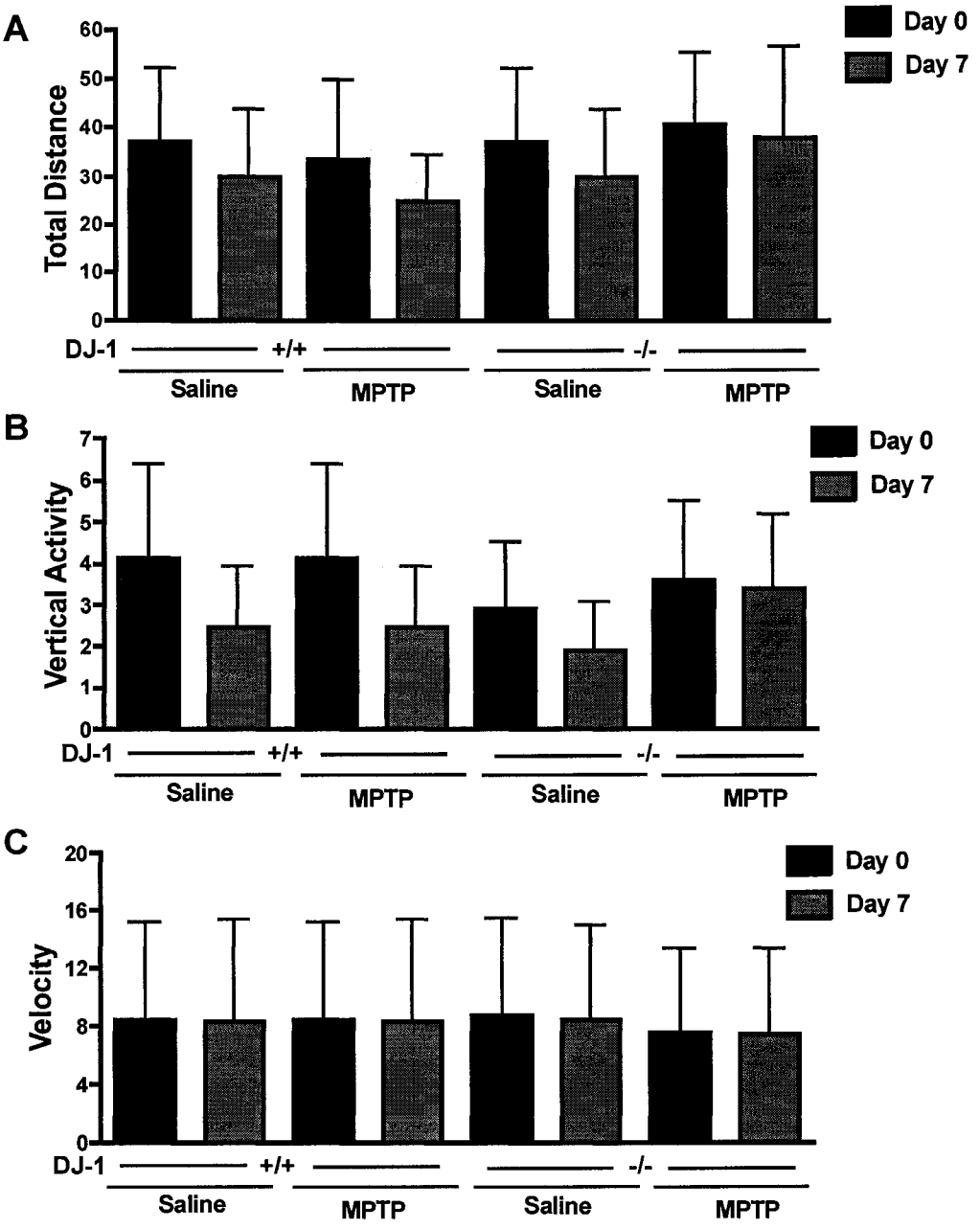

Figure 2.15. Locomotor activity of MPTP- or saline-treated *DJ-1*$^{+/+}$ or *DJ-1*$^{-/-}$ mice. Spontaneous locomotor activity was assessed in VersaMax activity chambers for 10 min both prior to MPTP or saline exposure, and again 7 d following treatment. No significant alterations are observed in total distance (cm), vertical activity (beam breaks), or velocity (cm/sec).

CHAPTER 3

DJ-1 MUTATION INDUCES ALTERATIONS IN CA^{2+} DYNAMICS IN ASTROCYTES

INTRODUCTION

Mutations in *DJ-1* cause early-onset Parkinson's disease (PD) due to lack of proper DJ-1 protein function (Bonifati *et al.*, 2003b). Approximately 90-95% of PD have a late onset (i.e., after ~ 55 years of age) and are not currently linked with any known specific genetic mutation(s). A subset of PD patients present with early onset PD, and many of these cases have been linked to mutations in genes including *Parkin* (Kitada *et al.*, 1998), *α-synuclein* (Polymeropoulos *et al.*, 1997), *PINK1* (Valente *et al.*, 2004), *UCHL1* (Leroy *et al.*, 1998), *LRRK2* (Paisan-Ruiz *et al.*, 2004), and *DJ-1* (Bonifati *et al.*, 2003b). *DJ-1* mutations are the second most common genetic mutation causing early-onset parkinsonism after mutations in *Parkin*, accounting for 1-2% of total genetically-linked cases (Abou-Sleiman *et al.*, 2003; Hague *et al.*, 2003b).

Initially, DJ-1 was identified as a protein able to transform NIH3T3 cells in cooperation with Ras (Nagakubo *et al.*, 1997). DJ-1 is currently classified as an oncogene (Nagakubo *et al.*, 1997; Kim *et al.*, 2005a) and overexpression and/or secretion may be associated with a variety of cancers including breast (Kim *et al.*, 2005a), non-small cell lung carcinoma (MacKeigan *et al.*, 2003), pancreatic (Melle *et al.*, 2007), thyroid (Srisomsap *et al.*, 2002), prostate (Grzmil *et al.*, 2004; Hod, 2004), uveal melanoma (Pardo *et al.*, 2006) and ovarian carcinoma (Davidson *et al.*, 2008). DJ-1 protein distribution is ubiquitous, and has been currently found to be present in all tissues studied to date, including neuronal and

non-neuronal tissues, and likely has an important role in normal cell homeostasis, which has yet to be fully elucidated.

The role DJ-1 may play in modulating neuro-glial interactions has not been investigated. Astrocytes are critical in maintaining the environment of the central nervous system they share with neurons and other glial cells. While neurons communicate predominantly through action potentials, astrocytes were originally considered to be non-excitable cells. However, in response to changes in the extracellular environment, including an action potential by neighboring neurons and numerous other stimuli, astrocytes respond by oscillations in intracellular calcium (Ca^{2+}) (Leybaert *et al.*, 1998). Specifically, activation of G-protein coupled receptors induces phospholipase C (PLC) to cleave phosphatidylinositol 4,5-biphosphate (PIP2) to diacylglycerol and inositol 1, 4, 5 triphosphate (IP3). In turn, IP3 stimulates the release of Ca^{2+} from intracellular stores. This signaling cascade can be triggered by a number of neurochemicals, including glutamate (Duffy and MacVicar, 1995; Porter and McCarthy, 1996; Pasti *et al.*, 1997), γ-aminobutyric acid (Kang *et al.*, 1998), norepinephrine (Duffy and MacVicar, 1995), acetylcholine (Shelton and McCarthy, 2000; Araque *et al.*, 2002), histamine (Shelton and McCarthy, 2000), adenosine (Porter and McCarthy, 1995), and ATP (Porter and McCarthy, 1995; Bowser and Khakh, 2004). After an astrocyte has been stimulated to release Ca^{2+}, a Ca^{2+} wave in turn propagates through neighboring astrocytes *in vitro* (Leybaert et al., 1998), though the extent that the cell culture system can recapitulate Ca^{2+} oscillations *in vivo* remains

controversial. Nevertheless, two major hypotheses exist to explain how the Ca^{2+} wave propagates through astrocytes: (1) Astrocytes release ATP, and ATP binds metabotrophic P2Y receptors on neighboring cells, simulating again the PLC-induced increase in IP3 (Guthrie *et al.*, 1999; Cotrina *et al.*, 2000; Fam *et al.*, 2000), or (2) IP3 itself diffuses through gap-junctions into adjacent astrocytes (Sanderson *et al.*, 1994; Venance *et al.*, 1997; Leybaert *et al.*, 1998). In all likelihood, both mechanisms probably contribute to astrocytic Ca^{2+} waves.

Increases in Ca^{2+} within the astrocyte also serve to modulate the surrounding microvasculature (Haydon and Carmignoto, 2006). Astrocytes produce many vasoactive products, including nitric oxide (Murphy *et al.*, 1993; Wiencken and Casagrande, 1999; Li *et al.*, 2003; Pawate *et al.*, 2004), ATP (Porter and McCarthy, 1995; Guthrie *et al.*, 1999; Queiroz *et al.*, 1999; Pasti *et al.*, 2001; Sul *et al.*, 2004), prostaglandins (Amruthesh *et al.*, 1993; Bezzi *et al.*, 1998; Wu *et al.*, 2002), and epoxyeicosatrieonic acids (EETs) (Amruthesh *et al.*, 1993; Alkayed *et al.*, 1996; Alkayed *et al.*, 1997). An increase in intracellular Ca^{2+} can stimulate phospholipase A_2 to cleave arachadonic acid (AA), which in turn regulates vasodilation or constriction. If AA is cleaved by COX2 to prostaglandin or by cytochrome P450 epoxygenase to EETs (Roman, 2002) within the astrocyte and subsequently released, the result is vasodilation. However, if AA itself enters the vascular smooth muscle, the muscle will convert AA into 20-hydroxyeicosatetraenoic acid (20-HETE), inducing vasoconstriction (Randriamboavonjy *et al.*, 2003). While these effects seem contradictory, it

highlights the importance of the fine control astrocytes have in modulating neural circulation, and much remains to be uncovered about the tight regulation of this system in the central nervous system.

Overall, astrocytes serve to integrate neuronal activity in concert with microcirculation, and protect the extracellular environment to assure these two functions work in unison with one another. While much research remains to fully explicate this complex system, it seems likely that coordination of blood flow to neuronal activity versus metabolic need (Sandor, 1999; Attwell and Iadecola, 2002) is mediated by neurotransmitter-induced astrocytic Ca^{2+} oscillations (reviewed by Haydon and Carmignoto, 2006). Also, astrocytes are critical regulators of the extracellular environment (Vernadakis, 1996), thus preventing excitotoxicity, and supplying neurons with antioxidants (Sagara *et al.*, 1993) as well as lactate, the primary oxidative substrate for neurons (Pellerin *et al.*, 1998; Bouzier-Sore *et al.*, 2003a; Bouzier-Sore *et al.*, 2003b). As such, disruption of Ca^{2+} signaling in the astrocyte could result in alterations in the delicate balance between blood flow and neuronal activity, as well as compromise the normal astrocytic trophic support of neurons.

Although PD is primarily characterized by degenerating dopaminergic neurons, the presence of reactive astrogliosis in affected regions implies dysfunction in these cells as well. Furthermore, high DJ-1 immunoreactivity is observed in reactive astrocytes (Neumann *et al.*, 2004), suggesting it may play a role in

modulating gliosis. All neuorological disorders that DJ-1 may modulate (see CHAPTER 2) are also beset by concurrent astrogliosis. DJ-1 is implicated in both Alzheimer's disease (Choi *et al.*, 2006) and ischemia (Aleyasin *et al.*, 2007; Yanagisawa *et al.*, 2007), which are each well established to be concomitantly plagued by aberrant neurovascular coupling, regulated by Ca^{2+} oscillations in astrocytes (Duffy and MacVicar, 1996). Therefore, in these studies, ATP-evoked intracellular Ca^{2+} waves were investigated in *DJ-1*$^{+/+}$ and *DJ-1*$^{-/-}$ astrocytes. ATP was selected because stimulation of astrocytes by the neurochemicals listed above activates the metabotrophic receptors, and leads to release of ATP, propagating the Ca^{2+} wave. Therefore, any alteration in the ATP-induced Ca^{2+} wave would likely affect the astrocytic responsiveness to all stimuli.

Studies conducted in this laboratory monitored intracellular Ca^{2+} waves in astrocytes exposed to three unique chemical agents: lipopolysaccharides (LPS), rotenone, or 2-chloro-4,6-diamino-1,3,5-triazine (DACT). LPS is a component of gram-negative bacterial cell walls and can induce a robust response in astrocytes, leading to production of proinflammatory mediators. Exposure of mice to systemic LPS induces progressive neurodegeneration of dopaminergic neurons, mimicking PD (Qin *et al.*, 2007). Many lines of evidence suggest inflammation is a causative or contributing factor in PD, not the least of which is the high concentrations of proinflammatory mediators found in brains of individuals with PD (Boka *et al.*, 1994; Mogi *et al.*, 1994a; Blum-Degen *et al.*, 1995; Whitton, 2007).

Rotenone, the classical mitochondrial complex I inhibitor, and was selected for two main reasons. Most importantly, inhibition of complex I is an attribute shared by other chemicals which induce PD, including MPTP (Ramsay *et al.*, 1986; Kindt *et al.*, 1987), and is observed in the brains of patients with sporadic PD (Parker and Swerdlow, 1998). Additionally, rotenone exposure in rats can recapitulate parkinsonism (Betarbet *et al.*, 2000; Alam and Schmidt, 2002), making it an attractive and relevant chemical model.

Finally, DACT, the primary metabolite of atrazine (2-chloro-4-ethylamino-6-isopropylamino-s-triazine) was utilized. Atrazine is currently the most common herbicide used in the United States, is found in a very high percentage of ground water samples, and has a long half-life (~200 days), making human exposure quite likely (ATSDR, 2003). Furthermore, exposure to chlorotriazines can induce deficiencies in parkinsonian-related neurochemicals (Das *et al.*, 2001; Das *et al.*, 2003; Filipov *et al.*, 2007). Many epidemiological studies suggest that pesticide exposure, rural living and well-water consumption are risk factors for PD. All these factors make atrazine an attractive chemical to investigate. In the body, atrazine is rapidly metabolized via sequential *N*-dealkylation reactions mediated by cytochrome P450 to DACT (Timchalk *et al.*, 1990). DACT is the predominant metabolite found in animals exposed to atrazine, and believed to be the active agent in atrazine-mediated reproductive disruption of the hypothalamic-pituitary axis (McMullin *et al.*, 2004). Research from our laboratory suggests exposure of

the gonadotrope cell line LβT2 to DACT induces a decrease in gonadotropin releasing hormone (GnRH)-evoked Ca^{2+} release through yet unknown mechanisms (data not shown). Therefore, we hypothesized that LPS, rotenone and/or DACT might alter the ATP-induced increase of intracellular Ca^{2+} in our primary cortical astrocytes, and further that *DJ-1*$^{-/-}$ astrocytes might be more susceptible to perturbations in Ca^{2+} than *DJ-1*$^{+/+}$ cells. Because each chemical targets distinct, specific mechanisms that may contribute to PD, delineating an increased susceptibility in our *DJ-1*$^{-/-}$ astrocytes to one or more of these chemicals might provide insight into how *DJ-1* mutation leads to PD.

MATERIALS AND METHODS

DJ-1 KNOCKOUT MOUSE: A gene-trap screening library conducted in embryonic stem cells was utilized, the *DJ-1* gene was mutated and we attained chimeric mice generated by BayGenomics. The precise location of the gene-trap was ascertained and a functional knockout was confirmed (see CHAPTER 2). Heterozygous mice were bred to establish a colony containing all three genotypes. Primary mouse cortical astrocytes were isolated from d1-d2 old pups and maintained as previously described (Allen *et al.*, 2000b).

INTRACELLULAR CA^{2+}: Astrocytes were cultured in 4-well chamber slides, treated with 0, 10, 25, or 50 μg/mL LPS for 72h, then exposed to 0, 50, 500, or 1000nM rotenone for 24h. These doses of rotenone were selected because previous studies have demonstrated that 10 nM to 1 μM caused dose-dependent

ATP depletion, oxidative damage, and even death (Sherer *et al.*, 2003b). In studies using DACT, astrocytes were exposed for 24h to 300μM DACT, as this dose has been demonstrated to decrease GnRH-evoked rise in intracellular calcium from LβT2 cells in our laboratory. Astrocytes were loaded with the intracellular Ca^{2+} indicator, Fluo 4 AM (2μM, excitation 490nm, emission 515nm, Invitrogen) for 30 min at 37°C. After dye loading, astrocytes were washed with and imaged in minimum essential media lacking phenol red and supplemented with 25mM HEPES. Images were collected every 15 sec for 10 min using a Zeiss Axiovert 200M microscope equipped with a Hammatsu ORCA-ER cooled charge-coupled device camera. After 1 min of baseline sampling, 1μM ATP was added to evoke an increase in intracellular Ca^{2+}. To assure adequate mixing of ATP upon addition, 100μL of 4x (4μM) ATP was added to 300μL of imaging media already on the slide. Also, one extra image was collected off the slide prior to collecting any images for analysis in order to give the astrocytes ample time to react to the added ATP. Images were analyzed using SlideBook software, and fluorescence was normalized to its average initial value per cell (F/F_0).

STATISTICAL ANALYSES: All statistical analyses were performed using GraphPad Prism software. Means were analyzed using ANOVA, and when they significantly differed ($p<0.05$), Tukey's *post hoc* test was employed to determine which means significantly differed from one another.

RESULTS

In *DJ-1*$^{+/+}$ cells, peak Ca^{2+} concentration significantly ($p<0.05$) increased in cells exposed to 10 or 50μg/mL LPS, but decreased in cells exposed to 25μg/mL compared to control levels (Figure 3.1). Final Ca^{2+} levels did not return to baseline levels in all LPS-exposed cells ($n \geq 198$, $p<0.05$). In contrast, peak Ca^{2+} concentration decreased in a dose-dependent manner in *DJ-1*$^{-/-}$ astrocytes exposed to LPS (Figure 3.2, $n \geq 67$, $p<0.05$). Final intracellular Ca^{2+} levels remained elevated throughout the duration of sampling in all samples, though astrocytes exposed to 50μg/mL LPS were significantly lower than the rest. As LPS tends to induce inflammation in astrocytes, it is curious that Ca^{2+} concentrations would increase in *DJ-1*$^{+/+}$ cells exposed to high (50μg/mL) levels of LPS. The dose-dependent decrease in LPS-treated *DJ-1*$^{-/-}$ cells is expected, and may represent an increased sensitivity of astrocytes to LPS due to *DJ-1* mutation. Moreover, the rate of decline in Ca^{2+} levels following ATP stimulation in *DJ-1*$^{-/-}$ astrocytes is slower than their *DJ-1*$^{+/+}$ counterparts. While this might suggest an impairment of Ca^{2+} reuptake from the cytosol or opening of ionotrophic channels allowing extracellular ATP to flow into the cell, in actuality the *DJ-1*$^{-/-}$ astrocytes tended to increase the frequency of secondary Ca^{2+} peaks in cells that responded initially to ATP, and this was not observed to as great an extent in *DJ-1*$^{+/+}$ cells. Interestingly, peak ATP-evoked intracellular Ca^{2+} was higher in untreated (0 LPS) *DJ-1*$^{-/-}$ astrocytes compared to *DJ-1*$^{+/+}$ ($F/F_0 = 1.60$ versus 1.39, respectively).

Peak Ca^{2+} concentration increased in *DJ-1*$^{+/+}$ cells exposed to 50 or 500nM rotenone (Figure 3.3). Final intracellular Ca^{2+} levels remained modestly though significantly elevated through the duration of sampling, with all rotenone-treated samples significantly more elevated than control ($n \geq 274$, $p<0.05$). In *DJ-1*$^{-/-}$ astrocytes, peak Ca^{2+} concentration was similar at all rotenone doses (Figure 3.4). Final intracellular Ca^{2+} levels remained elevated at all levels of rotenone exposure, though 50nM rotenone was significantly lower than all other doses ($n \geq 111$, $p<0.05$). Overall, intracellular Ca^{2+} waves demonstrate an increased susceptibility of *DJ-1*$^{-/-}$ astrocytes to alterations in Ca^{2+} dynamics mediated by LPS, and an increase in secondary Ca^{2+} waves noted in all *DJ-1*$^{-/-}$ cells, regardless of treatment. Therefore, mutation of *DJ-1* may induce alterations in astrocyte Ca^{2+} dynamics.

DACT-exposed *DJ-1*$^{+/-}$ astrocytes had a decrease in peak Ca^{2+} concentrations, consistent with data published by our laboratory in the LβT2 cell line (Figure 3.5). Interestingly, peak Ca^{2+} concentration was reached at 90 sec in DACT-treated cells, but at 60 sec (i.e., immediately after ATP was added) in cells exposed only to DSMO. *DJ-1*$^{-/-}$ astrocytes had significantly increased peak Ca^{2+} concentration after DACT treatment (Figure 3.5, $p<0.01$), though this peak was reached much later during sampling (90 sec) compared to all other treatment groups (60 sec). Final Ca^{2+} levels were significantly lower in DACT-treated *DJ-1*$^{+/+}$ astrocytes. Intracellular Ca^{2+} levels again remained elevated through the duration of imaging in all *DJ-1*$^{-/-}$ astrocytes, with DACT-treated cells having highest final Ca^{2+} levels

(p <0.001, n≥401). Again, this seemingly slow decline of intracellular Ca^{2+} in *DJ-1*$^{-/-}$ astrocytes appears to be, in reality, a compilation of numerous secondary waves in a portion of cells examined.

DISCUSSION AND CONCLUSIONS

Although exposure to LPS or rotenone did induce modest dysfunction in one or both genotypes, no clear pattern of toxin-induced alterations were evident. One phenotype that was consistent, however, was the sustained elevation of Ca^{2+} in *DJ-1*$^{-/-}$ astrocytes. Overall, individual *DJ-1*$^{-/-}$ cells had an obvious, anticipated increase in intracellular Ca^{2+} immediately following addition of ATP (i.e., 60 sec). However, a high percentage of these cells had secondary oscillations of Ca^{2+}, in excess of what was observed in *DJ-1*$^{+/+}$ astrocytes, causing the return to baseline to be delayed to beyond our sampling time.

Peak Ca^{2+} concentrations were higher in *DJ-1*$^{-/-}$ astrocytes compared to *DJ-1*$^{+/+}$, however, this value itself tended to be a fairly inconsistent indicator of reactivity of astrocytes to applied ATP. While it may indeed be a valid genotype-specific effect, as an absolute value, it was not consistent between experiments, and may not be the best indicator of astrocyte function in these mutant cells. While some alterations in the return to baseline in *DJ-1*$^{-/-}$ cells are evident, the mechanism is currently unclear. Furthermore, the overall trend is a return towards baseline, which is inhibited by continued secondary oscillations. Additional investigations, extending the duration of sampling, could shed further light on this issue.

Repeating these experiments in Ca^{2+}-free media could possibly help elucidate whether these secondary oscillations in *DJ-1*$^{-/-}$ astrocytes are due to entry of extracellular Ca^{2+} from the media or whether they are from calcium release from intracellular stores.

Overall, these data provide a glimpse into the possibility that alterations in Ca^{2+} dynamics may affect *DJ-1* related PD. Notably, *DJ-1*$^{-/-}$ astrocytes tended to be more sensitive to LPS than their *DJ-1*$^{+/+}$ counterparts. While the highest dose of LPS employed, 50μg/mL actually increased peak Ca^{2+} concentrations in our *DJ-1*$^{+/+}$ cells, this exposure severely retarded the cytosolic peak of Ca^{2+} in *DJ-1*$^{-/-}$ astrocytes. While this could be a specific alteration in *DJ-1*$^{-/-}$ intracellular Ca^{2+}, another explanation is overt cellular toxicity. Evident in Figure 2.4(F), exposure of astrocytes to 50μg/mL LPS resulted in fewer cells counted compared to control. Based upon observation alone, *DJ-1*$^{-/-}$ astrocytes tended have fewer numbers of cells on the chamber slides for analysis of Ca^{2+} compared to *DJ-1*$^{+/+}$. Therefore, it is possible that *DJ-1*$^{-/-}$ cells are more sensitive to LPS toxicity, especially at high levels, accounting for their blunted response to ATP stimulation. As LPS is a prototypical inducer of inflammation, a condition associated with PD, mutation of *DJ-1*$^{-/-}$ might increase astrocytic responsiveness to LPS which could contribute to *DJ-1* linked PD. Therefore, further investigation into the possibility of *DJ-1*-mediated alterations in neuroinflammation might be helpful in elucidating the mechanism(s) by which *DJ-1* mutation induces PD.

CHAPTER 3

FIGURES

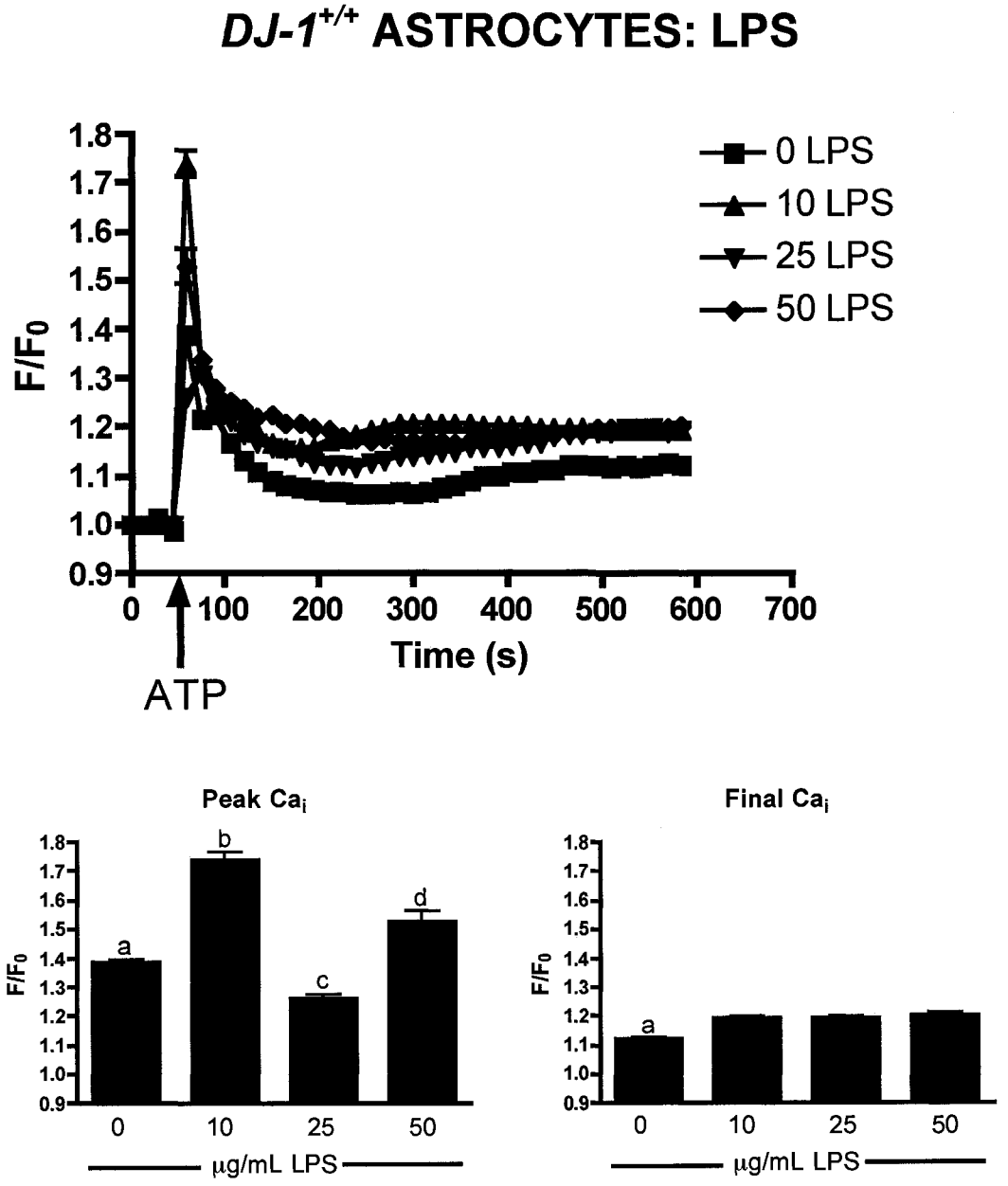

Figure 3.1. Intracellular Ca^{2+} transient peak in *DJ-1*$^{+/+}$ astrocytes following exposure to LPS. Astrocytes were exposed to 0, 10, 25, or 50μg/mL LPS for 72h, then treatments were removed and cells were allowed 24h to rest. After baseline sampling for 1 min, astrocytes were exposed to 1μM ATP and the intracellular Ca^{2+} concentration was monitored for 9 additional min. Peak Ca^{2+} concentration increased in cells exposed to 10 or 50μg/mL LPS, but decreased in cells exposed to 25μg/mL. Final Ca^{2+} levels did not return to baseline levels in all LPS-exposed cells ($n \geq 198$, $p<0.05$).

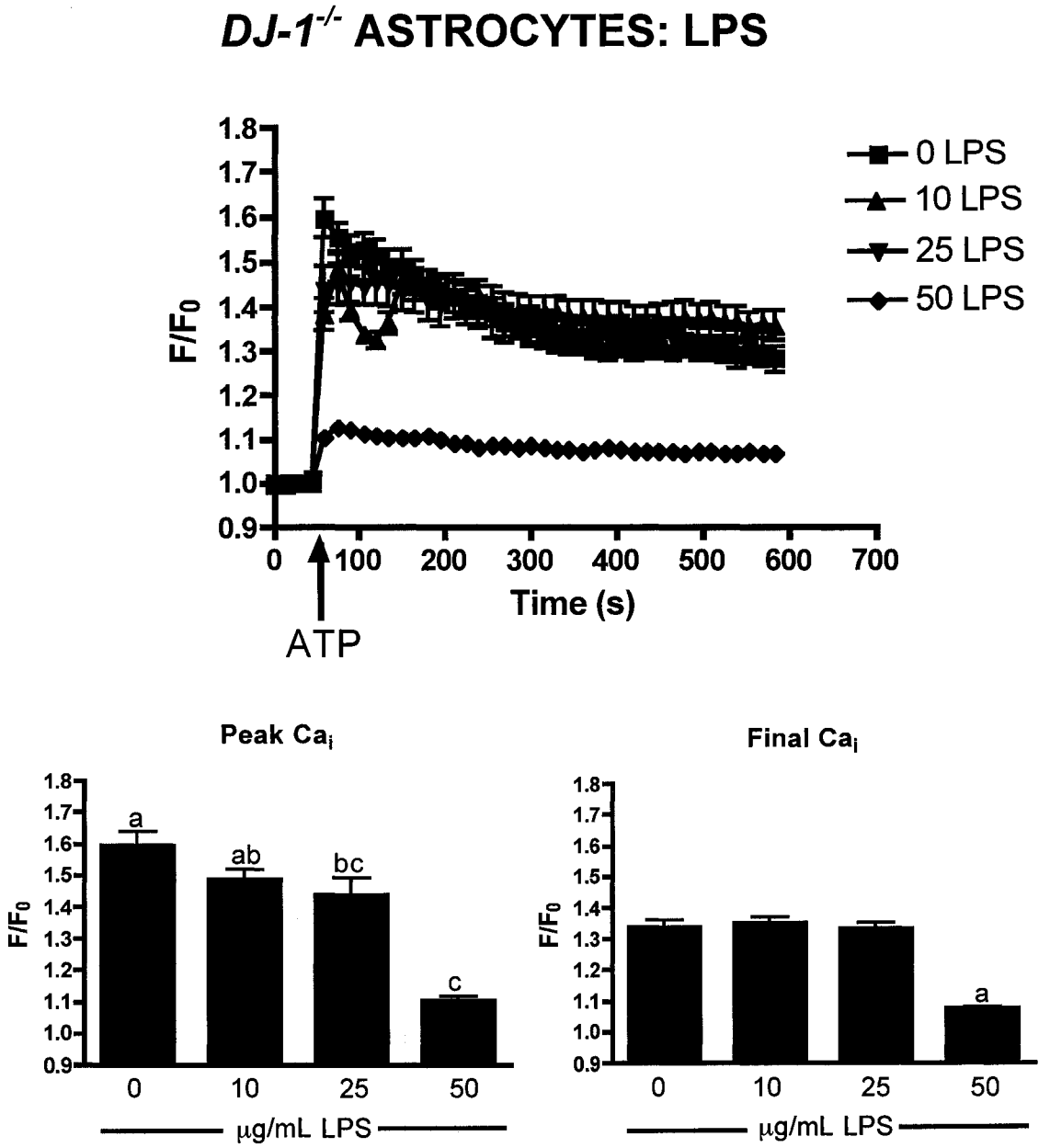

Figure 3.2. Intracellular Ca^{2+} peak in *DJ-1*$^{-/-}$ astrocytes following exposure to LPS. Astrocytes were exposed to 0, 10, 25, or 50μg/mL LPS for 72h, then treatments were removed and cells were allowed 24h to rest. After baseline sampling for 1 min, astrocytes were exposed to 1μM ATP and the intracellular Ca^{2+} concentration was monitored for 9 additional min. Peak Ca^{2+} concentration decreased in a dose-dependent manner in astrocytes exposed to LPS ($n \geq 67$, $p<0.05$). Final intracellular Ca^{2+} levels remained elevated throughout the duration of sampling, and only cells exposed to 50μg/mL LPS returned to baseline values.

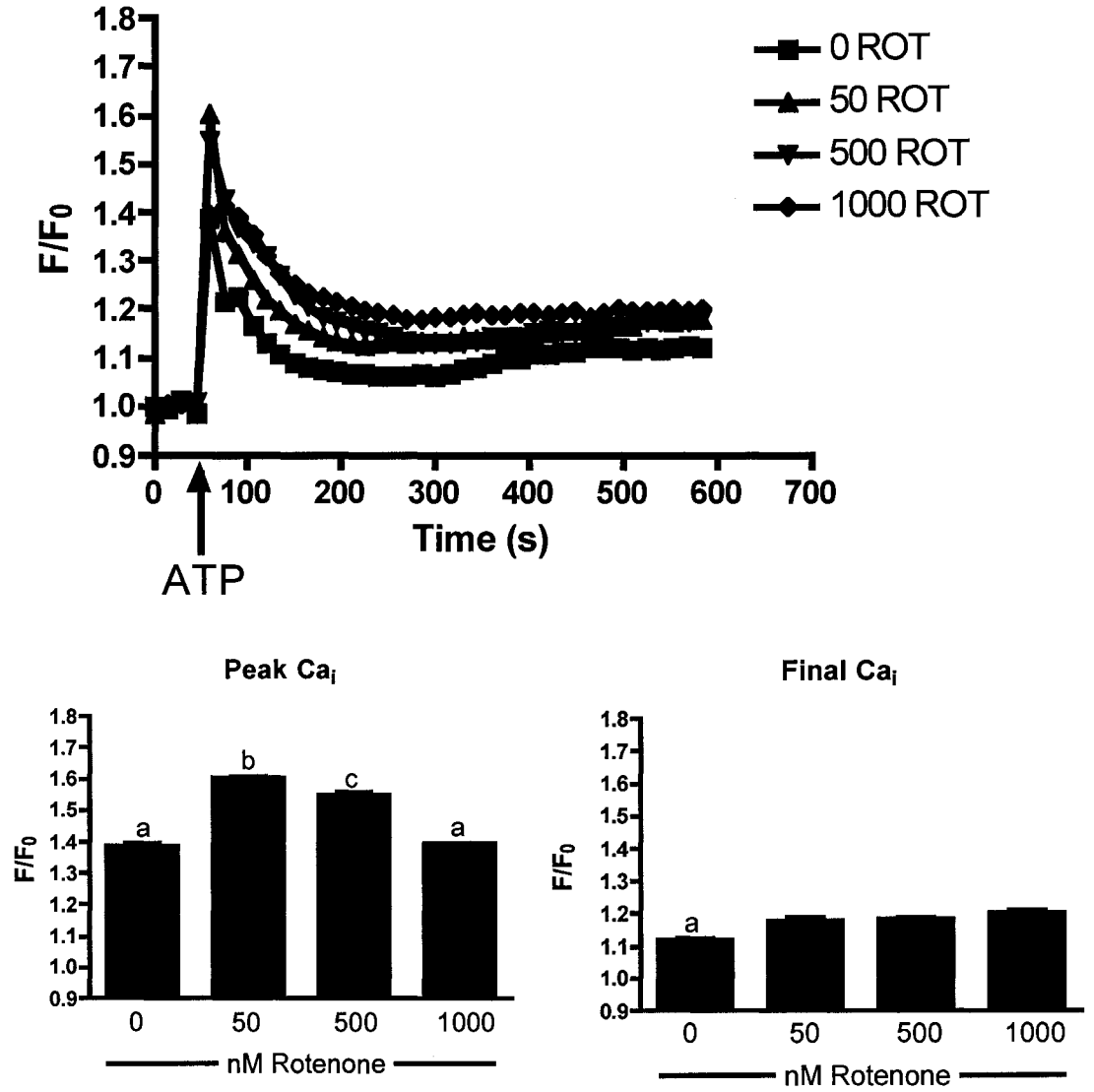

Figure 3.3. Intracellular Ca^{2+} peak in *DJ-1*$^{+/+}$ astrocytes following 24h exposure to rotenone. Astrocytes were exposed to 0, 50, 500, or 1000nM rotenone for 24h. After baseline sampling for 1 min, astrocytes were exposed to 1μM ATP and fluorescence was monitored for 9 additional min. Bars with differing letters significantly differ from one another ($p<0.05$). Peak Ca^{2+} concentration increased in cells exposed to 50 or 500nM rotenone ($p<0.05$). Final intracellular Ca^{2+} levels remained significantly elevated through the duration of sampling, with rotenone-treated samples more elevated than control ($n\geq274$, $p<0.05$).

DJ-1$^{-/-}$ ASTROCYTES: ROTENONE

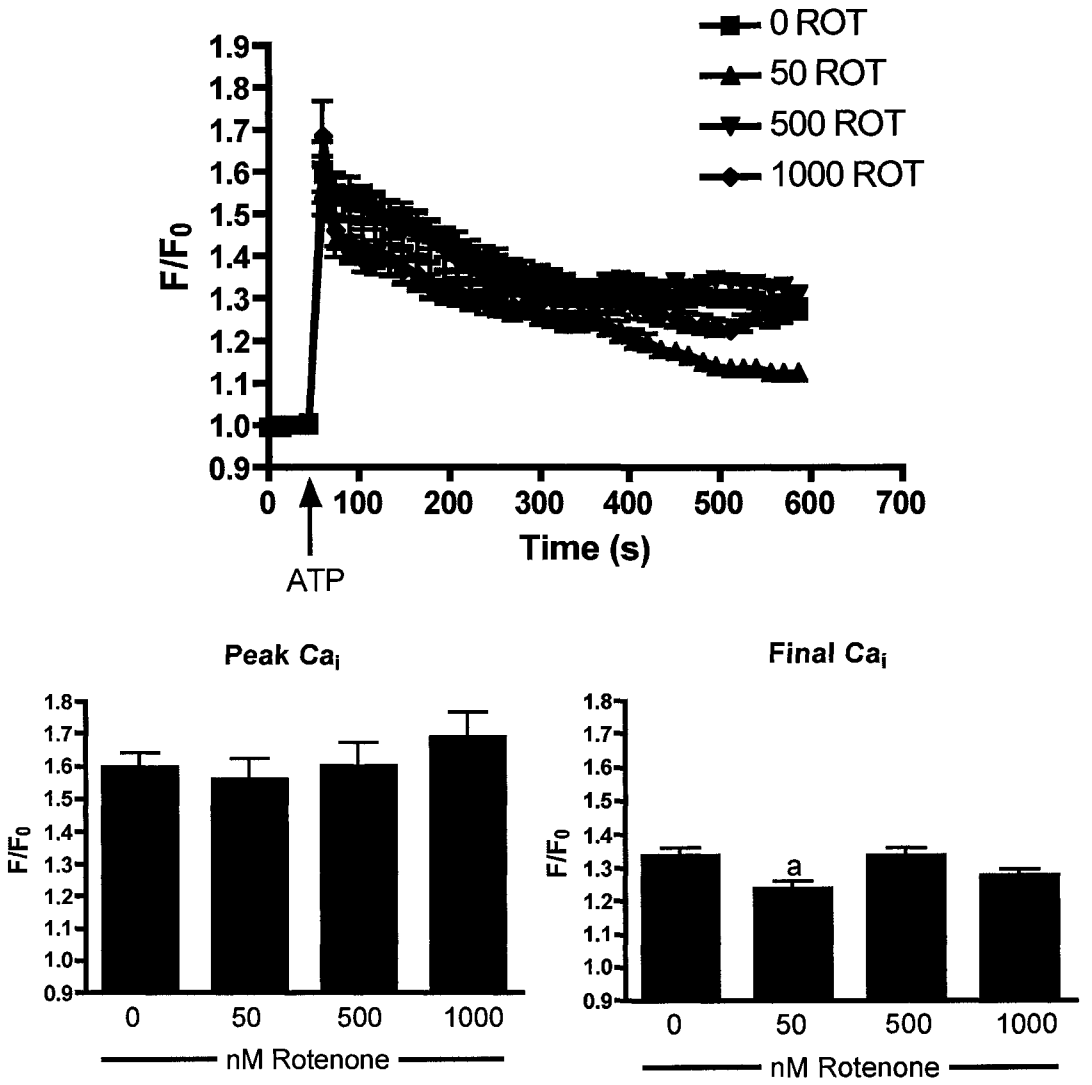

Figure 3.4. Intracellular Ca^{2+} peak in *DJ-1*$^{-/-}$ astrocytes following 24h exposure to rotenone. Astrocytes were exposed to 0, 50, 500, or 1000nM rotenone for 24h. After baseline sampling for 1 min, astrocytes were exposed to 1μM ATP and fluorescence was monitored for 9 additional min. Bars with differing letters significantly differ from one another ($p<0.05$). Peak Ca^{2+} concentration was similar at all rotenone doses. Final intracellular Ca^{2+} levels remained elevated at all levels or rotenone exposure, though 50nM rotenone was significantly lower than all other doses ($n\geq111$, $p<0.05$).

CALCIUM IN *DJ-1*$^{+/+}$, *DJ-1*$^{+/-}$ and *DJ-1*$^{-/-}$

ASTROCYTES: DACT

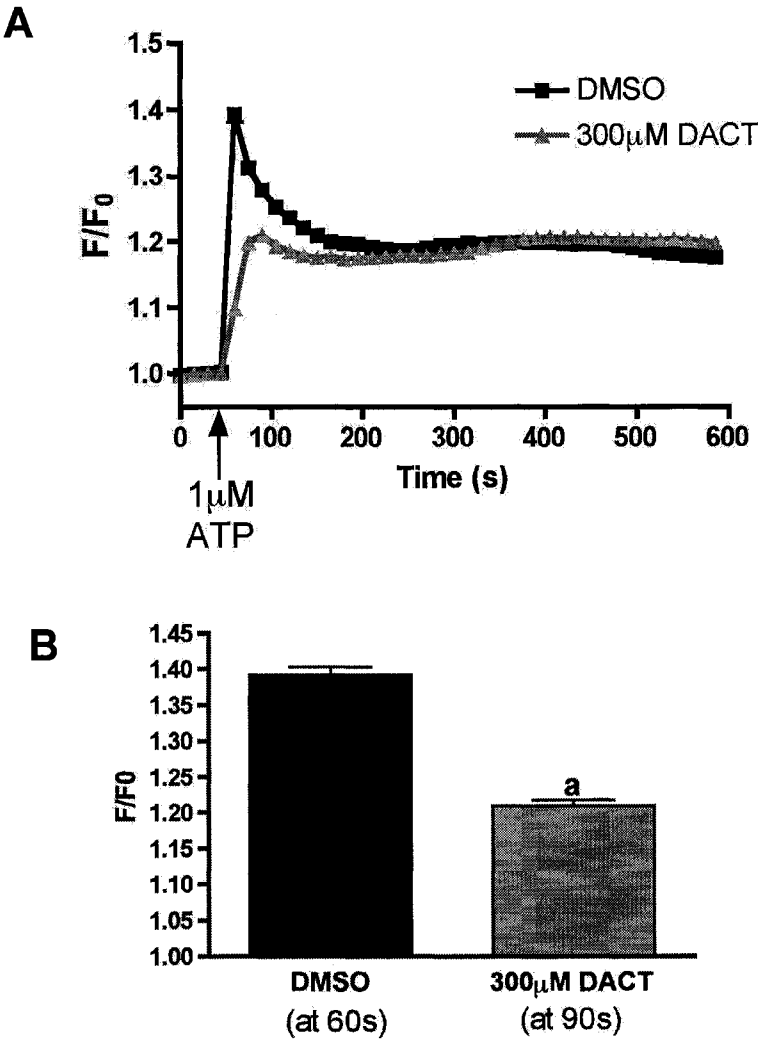

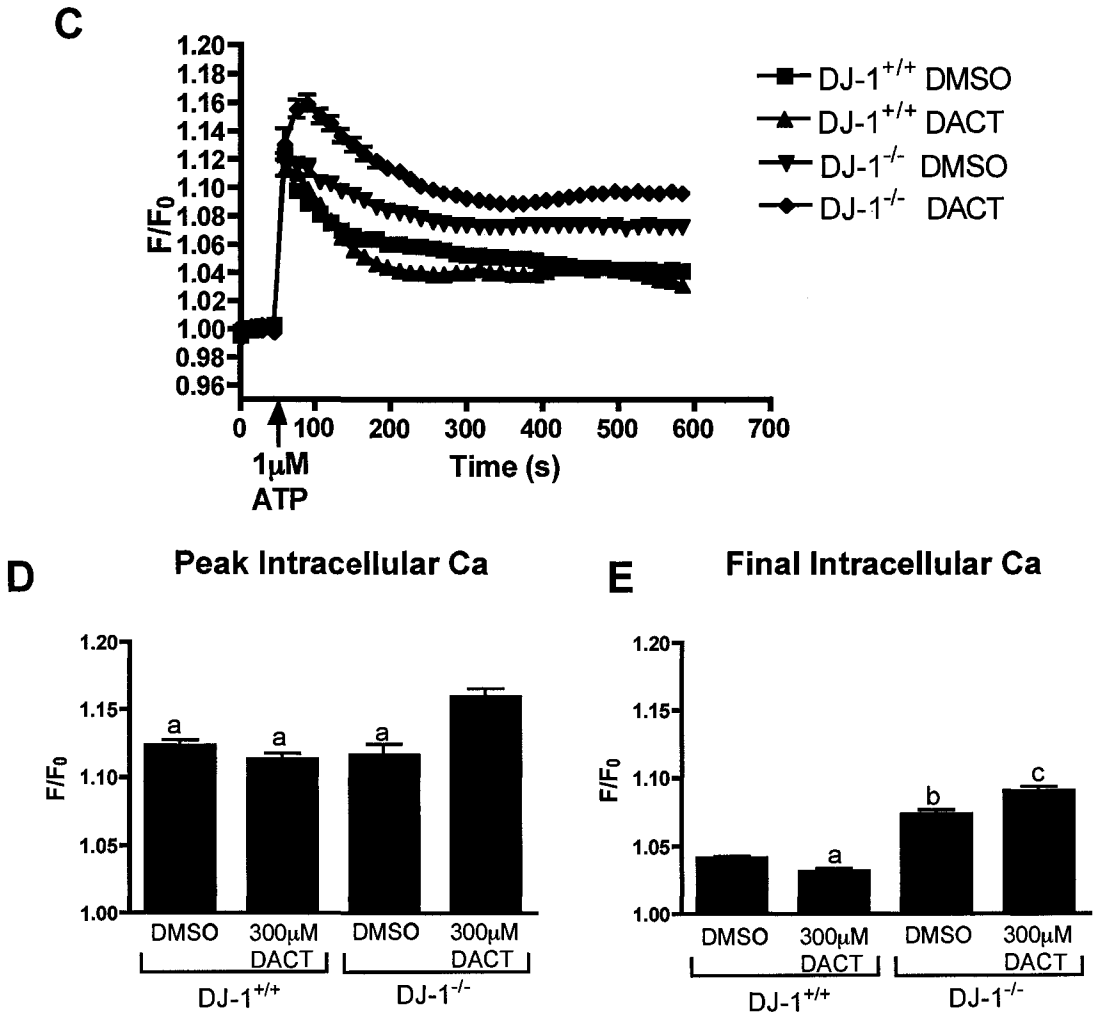

Figure 3.5. DACT increases and delays peak intracellular Ca^{2+} concentrations in *DJ-1*$^{+/-}$, *DJ-1*$^{-/-}$ but not *DJ-1*$^{+/+}$ primary cortical astrocytes. Astrocytes were exposed to 300μM DACT or DMSO for 24h, then the ATP-induced increase in intracellular Ca^{2+} was examined. Following baseline sampling, 1μM ATP was added. A, B: DACT significantly decreased peak intracellular Ca^{2+} concentrations (p <0.001, n≥351) in *DJ-1*$^{+/-}$ cells and tended to delay time to peak Ca^{2+} levels. C, D, E. DACT significantly increased peak Ca^{2+} concentration in *DJ-1*$^{-/-}$ astrocytes (p<0.01). Although final Ca^{2+} levels were significantly lower in DACT-treated *DJ-1*$^{+/+}$ astrocytes, intracellular levels remained elevated through the duration of imaging in all *DJ-1*$^{-/-}$ astrocytes, with DACT-treated cells having highest final Ca^{2+} levels (p <0.001, n≥401).

CHAPTER 4

DJ-1 MUTATION DECREASES *TNFα* EXPRESSION AND SECRETION IN ASTROCYTES

ABSTRACT

Mutations in *DJ-1* cause early-onset Parkinson's disease (PD). To study the physiological consequences of *DJ-1* mutation in the context of neuroinflammatory insult, a *DJ-1* knockout mouse was made, and primary cortical astrocytes were isolated. Astrocytes were isolated from *DJ-1*$^{+/+}$ and *DJ-1*$^{-/-}$ mice and exposed to 10μg/mL lipopolysaccharides (LPS) for 24h either alone or following 2h preexposure to inhibitors of MEK (U0126), JNK (JNK inhibitor II), or p38 (SB203580). RNA was then isolated, cDNA synthesized, and real-time PCR was used to assess expression of the proinflammatory mediators cyclooxygenase 2 (*COX2*), inducible nitric oxide synthetase (*NOS2*), or tumor necrosis factor α (*TNFα*). As anticipated, LPS induced expression of all three genes. LPS-induced expression of *COX2* decreased similarly in *DJ-1*$^{+/+}$ and *DJ-1*$^{-/-}$ astrocytes in response to inhibition of p38 but was unaffected by inhibition of MEK or JNK. In LPS-treated cells, no significant alterations in LPS-induced *NOS2* expression were observed in any inhibitor-treated cells. While expression of *TNFα* was not effected by the inhibitors in either genotype, *DJ-1*$^{-/-}$ astrocytes had consistently lower expression compared to *DJ-1*$^{+/+}$ counterparts. Secretion of TNFα into the culture media was also significantly decreased in *DJ-1*$^{-/-}$ astrocytes and inhibition of p38 decreased this secretion in both genotypes. To investigate LPS-stimulated upregulation of MAPKs, cells were treated with 10μg/mL LPS for 0, 5, 15, 30, 60, 90, or 120 min, protein was isolated and phosphorylated forms of ERK, JNK, p38, or AKT (Ser 473) were analyzed. Increased phosphorylation of all proteins was observed within 15 min of LPS exposure. Finally, to determine how rapidly

LPS can induce binding of p65 to the *NOS2* promoter, the chromatin immunoprecipitation (ChIP) assay was preformed on astrocytes exposed to 10μg/mL LPS for 1, 6, or 8 h. Binding of p65 to the *NOS2* promoter was detected at all time points analyzed. These data point to a lack of neuroprotection afforded by astrocytes to surrounding neurons is induced by *DJ-1* mutation.

INTRODUCTION

Neuroinflammation is a double-edged sword in neuronal survival and function, where transitory activation is neuroprotective (Perry *et al.*, 2002), but prolonged exposure induces neuronal death (Hirsch *et al.*, 1998). For example, astrocytes will produce cytokines following insult, and these molecules promote neuronal survival via interactions with their respective receptors on cell membranes as well as modulating neurotransmitter function (see below). In contrast, following prolonged activation, inflammation is associated with numerous neurodegenerative diseases, including PD (Boka *et al.*, 1994; Mogi *et al.*, 1994a; Hirsch *et al.*, 1998; Whitton, 2007). Therefore any alteration of the delicately coordinated neuroinflammatory response will be detrimental to neuronal viability.

Cytokines within the central nervous system (CNS) can be released from resident astrocytes, neurons, and/or microglia, or from cells in the periphery. Within the CNS, cytokines modulate neuronal viability through a variety of mechanisms. Interleukin (IL)-1 and IL-6 can modulate synaptic plasticity (Bellinger *et al.*, 1995; Li *et al.*, 1997). IL-1 can also enhance γ-aminobutyric acid

(GABA) inhibitory responses by affecting GABA receptors (Miller and Fahey, 1994). TNFα, IL-1α, IL-1β, and IL-6 prevent excitotoxicity induced by prolonged stimulation of the *N*-methyl-D-aspartic acid (NMDA) glutamate receptors via affecting receptor function and/or the signaling cascades secondary to receptor activation (Cheng *et al.*, 1994; Barger *et al.*, 1995; Bruce *et al.*, 1996; Carlson *et al.*, 1998). Excess NMDA receptor activation causes uncontrolled increases in intracellular calcium within the neuron, leading to neuronal apoptosis via excitotoxicity, a condition associated with neurodegeneration, ischemia, and other neurological disorders (Beal, 1992; Beal, 1994; Whetsell, 1996; Beal, 1998). Therefore, release of cytokines by astrocytes is critical to maintaining neuronal viability (Maeda *et al.*, 1994; Hori *et al.*, 1996).

TNFα is particularly significant in neuronal homeostasis. Its pleiotropic effects in the CNS span the gamut of neuronal function, from regulation of electrophysiology to transcription. In fact, TNFα is known to regulate calcium homeostasis, the synthesis and release of neuronal monoamines and glutamate, potassium and calcium ion channel regulation, production of growth factors and cytokines, as well as numerous second messengers (Jarskog *et al.*, 1997; Pan *et al.*, 1997; De Simoni and Imeri, 1998; Munoz-Fernandez and Fresno, 1998; Vitkovic *et al.*, 2000; Perry *et al.*, 2002). Furthermore, both TNFα and its receptors are constitutively expressed in various regions of the brain including the cortex, striatum, and thalamus, suggesting a role in normal cellular homeostasis (Vitkovic *et al.*, 2000). Astrocytes and oligodendrocytes

predominantly express TNFα receptor type 1 (TNFR1), though all other neuronal cell types express both TNFR1 and TNFα receptor type 2 (Dopp *et al.*, 1997; Munoz-Fernandez and Fresno, 1998). While the role(s) of TNFα in normal brain function remain unclear, it is likely significant in sleep, as its expression is highest during peak periods of sleep (Bredow *et al.*, 1997). In support, mice lacking TNFR sleep less than control animals (Krueger *et al.*, 1998). TNFα is also probably significant during development, as high levels are observed during the maturation of astrocytes and neurons, but decreases once the cells reach maturity (Munoz-Fernandez and Fresno, 1998). Overall, TNFα likely has a significant role in normal homeostasis within the CNS, including brain regions affected in PD.

Inflammation is likely a contributing factor to the development and propagation of PD. Increases in proinflammatory cytokines have been observed in the striatum of PD brains, including TNFα, IL1-β, and IL-6 (Mogi *et al.*, 1994a; Mogi *et al.*, 1994b; Blum-Degen *et al.*, 1995; Muller *et al.*, 1998). Furthermore, activation of glia has been described in patients with PD and these cells can express and secrete proinflammatory cytokines such as TNFα, IL-1β, and interferon-γ. Significantly, genetic interdiction against proinflammatory proteins including COX2 (Feng *et al.*, 2003), nicotinamide adenine dinucleotide phosphate (NADPH) oxidase (Wu *et al.*, 2003), and both receptors for TNFα (Qin *et al.*, 2007), prevents MPTP-induced degeneration of dopaminergic neurons.

The Gram-negative bacterial endotoxin LPS can initiate neuronal cell loss within the substantia nigra in experimental models (Herrera *et al.*, 2000; Ling *et al.*, 2002; Qin *et al.*, 2007). LPS acts through toll-like receptors to increase the expression of numerous proinflammatory mediators, including IL-1 (Sharif *et al.*, 1993) and-6 (Chung and Benveniste, 1990), as well as mitogen-activated protein kinases (Willis and Nisen, 1996; Schumann *et al.*, 1998), TNFα (Sawada *et al.*, 1989; Chung and Benveniste, 1990), and NOS2 (Simmons and Murphy, 1992). TNFα binds TNF-receptor 1, triggering Fas-mediated apoptosis, resulting in activation of caspase 8 and subsequently the caspase cascade (Ware *et al.*, 1996). Inducible nitric oxide synthetase (NOS2 or iNOS) produces high levels of nitric oxide (NO), which in turn reacts with superoxide radicals to form peroxynitrite, a highly reactive nitrogen species capable of nitrating tyrosine residues, and compromising protein function (Szabo *et al.*, 1995). Recently, LPS-induced inflammation was demonstrated to induce dysfunction of mitochondrial complexes I and II in the substantia nigra as well as the striatum in rats with the prototypical increases in proinflammatory genes, COX2 and NOS2 (Hunter *et al.*, 2007). Therefore, LPS effectively induces neuroinflammation and can also recapitulate other parkinsonian characteristics, including mitochondrial dysfunction.

Animals exposed to LPS provide excellent evidence that neuroinflammation is significant in PD. Intraperitoneal injection of a single dose of LPS in adult mice induces a 23% loss of dopaminergic neurons in the substantia nigra 5 months

after injection, and progressed to 47% lost by 8 months after injection (Qin *et al.*, 2007). Notably, LPS-treated mice had significantly elevated brain TNFα levels for 10 months following injection, though levels in the liver and serum had returned to normal levels within 1 week or 9 hours, respectively. Upregulation of MCP-1, NFκB p65, IL-1β, and TNFα were observed in LPS-treated mice, but not in TNF-1R/2R knockouts (Qin *et al.*, 2007). While it is yet unclear how TNFα levels are sustained at an elevated level so long after exposure, given PD's progressive nature, this observation is especially intriguing. Maternal exposure to bacterial LPS during pregnancy decreases the number of dopaminergic neurons in offspring (Ling *et al.*, 2002; Carvey *et al.*, 2003), likely due to production of proinflammatory cytokines including TNFα, IL-1 α, IL-1β, IL-6, IFN-γ and others (Carvey *et al.*, 2003). Indeed, human exposure to LPS during prenatal development occurs through maternal bacterial vaginosis, a condition with a 14% incidence rate (Thorsen *et al.*, 1998). Additionally, LPS exposure *in utero* has been shown to decrease the number of dopaminergic neurons formed as well as brain dopamine levels in offspring (Bakos *et al.*, 2004), which may predispose individuals to development of PD.

Increasing evidence indicates that PD development may represent a labyrinth of interactions occurring over time, with contributing factors including genetic predisposition, innate attributes of the nigrostriatal system, as well as exposure to environmental toxins (Olanow and Tatton, 1999; Kidd, 2000). Thus, a model utilizing toxin exposure coupled with a genetic predisposition is a biologically

reasonable model for studying the complexity of PD. Transitory elevations in cytokines can be neuroprotective, especially through inhibition of excitotoxicty, though prolonged exposure is equally detrimental. As proinflammatory mediators are significant in promoting neuronal viability, and prolonged inflammation is significant in the pathogenesis of neurodegeneration, alterations in expression of genes related to inflammation were explored in LPS-exposed astrocytes from *DJ-1* mutant mice.

MATERIALS AND METHODS

DJ-1 KNOCKOUT MICE: A gene-trap screening library conducted in embryonic stem cells was utilized, *DJ-1* gene was mutated and chimeric mice were generated (BayGenomics). The precise location of the gene-trap was ascertained and a functional knockout was confirmed via real-time PCR and Western blotting (see CHAPTER 2). Heterozygous mice were bred to establish a colony containing all three genotypes. Primary mouse cortical astrocytes were isolated and maintained as previously described (Allen *et al.*, 2000b).

REAL-TIME PCR: As astrocytes are known to increase expression of proinflammatory proteins following exposure to numerous neurotoxins, we investigated whether *DJ-1*$^{-/-}$ primary astrocytes would display differential reactivity to the inflammatory stimulus LPS. Expression of all these genes is partially dependent upon stimulation by MAPK pathways. To assess which protein(s) of the MAPK pathways are involved in *COX2, NOS2,* and *TNF*α increases following

LPS exposure in astrocytes, we utilized a MEK inhibitor (10μM U0126, Cell Signaling), a p38 inhibitor (30μM SB203580, Calbiochem), or an inhibitor of JNK (10μM JNK Inhibitor II, Calbiochem). Astrocytes were subsequently exposed to PBS or 10μg/mL LPS for 24h, RNA was isolated via the RNeasy Kit (Qiagen) including DNase-treatment on column, per manufacturer's instructions. cDNA was synthesized using iScript (BioRad) per manufacturer's instructions to assess expression of *COX2*, *NOS2*, and *TNFα* via real-time PCR. Relative expression of *COX2* (5' - GGA GTC TGG AAC ATT GTG AAC - 3', 5' - GTA GTA GGA GAG GTT GGA GAA G - 3'), *NOS2* (5' - TCA CGC TTG GGT CTT GTT - 3', 5' - CAG GTC ACT TTG GTA GGA TTT G - 3') or *TNFα* (5' - GCA CCA CCA TCA AGG ACT C - 3', 5' - GAA AGG TCT GAA GGT AGG AAG G - 3') was measured using a BioRad iCycler. Expression was measured via SYBR green incorporation (BioRad), and samples were normalized to *β-actin* (5'-GAC AGG ATG CAG AAG GAG ATT ACT G-3', 5'-GCT GAT CCA CAT CTG CTG GAA-3') via the delta-delta C_T method (Livak and Schmittgen, 2001). As a negative control, samples without reverse transcriptase were also analyzed to assure no DNA contamination was present. *COX2* and *TNFα* expression was analyzed relative to *DJ-1*$^{+/+}$ astrocytes exposed to PBS and DMSO. In all PBS-treated samples, *NOS2* expression was beyond the detection limit, so expression of *NOS2* was analyzed relative to LPS-exposed *DJ-1*$^{+/+}$ levels.

SECRETED TNFα: Astrocytes were cultured as described above in "REAL-TIME PCR," media was collected and immediately stored at -80°C for later analysis.

TNFα levels in culture media samples were determined via an enzyme-linked immunosorbent assay (ELISA, eBiosciences) per manufacturer's instructions.

PHOSPHORYLATION OF KINASES: Primary cortical astrocytes were cultured in serum-free media for 24h, then subsequently exposed to 10μg/mL LPS for 0, 5, 15, 30, 60, 90, or 120 min. To isolate protein, cells were lysed in buffer (50mM Tris, 150mM NaCl, 0.1% SDS, 1% nonidet P-40, 0.5% Na deoxycholate, 2mM Na orthovanadate) supplemented with complete mini protease cocktail inhibitors (Roche). Samples were sonicated for 10 sec at 30% output, placed on ice for 20 min, then centrifuged at 14,000 rpm for 10 min at 4°C. Production of phospho (P) -ERK, -JNK, -p38, or -AKT (ser 473) was analyzed. Protein was subjected to SDS-PAGE, electrotransferred to PVDF, and probed for P-kinases (Cell Signaling, Table 4.1). Protein was detected via chemiluminescence (Pierce). Each blot was stripped in pre-warmed (55-60°C) stripping buffer (6.25mM Tris, 2% SDS, 0.7% β-mercaptoethanol) for 1h at room temperature, and reprobed for non-phosphorylated forms of each MAPK to assure equal loading (data not shown).

NOS2 IMMUNOFLUORESCENCE: NOS2 protein levels in astrocytes were measured using immunofluorescence. Briefly, astrocytes plated on glass coverslips were treated for 24h with 50μM manganese (Mn), cytokines (1ng/mL TNFα + 10pg/mL interferon-γ), 10μg/mL LPS, or manganese in combination with cytokines or LPS. Cells were fixed with methanol, permeabilized with 0.01%

Triton X-100 and then probed for the protein of interest. Primary monoclonal antibody for GFAP and polyclonal antibodies for NOS2 (BD Pharmingen, SanDeigo CA) and phosphorylated ERK (Cell Signaling, Danvers MA) were used at 1:1000, 1:400 and 1:100 respectively. Protein levels were visualized via fluorescence microscopy following hybridization of Alexa Fluor- 488 or 647-labeled secondary antibodies. Fluorescence was normalized to the number of cells assessed. All analysis was accomplished using SlideBook software.

CHROMATIN IMMUNOPRECIPITATION ASSAY: To determine whether LPS induces p65 NFκB binding to the promoter regions of NOS2, the chromatin immunoprecipitation (ChIP) assay was employed. Astrocytes were exposed to PBS or 10μg/mL LPS for 0, 1, 6, or 8 h. Cells were cross-linked with formaldehyde (1%), then detached from the culture plate (5mM PIPES, 85mM KCl, 0.5% NP-40, supplemented with Complete Mini Protease Inhibitor cocktail (Roche)), and pelleted via centrifugation at 5000 RPM for 5 min. Supernatant was discarded, and cells were lysed using nuclear lysis buffer (50mM Tris pH 8.1, 10mM EDTA, 1% SDS, supplemented with Complete Mini Protease Inhibitor cocktail (Roche)) to isolate nuclear protein. Samples were incubated for 1 h with pre-blocked salmon sperm DNA Protein A agarose beads (Upstate) to pull down any non-specific proteins, and then incubated with an anti-p65 antibody (2μg, Santa Cruz) overnight. One untreated sample was not exposed to antibody in order to control for non-specific pull-down by the beads. Prior to antibody exposure, ten percent input controls were removed from samples to assure DNA

degradation had not occurred. Cross-linking was reversed and DNA was extracted via phenol-chloroform (Riccio et al. 2006). To assess if p65 binds to *NOS2* promoter, PCR was utilized with specific primers flanking the proximal κB response element (-87 to -76) found on *NOS2* promoter (5' - ATG GCC TTG CAT GAG GAT ACA CCA - 3', 5' - GAG TCT CAG TCT TCA ACT CCC TGT - 3').

STATISTICAL ANALYSES: All statistical analyses were performed using GraphPad Prism software. Means were analyzed using ANOVA, and they significantly differed ($p<0.05$), Tukey's *post hoc* test was employed.

RESULTS

Interestingly, *DJ-1*$^{+/+}$ and *DJ-1*$^{-/-}$ astrocytes had similar levels of induction of *COX2* (Figure 4.1) and *NOS2* (Figure 4.2) following exposure to LPS, but the relative expression of *TNFα* was significantly decreased in *DJ-1*$^{-/-}$ cells (Figure 4.3). *COX2* expression was not affected by genotype, or by preincubation with U0126 or JNK inhibitor II, however inhibition of p38 significantly decreased *COX2* upregulation (Figure 4.1). Expression of *NOS2* was below our detection limits in all PBS-treated samples, which is consistent with reports that this gene is not constitutively expressed in astrocytes (Moreno *et al.*, 2008). No statistical differences in *NOS2* expression were noted when any of the inhibitors (Figure 4.2) were used or between genotypes ($p>0.05$), however inhibition of JNK and p38 modestly decreased LPS-induced increases in *NOS2* expression. Finally, none of the inhibitors utilized in this study statistically altered *TNFα* expression in

either genotype. Notably, *TNFα* expression was consistently lower in *DJ-1*$^{-/-}$ astrocytes, regardless of treatment with inhibitors (Figure 4.3).

To verify that decreased expression of *TNFα* in *DJ-1*$^{-/-}$ astrocytes is physiologically relevant, secretion of TNFα into the culture media was analyzed. Levels of TNFα in all PBS-treated samples were below the assay detection limit (8pg/mL); therefore, only LPS-treated samples are graphically represented (Figure 4.4). Basal LPS-induced secretion of TNFα (i.e., DMSO-treated samples) into media samples was lower from *DJ-1*$^{-/-}$ compared to *DJ-1*$^{+/+}$ astrocytes ($p<0.001$). Inhibition of JNK significantly decreased levels of secreted TNFα into *DJ-1*$^{+/+}$ but not *DJ-1*$^{-/-}$ media. Inhibition of p38 decreased secretion of TNFα from both *DJ-1*$^{+/+}$ and *DJ-1*$^{-/-}$ astrocytes. In all treatment scenarios, the concentration of TNFα was significantly lower in *DJ-1*$^{-/-}$ versus *DJ-1*$^{+/+}$ media ($p<0.05$).

In order to validate upregulation of NOS2 protein following exposure to LPS and other treatments, astrocytes were probed for NOS2. Following exposure to LPS, NOS2 levels were insignificantly lower in *DJ-1*$^{-/-}$ cells in all experimental conditions (Figure 4.5). Only coexposure to cytokines and LPS significantly increased NOS2 production in either *DJ-1*$^{+/+}$ or *DJ-1*$^{-/-}$ above the level observed in vehicle-exposed cells.

To determine the appropriate time to assess LPS-induced phosphorylation of ERK, JNK, p38 or AKT, a time-course following LPS exposure was conducted,

and protein was extracted and assayed by Western blotting as described in CHAPTER 2. By 5 min following LPS exposure, all protein phosphorylation levels increased (Figure 4.6). Phospho-ERK increased at 5 and 15 min, and by 120 min was back to baseline values. Phospho-JNK increased also at 5 and 15 min, and stayed elevated through 120 min. Phospho-p38 increased at 5 and 15 min, and subsequent times were similar to time 0 values. Phospho-Akt (Ser 473) increased at 5 and 15 min as well, and then quickly returned to baseline levels.

The ChIP assay was used to determine how soon after LPS exposure binding of p65 could be detected at the NOS2 promoter. Following 1 h of exposure, p65 NFκB binding was detected at the NOS2 promoter region, and that binding was also detected at all other time points analyzed (Figure 4.7). Input controls confirmed that lack of binding at 0h was not due to sample degradation.

DISCUSSION AND CONCLUSIONS

Our data describing a decline in expressed and released TNFα from *DJ-1*$^{-/-}$ cells is first in reporting any alteration of any cytokine attributable to mutation of *DJ-1*. It is noteworthy that upregulation of these factors in astrocytes is primarily designed as a cytoprotective effect, though prolonged exposure to proinflammatory mediators is detrimental to neurons. Therefore, while *DJ-1*$^{-/-}$ mutation might not exacerbate effects during later stages of PD when pathogenic levels of cytokines are observed, it is possible that mutation of *DJ-1*$^{-/-}$ in fact promotes early degeneration of dopaminergic neurons by failing to provide

sufficient preventative/protective measures against neuronal demise. Specifically, TNFα has been shown to prevent excitotoxicity, and mice lacking TNF receptor-2 (Fontaine *et al.*, 2002) are more susceptible to ischemic neurotoxicity. Also, pretreatment of cultured mesencephalic neurons with TNFα decreased excitotoxicity in a dose-dependent manner (Shinpo *et al.*, 1999) and inhibition of TNFα via siRNA increases 6-hydroxydopamine-induced striatal degeneration (Gemma *et al.*, 2007), highlighting the neuroprotective role of TNFα in the CNS. Therefore, it is possible that decrease in TNFα expression and secretion induced by *DJ-1* mutation decreases astrocytic support of neuronal viability during early neurodegeneration.

As expression of *COX2, NOS2,* and *TNFα* are all upregulated in response to LPS, an effect predominantly mediated by NFκB, it is surprising that *DJ-1*$^{-/-}$ astrocytes have lower expression of only *TNFα*. By analyzing levels of TNFα in media, we have verified that decreased expression does lead to a decline in secreted levels of TNFα by *DJ-1*$^{-/-}$ astrocytes. The mouse *TNFα* promoter has numerous κB sites (Kuprash *et al.*, 1999). It is possible that mutation of *DJ-1* prevents a key coactivator from participating in NFκB binding, thus resulting in the blunted response observed in our studies. DJ-1 is known to prevent PIASχα from negatively regulating the androgen receptor (Takahashi *et al.*, 2001), so removal of DJ-1 might negatively affect genes downstream of this protein, and a yet unidentified protein could mediate similar effects in *TNFα* regulation. A recent report by Mo and colleagues suggests that MEKK1 requires functional DJ-1 for

full activation (Mo *et al.*, 2008). As MEKK1 phosphorylates and activates IκB kinase (Lee *et al.*, 1998), it is possible that mutation of *DJ-1* decreases overall phosphorylation of IκB, by eliminating its activation via MEKK1. Because TNFα has numerous κB binding sites in it promoter, it may not be fully activated, thereby leading to a decrease in LPS-stimulated expression. Other proteins that are not known to regulate *COX2* or *NOS2*, including Bcl3 (Hirotani *et al.*, 2005), Atf2 (Novotny *et al.*, 1998), Egr1 (Shi *et al.*, 2002b; Shi *et al.*, 2002a), and Stat proteins 3, 5a, 5b, and 6 (Lu *et al.*, 1998; Chappell *et al.*, 2000), also regulate the *TNFα* promoter. While DJ-1 interaction with these proteins has not been studied, it is possible that DJ-1 transiently interacts with one or more of these proteins, or acts further upstream to modulate regulation of *TNFα*.

Inhibition of MEK, p38, or JNK did not induce differential expression of proinflammatory mediators in *DJ-1*$^{+/+}$ versus *DJ-1*$^{-/-}$ astrocytes. However, we established that expression of our three genes of interest did not respond identically to inhibition of MAPKs. Inhibition of p38 alone decreased expression of *COX2*. Although not statistically significant, inhibition of p38 tended to decrease expression of *NOS2* in both *DJ-1*$^{+/+}$ (p=0.11) and *DJ-1*$^{-/-}$ (p=0.07) astrocytes. Neither MEK nor JNK inhibition affected expression of *NOS2*. No expression changes in *COX2* were induced by inhibition of MEK, JNK, or p38. However, expression of *COX2* was lower in *DJ-1*$^{-/-}$ astrocytes. Interestingly, MEK inhibition did not affect secretion of TNFα in either genotype, whereas significant decreases were observed in *DJ-1*$^{+/+}$ astrocytes treated with JNK inhibitor II, and

inhibition of p38 decreased secretion in both genotypes. We verified that these concentrations of inhibitors did indeed decrease phosphorylation of ERK (U0126), JNK (JNK inhibitor II), and p38 (SB203580, data not shown). As neuroinflammation and reactive astrocytosis are clearly involved in the pathogenesis of PD as well as many other neurological disorders, the response of astrocytes to proinflammatory stimuli, such as LPS warrants investigation. While we would have anticipated that mutation of *DJ-1* would increase expression of proinflammatory proteins following LPS exposure, upregulation of *TNFα* was lower in *DJ-1*$^{+/+}$ astrocytes compared to *DJ-1*$^{+/+}$ cells. No other data to date has demonstrated alterations in *TNFα* expression due to knockout, knockdown, or even overexpression of *DJ-1*; therefore how this expression is decreased is unclear. Because the etiology of PD is still enigmatic, the early neuronal changes that occur with this disease are still largely unknown. Thus, whether mutation of *DJ-1*$^{-/-}$ would increase neuronal degeneration via lack of protective cytokine secretion is unclear in the context of development of PD. However, given the cytoprotective effects of TNFα, it is likely that decreasing the secretion of this cytokine from astrocytes would be detrimental to neuronal viability.

NOS2 protein production increased following coexposure to 10μg/mL LPS in combination with 50μM Mn, but not to either treatment individually. Interestingly, *DJ-1*$^{-/-}$ astrocytes tended to have lower NOS2 levels in all treatment regimes, though it was not significantly lower. Subsequent studies in our laboratory have

indicated that maximal production of NOS2 protein occurs approximately 8h following exposure to LPS (data not shown). So, while LPS alone should be sufficient to induce NOS2, it is possible that our 24h time point was beyond the ideal time to analyze protein production of NOS2, and therefore may have declined to levels indistinguishable statistically from baseline.

Numerous phosphorylation cascades have been implicated in LPS-induced upregulation of proinflammatory mediators (Zhu *et al.*, 2000), including *COX2*, *NOS2*, and *TNFα*. To determine actual phosphorylation of proteins following LPS exposure, immunoblotting of P-ERK, P-JNK, P- p38, and P-AKT (ser 473) was monitored over time. While these preliminary studies provide no insight into genotype specific alterations or lack thereof in protein phosphorylation, the exposure time of LPS has been verified, so that phosphorylation of these proteins under LPS-stimulated conditions can be ascertained when *DJ-1*$^{-/-}$ astrocytes and/or inhibitors are used. This will provide further insight into the pathways controlling expression of *COX2*, *NOS2*, and *TNFα* in our *DJ-1*$^{+/+}$ and *DJ-1*$^{-/-}$ astrocytes.

In summary, mutation of *DJ-1* decreases LPS-induced expression of *TNFα* and its secretion through yet unknown mechanisms. This finding is the first to suggest TNFα induction could be influenced by DJ-1, therefore, possibly providing insight into DJ-1's role in cellular homeostasis. As anticipated, LPS rapidly induced phosphorylation of ERK, JNK, p38 and AKT, proteins that may contribute to the

differential expression of TNFα in our *DJ-1*$^{-/-}$ astrocytes. Furthermore, within an hour of exposure to LPS, p65 binding to the NOS2 proximal κB site was detected, therefore we can successfully detect, via the ChIP assay, any genotype specific alterations in binding of NFκB to the promoters of NOS2, COX2 or TNFα. Future studies are needed to discern the mechanism by which DJ-1 alters LPS-induced TNFα expression and secretion, and what the physiological consequences of this alteration are within the context of DJ-1 related disease(s).

CHAPTER 4

TABLE AND FIGURES

COX2 EXPRESSION

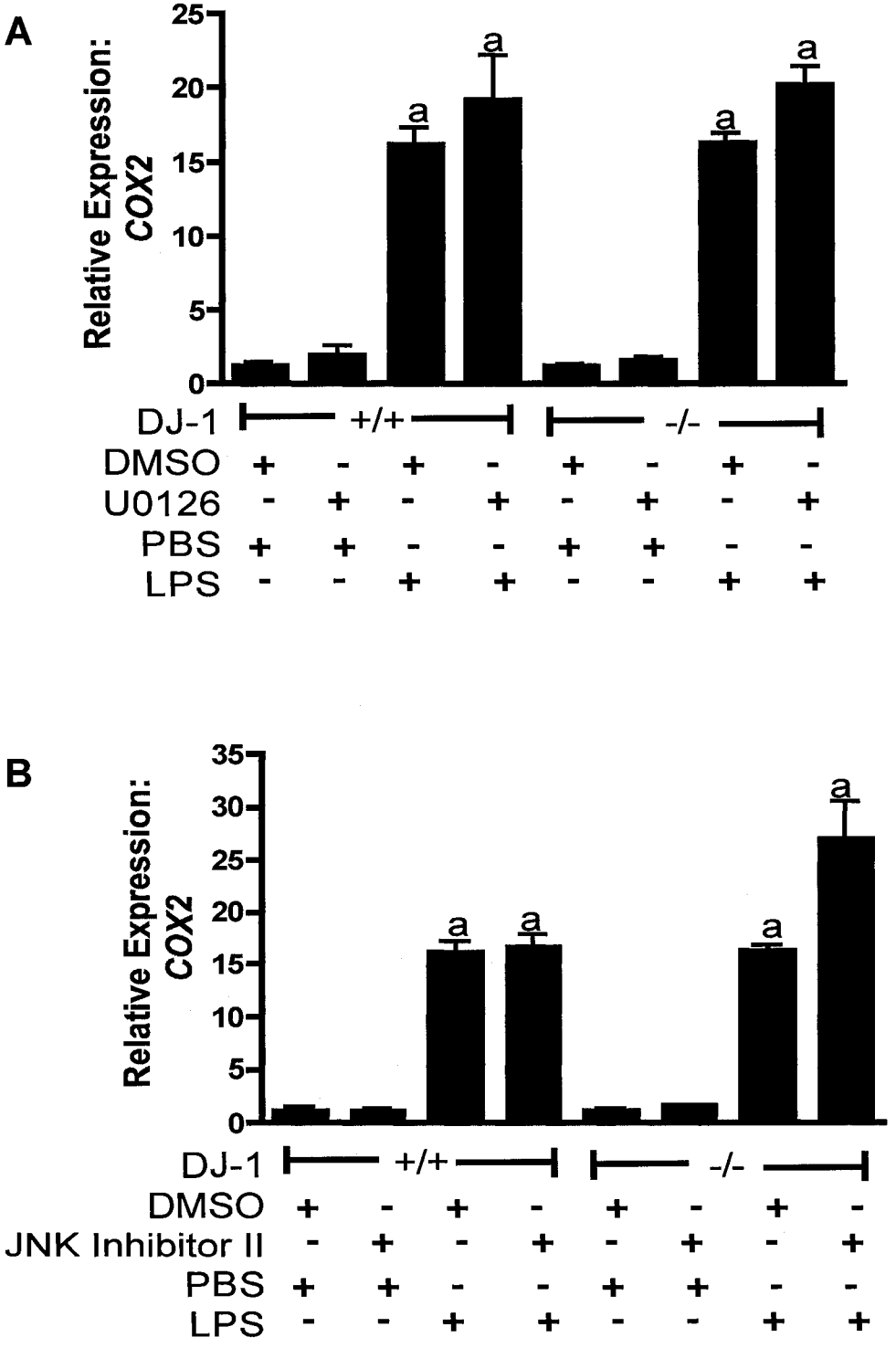

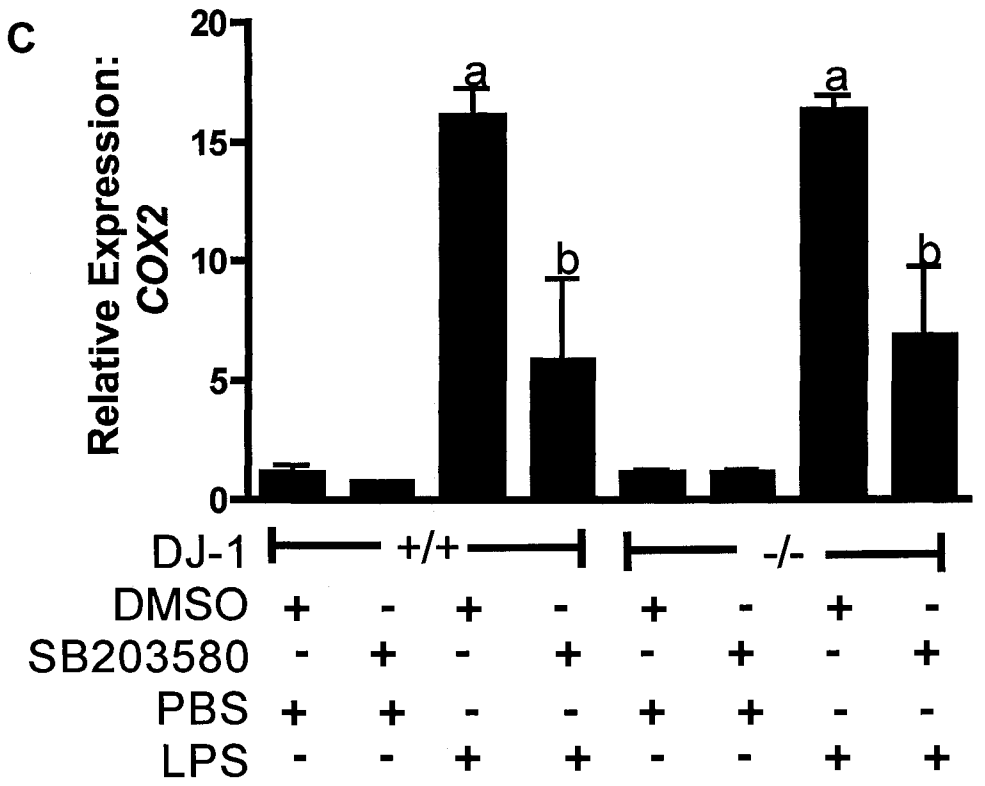

Figure 4.1. LPS-induced relative expression of *COX2* decreases with inhibition of p38 but not MEK or JNK. Astrocytes were exposed to DMSO, U0126 (MEK inhibitor, 10μM), JNK inhibitor II (10μM), or SB203580 (p38 inhibitor, 30μM) for 2h, then PBS or 10μg/mL LPS for 24h, and RNA was isolated. Expression of *COX2* was determined via real-time PCR, and values are expressed relative to *DJ-1*$^{+/+}$ cells exposed to DMSO and PBS. Bars with differing letters significantly differ from one another ($p<0.05$). LPS significantly increased expression of *COX2* in all exposed samples (A,B,C, $p<0.001$). No genotype-specific alterations occurred, but inhibition of p38 (C) decreased *COX2* relative expression in both genotypes ($p<0.05$).

NOS2 EXPRESSION

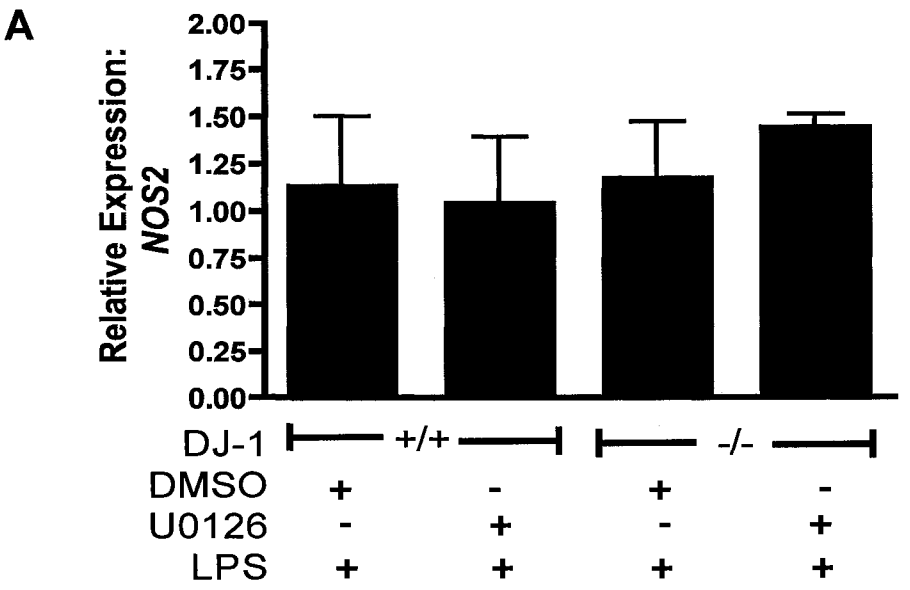

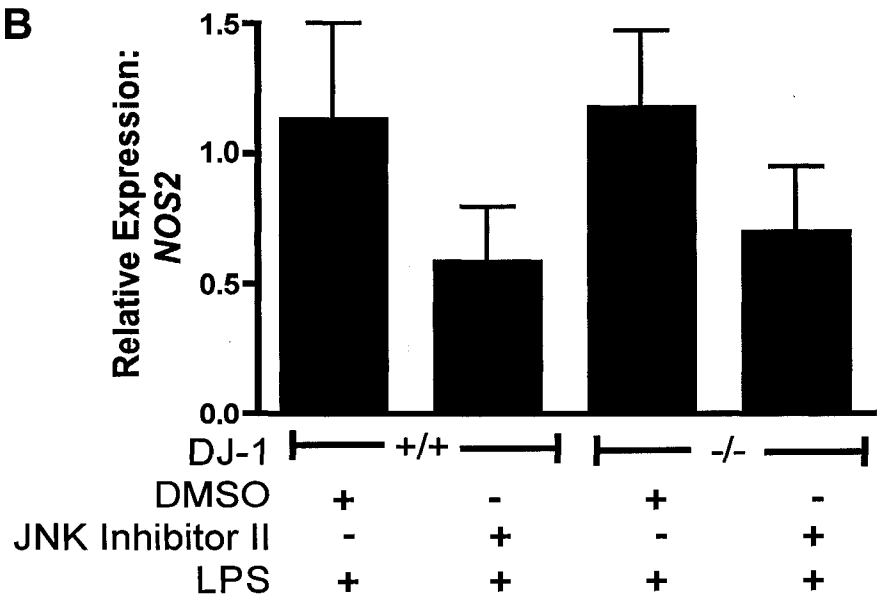

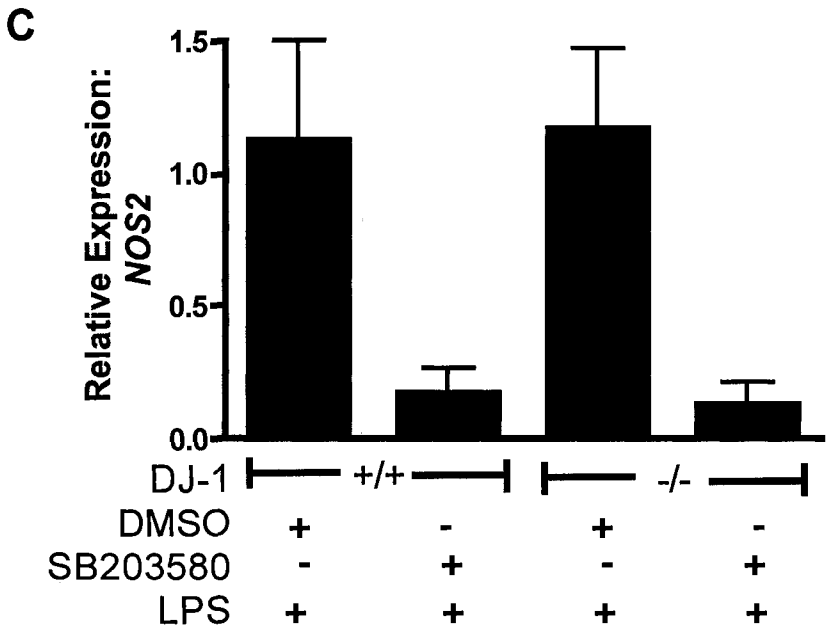

Figure 4.2. LPS-induced relative expression of *NOS2* tends to decrease with inhibition of p38 but not MEK or JNK. Astrocytes were exposed to DMSO, U0126 (MEK inhibitor, 10μM), JNK inhibitor II (10μM), or SB203580 (p38 inhibitor, 30μM) for 2h, then PBS or 10μg/mL LPS for 24h, and RNA was isolated. Expression of *NOS2* was determined via real-time PCR, and values are expressed relative to *DJ-1*$^{+/+}$ cells exposed to DMSO and LPS, as all expression levels in PBS-treated samples were too low to detect. Bars with differing letters significantly differ from one another ($p<0.05$). *NOS2* expression was similar in all groups (A,B,C $p>0.05$), though p38 inhibition tended to decrease expression (C, *DJ-1*$^{+/+}$ $p=0.11$, *DJ-1*$^{-/-}$ $p=0.07$).

TNFα EXPRESSION

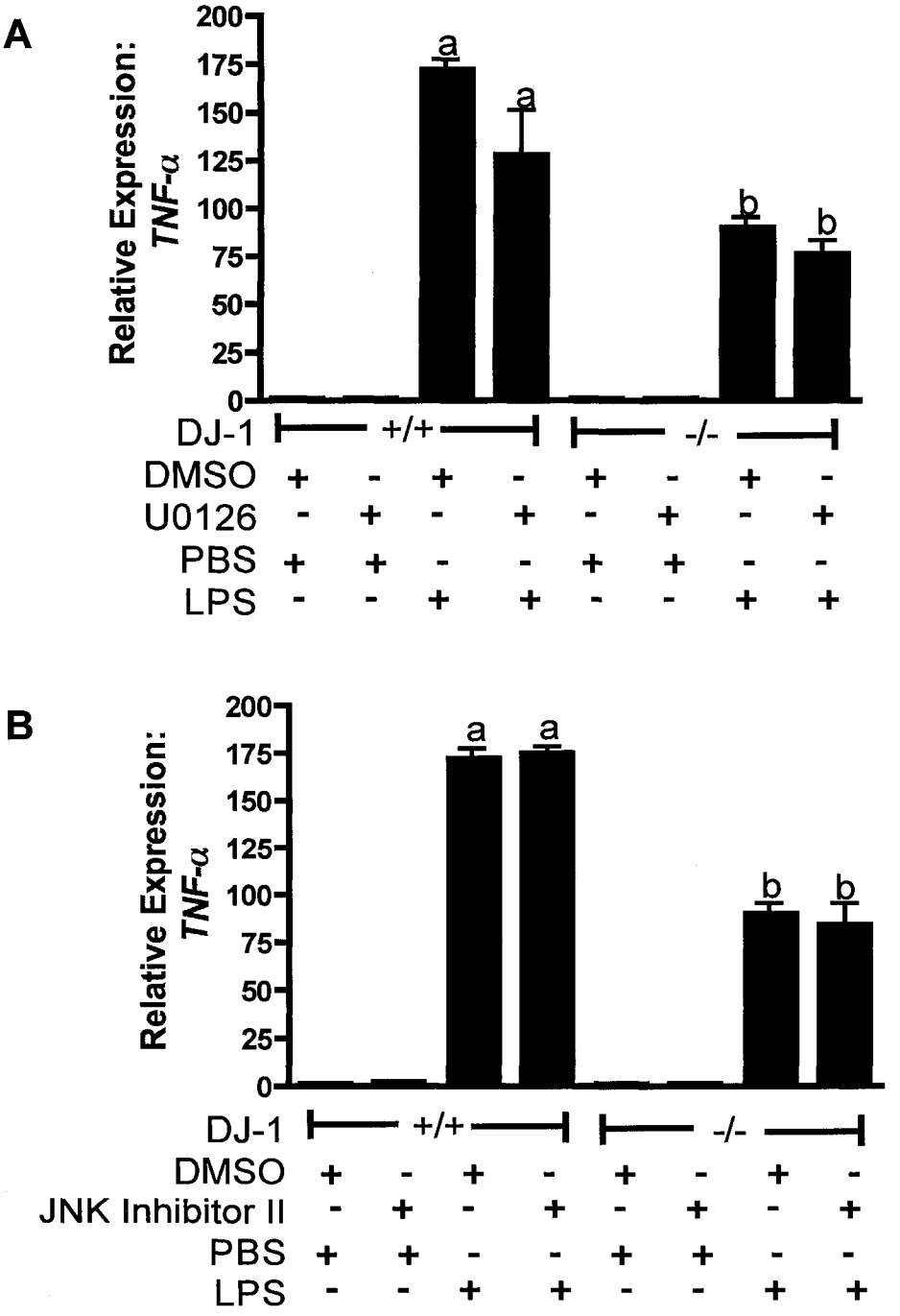

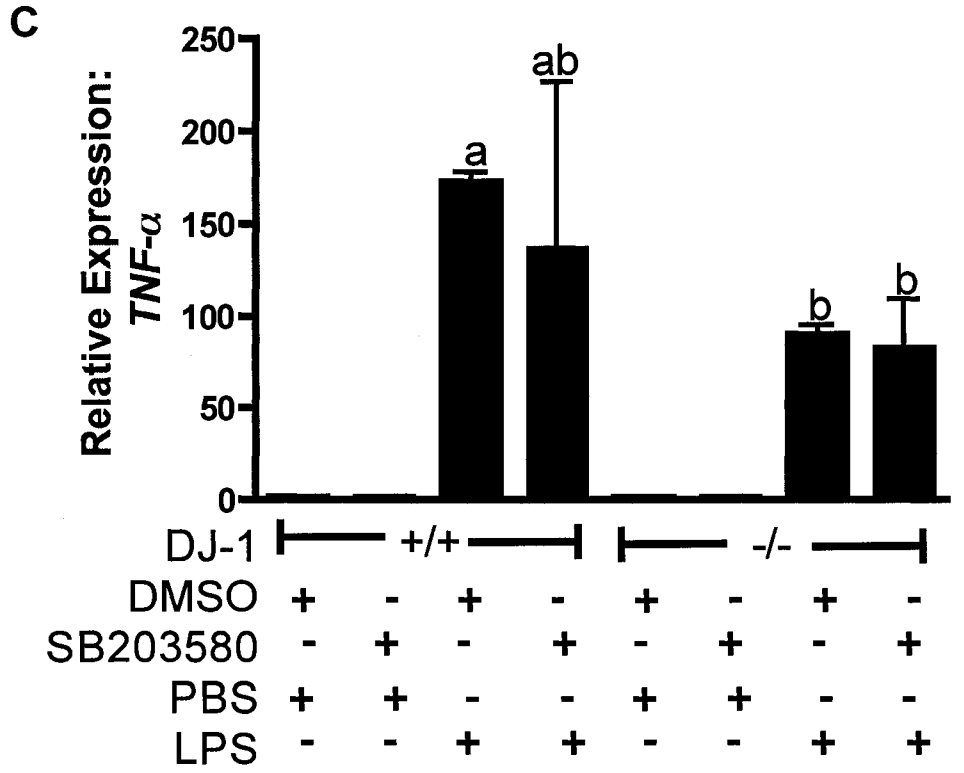

Figure 4.3. LPS-induced relative expression of *TNFα* is lower in *DJ-1*$^{-/-}$ astrocytes, and does not decrease following inhibition of MEK, JNK, or p38. Astrocytes were exposed to DMSO, U0126 (MEK inhibitor, 10μM), JNK inhibitor II (10μM), or SB203580 (p38 inhibitor, 30μM) for 2h, then PBS or 10μg/mL LPS for 24h, and RNA was isolated. Expression of *TNFα* was determined via real-time PCR, and values are expressed relative to *DJ-1*$^{+/+}$ cells exposed to DMSO and PBS. Bars with differing letters significantly differ from one another ($p<0.05$). *TNFα* expression was significantly lower in all *DJ-1*$^{-/-}$ cells regardless of exposure to inhibitor ($p<0.01$). No inhibitor altered expression of *TNFα*.

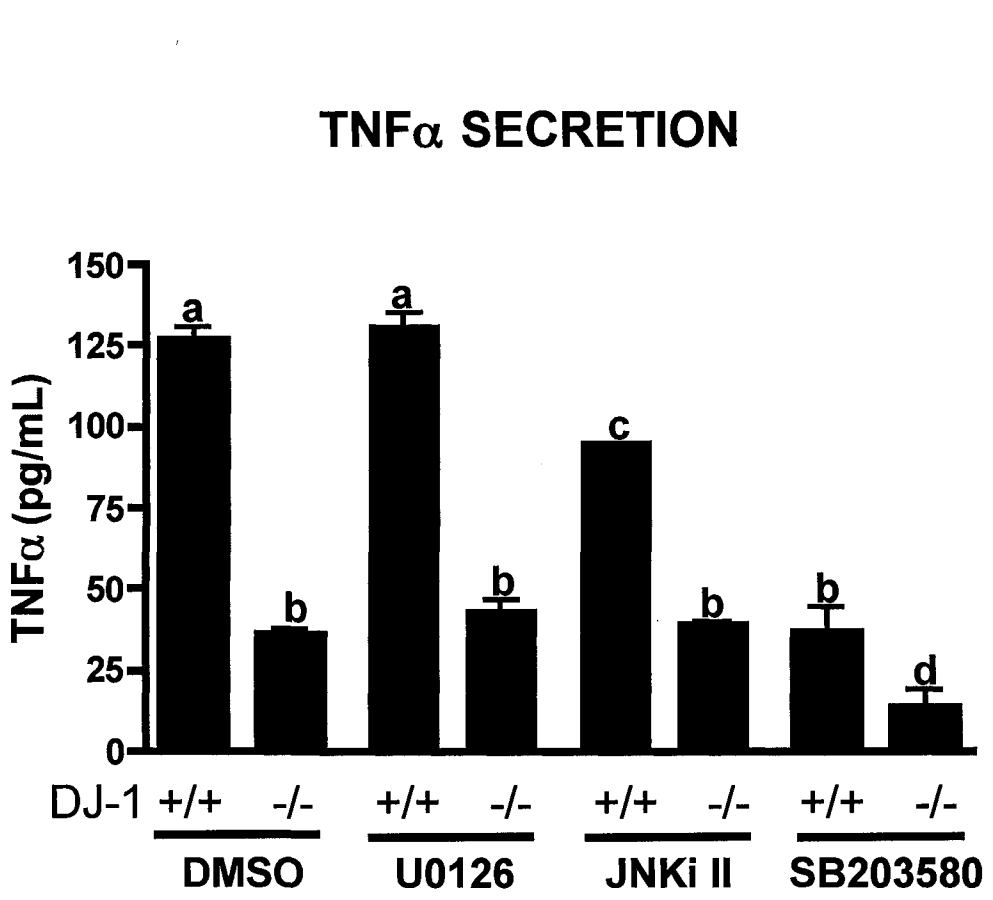

Figure 4.4. Mutation of *DJ-1*$^{-/-}$ decreases secretion of TNFα from astrocytes exposed to LPS. Astrocytes were exposed to DMSO, U0126 (MEK inhibitor, 10μM), JNK inhibitor II (JNKi II,10μM), or SB203580 (p38 inhibitor, 30μM) for 2h, then PBS or 10μg/mL LPS for 24h, and culture media was collected. Secretion of TNFα into culture media was determined via ELISA (eBiosciences). Bars with differing letters significantly differ from one another ($p<0.05$). Levels of TNFα in all PBS-treated samples were below the assay detection limit (8pg/mL). Without exposure to inhibitors, LPS-induced secretion of TNFα was lower in *DJ-1*$^{-/-}$ compared to *DJ-1*$^{+/+}$ ($p<0.001$). Inhibition of JNK decreased levels of TNFα in *DJ-1*$^{+/+}$ media ($p<0.01$). Inhibition of p38 decreased secretion of TNFα from both *DJ-1*$^{+/+}$ and *DJ-1*$^{-/-}$ astrocytes ($p<0.05$).

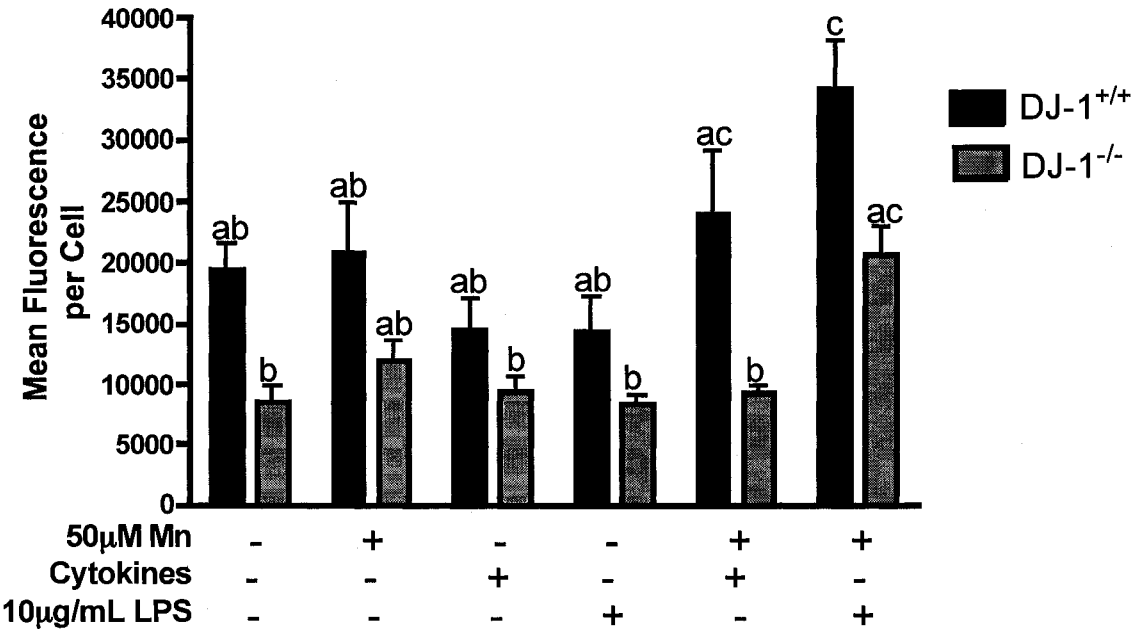

Figure 4.5. NOS2 production increases with coexposure to manganese and LPS. Primary astrocytes were exposed to 50μM manganese (Mn), cytokines (1ng/mL tumor necrosis factor α and 10pg/mL interferon γ), 10μg/mL LPS, or manganese in combination with cytokines or LPS for 24h. NOS2 was detected via immunofluorescence, and expressed per number of cells assessed. Bars with differing letters significantly differ ($p<0.05$).

Table 4.1. Antibody concentrations and amount of protein used in immunoblots. Antibodies were attained from Cell Signaling Technologies and immunoblot parameters were optimized for each.

Phospho Protein	Antibody Concentration	Protein Loaded (μg)
ERK	1:4,000	10
JNK	1:2,000	15
p38	1:1,000	15
AKT (ser 473)	1:1,000	15

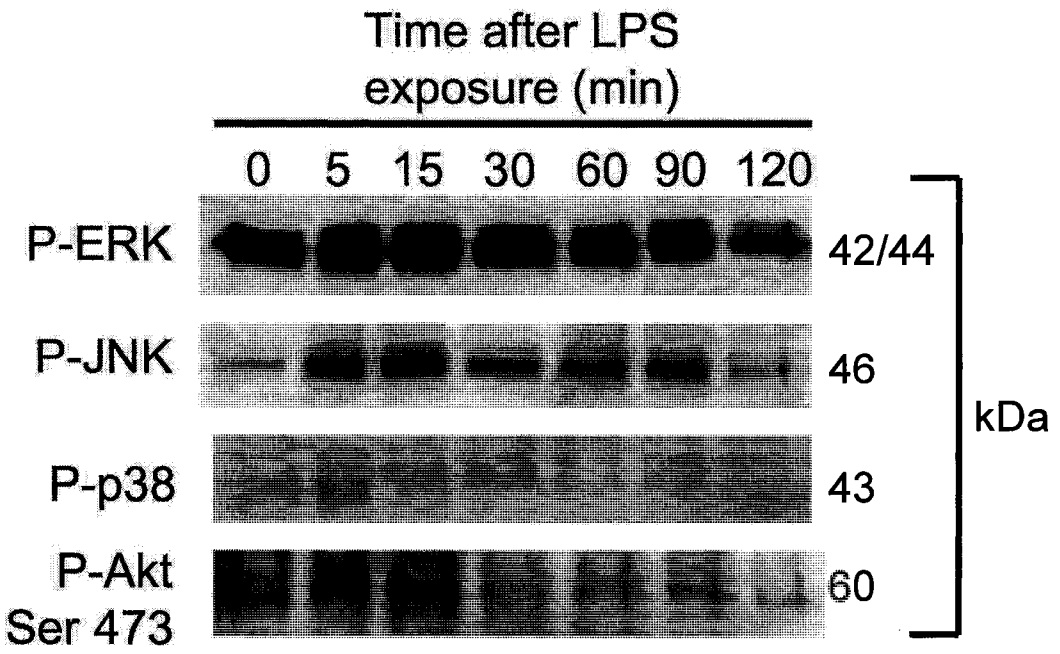

Figure 4.6. LPS induces rapid phosphorylation of MAPK proteins. Astrocytes were serum-starved for 24h, and then exposed to 10μg/mL LPS for 0, 5, 15, 30, 60, 90, or 120 min. Protein was isolated and expression of phospho-ERK, phospho-JNK, phospho-p38, or phospho-AKT (ser 473) was analyzed. Phospho-ERK increased at 5 and 15 min, and by 120 min at below baseline values. Phospho-JNK (46kDa) increased also at 5 and 15 min, and stayed elevated until 120 min, although the 54kDa form was not detected. Phospho-p38 increased at 5 and 15 min, and subsequent times were similar to time 0 values. P-Akt (Ser 473) increased at 5 and 15 min as well, then quickly returns to baseline levels.

CHROMATIN IMMUNOPRECIPITATION ASSAY

Samples

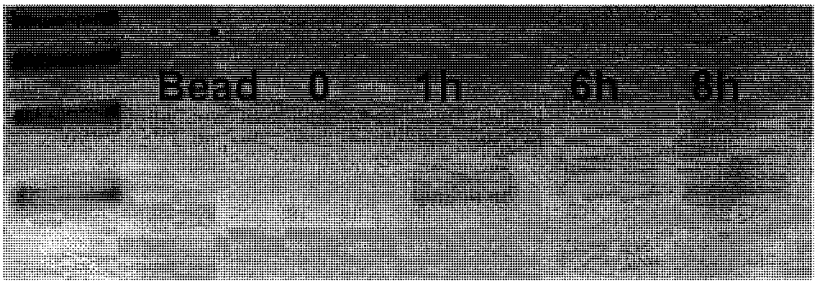

Input Controls

Figure 4.7. LPS induces binding of NFκB to the NOS2 promoter. The chromatin immunoprecipitation assay was employed to analyze astrocytes exposed to 10μg/mL LPS for 0, 1, 6, or 8h with an anti-p65 antibody and primers designed to flank the proximal κB response elements of the NOS2 promoter. Following 1h of exposure, NFκB binding was detected at the NOS2 promoter region. Input controls unexposed to antibody were sampled to assure that a lack PCR product following exposure to antibody was not due to degradation of DNA.

CHAPTER 5

CONCLUSIONS

FINAL CONCLUSIONS

As the percentage of the population 65 years and older increases, also will the incidence of neurodegenerative diseases such as PD, and the demand for novel, effective therapeutic strategies. The experiments proposed herein are the first step towards elucidating the physiological significance of *DJ-1* mutation in astrocytes. Indeed further investigation into the contribution of DJ-1 in neurological dysfunction may produce novel mechanism for describing PD etiology as our model incorporates a number of factors, which putatively contribute to development. Furthermore, by unraveling *DJ-1*'s role in PD, we may highlight new targets for therapeutics to combat this crippling neurodegenerative ailment.

Decrease in resting mitochondrial membrane potential in *DJ-1*$^{-/-}$ astrocytes is noteworthy because not only are glia critical in maintaining neuronal vitality, but subtle perturbations in their function may provide an environment less conducive to neuronal function. Furthermore, astrocytes supply neurons with lactate, their primary oxidative substrate, and utilize glutamine synthase to convert glutamate released by neurons into glutamine, which they subsequently release to neurons in order to provide neurotransmitters required for neuronal function. Also, astrocytes are extremely critical in regulating the extracellular environment, including uptake of neurotransmitters to prevent excitotoxicity, modulating the delicate balance between vasoconstriction and vasodilation, as well as too many

other roles to name. If astrocytes experience subtle alterations in their own physiology, they may be less able or likely to provide neurons with the numerous substrates required to sustain neuronal vitality. Furthermore, the overt phenotype observed would be neuronal cell death, despite the dysfunction occurring in the astrocyte, making the true physiological mechanism insidious. Maintaining the mitochondrial membrane potential is critical not only for production of ATP, but also regulating apoptosis, sequestering intracellular compounds, and maintaining the oxidative environment of the cell. In an astrocyte, who bears the double burden of supplying nutrients and antioxidants to itself as well as neurons, compromising this tightly controlled gradient is likely detrimental to both cell types. Though rotenone did not exacerbate this phenotype, other mitochondrial toxins, perhaps functioning through different mechanism(s) of action might do so, inducing a significant mitochondrial phenotype in *DJ-1*$^{-/-}$ astrocytes.

VEGF expression is critical in not only neurodegeneration, but also carcinogenesis. In cancer, the ability of initiated cells to induce *VEGF* differentiates tumor size, as angiogenesis is necessary for tumors to receive sufficient blood flow to flourish. The contribution of VEGF to neurodegenerative disease remains largely unknown, as alterations in vascular regulation are just beginning to be appreciated as a major factor in neuropathogenesis. In neural tissues, decline in VEGF may negatively impact vascular regulation in the CNS, which in turn would affect blood flow. Though it is unlikely that mutation of *DJ-1*

induces neurodegeneration primarily by suppression of *VEGF* expression, especially at such modest levels, this may contribute to furthering disease progression. While our seemingly opposite expression of *VEGF* and *HIF1α* in lung tissue is difficult to interpret, it is notable that alterations in expression of both genes occur in animals harboring mutation of *DJ-1* without treatment, especially as DJ-1 may contribute to carcinogenesis in this tissue. As overexpression of *DJ-1* is associated with carcinogenesis, perhaps mutation DJ-1 is protective against development of carcinogenesis in many tissues. However, it is unlikely that upregulation of the proangiogenic factor VEGF would be the mechanism of protection, as this would promote development of carcinogenesis. While down-regulation of *HIF1α* would be more conducive to decreasing carcinogenic potential, one of this proteins primary targets in promoting carcinogenicity is inducing expression of *VEGF*, so this is again an unlikely linkage between DJ-1 and cancer. Clearly, much research in this area is needed to fully elucidate the contribution of DJ-1 to regulation of neurovascular coupling and angiogenesis.

Because astrocytes react to various stimuli via increases in intracellular Ca^{2+} levels, altering these signaling mechanisms can significantly impact various trphic and cell-cell communication parameters. Although our Ca^{2+} trace graphs depict a delayed return to baseline levels, in actuality the increase in number of Ca^{2+} oscillations in our *DJ-1*$^{-/-}$ astrocytes accounts for the Ca^{2+} trace. Though perhaps not the ideal depiction of the overall activity of the astrocytes, the

increase in frequency of intracellular Ca^{2+} events is, in itself, a significant finding. Because it is critical in so many aspects of astrocyte function, regulation of Ca^{2+} in the astrocyte is tightly controlled, and our data reveals that *DJ-1*$^{-/-}$ astrocytes likely have some basic alterations in this system. The physiological significance of this finding requires further investigation, however, it is likely that astrocyte dynamics are not properly functioning, resulting in alterations in perhaps extracellular concentrations of potassium, ATP, or neurotransmitters, or even neurovascular coupling.

The link between altered intracellular Ca^{2+} signaling in *DJ-1*$^{-/-}$ astrocytes and decreased expression of *VEGF* may point to deficits in normal functional hyperemia in *DJ-1*$^{-/-}$ mice. In fact, as *DJ-1*$^{-/-}$ but not *DJ-1*$^{+/+}$ astrocytes exposed to 50μg/mL LPS failed to produce a meaningful peak in intracellular calcium following exposure to ATP, it is possible they would be unable to stimulate vasodilation following an action potential. Therefore, through both decreased *VEGF* expression as well as insufficient intracellular Ca^{2+} levels being attained, the surrounding tissue would likely suffer increased hypoxia. Increases in intracellular Ca^{2+} must reach a critical threshold in order to stimulate opening of the BK potassium channel (Filosa *et al.*, 2006). Release of potassium from astrocytic endfeet results in hyperpolarization of the arteriolar smooth muscle cells, causing dilation in a Ca^{2+} dependant manner, thus increasing blood flow (Filosa *et al.*, 2006). Inability of *DJ-1*$^{-/-}$ astrocytes to reach this threshold would result in decreased perfusion following an action potential, preventing

replenishment of affected astrocytes and an increasingly hypoxic environment. Hypoxic conditions normally drive expression of *VEGF* (See CHAPTER 2), but as *DJ-1*$^{-/-}$ neural tissue expresses less than *DJ-1*$^{+/+}$ counterparts, under-expression of this proangiogenic factor might well serve to exacerbate the hypoxic phenotype, accelerating neuronal degeneration. However, it is important to note that alterations in expression of *HIF1α,* a gene who is even named for its classical induction by hypoxia, are not observed. Therefore, either induction of *HIF1α* is not observed due to the experimental design (i.e., no chemical treatment, one time point during early adulthood), or hypoxia is not occurring in these animals. Exploration into the possibility that *DJ-1*$^{-/-}$ leads to increased hypoxia could prove interesting, and would also serve to link alterations in DJ-1 with additional neurological conditions.

Alterations in *TNFα* are intriguing in the context of *DJ-1* mutation induced PD. High levels of TNFα can activate proinflammatory processes through interactions with the TNFα receptors, a mechanism thought to contribute to neuronal degeneration in PD. However, TNFα is released from cells in response to stress predominantly as a cytoprotective element, serving to prevent further injury, and has an important role in normal neuronal viability. We observed a decrease in *TNFα* expression in our *DJ-1*$^{-/-}$ astrocytes while expression of *COX2* and *NOS2* remained unchanged, and release of TNFα into the culture media was consistent with this decline. Clearly, mutation of *DJ-1* in not exacerbating the neuroinflammatory response, however inhibiting synthesis and release of TNFα

is perhaps a subtler neurotoxic event. In fact, as TNFα may prevent against neuronal injury, especially excitotoxicity, it is possible that mutation of *DJ-1* may increase neuronal susceptibility to this injury by preventing secretion of normal neuroprotective cytokines. Further investigations into this phenotype are required, but determining whether this decrease in cytokine secretion from neighboring astrocytes translates into compromising neuronal viability could prove quite interesting in PD.

Based upon these studies, investigating the possibility that mutation of *DJ-1* decreases secretion of cytoprotective endogenous compounds, such as neurotrophic factors, from astrocytes is the next logical step. Towards this end, coculture of primary cells could provide direct evidence that *DJ-1* mutation decreases astrocytic support of neuronal viability. Pairing *DJ-1*$^{+/+}$ astrocytes with *DJ-1*$^{+/+}$ or *DJ-1*$^{-/-}$ neurons and assessing cell death compared to *DJ-1*$^{-/-}$ astrocytes cultured with the same neurons would indicate whether *DJ-1* mutation prevents astrocytic support of neuronal viability. Furthermore, assessment of the culture media for secreted cytokines could indicate if alterations in neurotrophic factors aside from TNFα are induced by mutation of *DJ-1.* In addition to LPS, treatment with glutamate, could be employed in these experiments to mimic excitotoxicity-mediated neuronal degeneration of PD. Astrocytes can be cultured on wire mesh inserts, which are capable of remaining in suspension above the plated neurons. Therefore, any change in neuronal viability would be attributable to secreted factors rather than direct contact between the two cell types. Further, this allows

physical separation after exposure of neurons to astrocytes, permitting further molecular characterization of each. Secondly, *in vivo* experimentation would be a powerful mechanism to further explore the possibility that astrocytes fail to produce sufficient neurotrophic support. As systemic LPS exposure is capable of inducing progressive neurodegeneration, *DJ-1*$^{+/+}$ or *DJ-1*$^{-/-}$ mice could be exposed to this compound. Further, a cytokine array could be utilized to determine *in vivo* what compounds are being differentially regulated in *DJ-1*$^{-/-}$ compared to *DJ-1*$^{+/+}$ mice. These experiments could be useful in determining whether or not decrease in cytokine production from astrocytes, induced by mutation of *DJ-1* would concomitantly compromise neuronal viability.

Though much information presented does not provide a definitive role for DJ-1 in physiology, it is noteworthy that this protein has only gained substantial interest within the last few years. Because multiple roles for DJ-1, interacting with numerous proteins, have been suggested, it is likely this protein may mediate a number of cellular responses, which remain to be fully discerned. Its ubiquitous expression throughout the body also suggests it may function as a stress-response protein, though no overt experimental evidence suggests this at present. However, because DJ-1 is implicated in a myriad of conditions, research into this intriguing protein warrants further investigation, whether as a breast cancer target, a potential therapeutic to decrease ischemia/reperfusion injury, or prevention of neurological disorders. Therefore, the studies described here provide further information as to the role of DJ-1 in cellular physiology.

LITERATURE CITED

Abou-Sleiman, P. M., Healy, D. G., Quinn, N., Lees, A. J., and Wood, N. W. (2003). The role of pathogenic DJ-1 mutations in Parkinson's disease. *Ann Neurol* **54**, 283-286.

Alam, M., and Schmidt, W. J. (2002). Rotenone destroys dopaminergic neurons and induces parkinsonian symptoms in rats. *Behav Brain Res* **136**, 317-324.

Aleyasin, H., Rousseaux, M. W., Phillips, M., Kim, R. H., Bland, R. J., Callaghan, S., Slack, R. S., During, M. J., Mak, T. W., and Park, D. S. (2007). The Parkinson's disease gene DJ-1 is also a key regulator of stroke-induced damage. *Proc Natl Acad Sci U S A* **104**, 18748-18753.

Alkayed, N. J., Birks, E. K., Hudetz, A. G., Roman, R. J., Henderson, L., and Harder, D. R. (1996). Inhibition of brain P-450 arachidonic acid epoxygenase decreases baseline cerebral blood flow. *Am J Physiol* **271**, H1541-1546.

Alkayed, N. J., Birks, E. K., Narayanan, J., Petrie, K. A., Kohler-Cabot, A. E., and Harder, D. R. (1997). Role of P-450 arachidonic acid epoxygenase in the response of cerebral blood flow to glutamate in rats. *Stroke* **28**, 1066-1072.

Allen, J. W., Mutkus, L. A., and Aschner, M. (2000a). Isolation of neonatal rat cortical astrocytes for primary cultures. *Current Protocols in Toxicology*, 12.14.11-12.14.15.

Allen, J. W., Mutkus, L. A., and Aschner, M. (2000b). Isolation of neonatal rat cortical astrocytes for primary cultures. In *Current Protocols in Toxicology*, pp. 12.14.11-12.14.15. John Wiley & Sons, Inc.

Amruthesh, S. C., Boerschel, M. F., McKinney, J. S., Willoughby, K. A., and Ellis, E. F. (1993). Metabolism of arachidonic acid to epoxyeicosatrienoic acids, hydroxyeicosatetraenoic acids, and prostaglandins in cultured rat hippocampal astrocytes. *J Neurochem* **61**, 150-159.

Andres-Mateos, E., Perier, C., Zhang, L., Blanchard-Fillion, B., Greco, T. M., Thomas, B., Ko, H. S., Sasaki, M., Ischiropoulos, H., Przedborski, S., Dawson, T. M., and Dawson, V. L. (2007). DJ-1 gene deletion reveals that DJ-1 is an atypical peroxiredoxin-like peroxidase. *Proc Natl Acad Sci U S A* **104**, 14807-14812.

Araque, A., Martin, E. D., Perea, G., Arellano, J. I., and Buno, W. (2002). Synaptically released acetylcholine evokes Ca2+ elevations in astrocytes in hippocampal slices. *J Neurosci* **22**, 2443-2450.

ATSDR (2003). Toxicological profile for Atrazine. . (P. H. Service, Ed.). U.S. Department of Health and Human Services, Atlanta, GA.

Attwell, D., and Iadecola, C. (2002). The neural basis of functional brain imaging signals. *Trends Neurosci* **25**, 621-625.

Bader, V., Ran Zhu, X., Lubbert, H., and Stichel, C. C. (2005). Expression of DJ-1 in the adult mouse CNS. *Brain Res* **1041**, 102-111.

Bai, G., Rama Rao, K. V., Murthy, C. R., Panickar, K. S., Jayakumar, A. R., and Norenberg, M. D. (2001). Ammonia induces the mitochondrial permeability

transition in primary cultures of rat astrocytes. *J Neurosci Res* **66**, 981-991.

Bai, J., and Cederbaum, A. I. (2001). Mitochondrial catalase and oxidative injury. *Biol Signals Recept* **10**, 189-199.

Bakos, J., Duncko, R., Makatsori, A., Pirnik, Z., Kiss, A., and Jezova, D. (2004). Prenatal immune challenge affects growth, behavior, and brain dopamine in offspring. *Ann N Y Acad Sci* **1018**, 281-287.

Bandopadhyay, R., Kingsbury, A. E., Cookson, M. R., Reid, A. R., Evans, I. M., Hope, A. D., Pittman, A. M., Lashley, T., Canet-Aviles, R., Miller, D. W., McLendon, C., Strand, C., Leonard, A. J., Abou-Sleiman, P. M., Healy, D. G., Ariga, H., Wood, N. W., de Silva, R., Revesz, T., Hardy, J. A., and Lees, A. J. (2004). The expression of DJ-1 (PARK7) in normal human CNS and idiopathic Parkinson's disease. *Brain* **127**, 420-430.

Barde, Y. A., Edgar, D., and Thoenen, H. (1982). Purification of a new neurotrophic factor from mammalian brain. *Embo J* **1**, 549-553.

Barger, S. W., Horster, D., Furukawa, K., Goodman, Y., Krieglstein, J., and Mattson, M. P. (1995). Tumor necrosis factors alpha and beta protect neurons against amyloid beta-peptide toxicity: evidence for involvement of a kappa B-binding factor and attenuation of peroxide and Ca2+ accumulation. *Proc Natl Acad Sci U S A* **92**, 9328-9332.

Bashkatova, V., Alam, M., Vanin, A., and Schmidt, W. J. (2004). Chronic administration of rotenone increases levels of nitric oxide and lipid peroxidation products in rat brain. *Exp Neurol* **186**, 235-241.

Beal, M. F. (1992). Mechanisms of excitotoxicity in neurologic diseases. *Faseb J* **6**, 3338-3344.

Beal, M. F. (1994). Huntington's disease, energy, and excitotoxicity. *Neurobiol Aging* **15**, 275-276.

Beal, M. F. (1998). Excitotoxicity and nitric oxide in Parkinson's disease pathogenesis. *Ann Neurol* **44**, S110-114.

Bellinger, F. P., Madamba, S. G., Campbell, I. L., and Siggins, G. R. (1995). Reduced long-term potentiation in the dentate gyrus of transgenic mice with cerebral overexpression of interleukin-6. *Neurosci Lett* **198**, 95-98.

Benveniste, E. N. (1998). Cytokine actions in the central nervous system. *Cytokine Growth Factor Rev* **9**, 259-275.

Benveniste, O., Vaslin, B., Le Grand, R., and Dormont, D. (1998). Comparing IL-6, TNF-alpha, and IL-1beta responses to acute infection with attenuated nef-truncated or pathogenic SIVmac251 in macaque peripheral blood mononuclear cells. *J Acquir Immune Defic Syndr Hum Retrovirol* **18**, 389-390.

Betarbet, R., Canet-Aviles, R. M., Sherer, T. B., Mastroberardino, P. G., McLendon, C., Kim, J. H., Lund, S., Na, H. M., Taylor, G., Bence, N. F., Kopito, R., Seo, B. B., Yagi, T., Yagi, A., Klinefelter, G., Cookson, M. R., and Greenamyre, J. T. (2006a). Intersecting pathways to neurodegeneration in Parkinson's disease: Effects of the pesticide rotenone on DJ-1, alpha-synuclein, and the ubiquitin-proteasome system. *Neurobiol Dis.*

Betarbet, R., Canet-Aviles, R. M., Sherer, T. B., Mastroberardino, P. G., McLendon, C., Kim, J. H., Lund, S., Na, H. M., Taylor, G., Bence, N. F., Kopito, R., Seo, B. B., Yagi, T., Yagi, A., Klinefelter, G., Cookson, M. R., and Greenamyre, J. T. (2006b). Intersecting pathways to neurodegeneration in Parkinson's disease: effects of the pesticide rotenone on DJ-1, alpha-synuclein, and the ubiquitin-proteasome system. *Neurobiol Dis* **22**, 404-420.

Betarbet, R., Sherer, T. B., MacKenzie, G., Garcia-Osuna, M., Panov, A. V., and Greenamyre, J. T. (2000). Chronic systemic pesticide exposure reproduces features of Parkinson's disease. *Nat Neurosci* **3**, 1301-1306.

Bezzi, P., Carmignoto, G., Pasti, L., Vesce, S., Rossi, D., Rizzini, B. L., Pozzan, T., and Volterra, A. (1998). Prostaglandins stimulate calcium-dependent glutamate release in astrocytes. *Nature* **391**, 281-285.

Blackinton, J., Ahmad, R., Miller, D. W., van der Brug, M. P., Canet-Aviles, R. M., Hague, S. M., Kaleem, M., and Cookson, M. R. (2005). Effects of DJ-1 mutations and polymorphisms on protein stability and subcellular localization. *Brain Res Mol Brain Res* **134**, 76-83.

Blum-Degen, D., Muller, T., Kuhn, W., Gerlach, M., Przuntek, H., and Riederer, P. (1995). Interleukin-1 beta and interleukin-6 are elevated in the cerebrospinal fluid of Alzheimer's and de novo Parkinson's disease patients. *Neurosci Lett* **202**, 17-20.

Boka, G., Anglade, P., Wallach, D., Javoy-Agid, F., Agid, Y., and Hirsch, E. C. (1994). Immunocytochemical analysis of tumor necrosis factor and its receptors in Parkinson's disease. *Neurosci Lett* **172**, 151-154.

Bonifati, V., Rizzu, P., Squitieri, F., Krieger, E., Vanacore, N., van Swieten, J. C., Brice, A., van Duijn, C. M., Oostra, B., Meco, G., and Heutink, P. (2003a). DJ-1(PARK7), a novel gene for autosomal recessive, early onset parkinsonism. *Neurol Sci* **24**, 159-160.

Bonifati, V., Rizzu, P., van Baren, M. J., Schaap, O., Breedveld, G. J., Krieger, E., Dekker, M. C., Squitieri, F., Ibanez, P., Joosse, M., van Dongen, J. W., Vanacore, N., van Swieten, J. C., Brice, A., Meco, G., van Duijn, C. M., Oostra, B. A., and Heutink, P. (2003b). Mutations in the DJ-1 gene associated with autosomal recessive early-onset parkinsonism. *Science* **299**, 256-259.

Borrett, D., and Becker, L. E. (1985). Alexander's disease. A disease of astrocytes. *Brain* **108 (Pt 2)**, 367-385.

Bouzier-Sore, A. K., Serres, S., Canioni, P., and Merle, M. (2003a). Lactate involvement in neuron-glia metabolic interaction: (13)C-NMR spectroscopy contribution. *Biochimie* **85**, 841-848.

Bouzier-Sore, A. K., Voisin, P., Canioni, P., Magistretti, P. J., and Pellerin, L. (2003b). Lactate is a preferential oxidative energy substrate over glucose for neurons in culture. *J Cereb Blood Flow Metab* **23**, 1298-1306.

Bowser, D. N., and Khakh, B. S. (2004). ATP excites interneurons and astrocytes to increase synaptic inhibition in neuronal networks. *J Neurosci* **24**, 8606-8620.

Bredow, S., Guha-Thakurta, N., Taishi, P., Obal, F., Jr., and Krueger, J. M. (1997). Diurnal variations of tumor necrosis factor alpha mRNA and alpha-tubulin mRNA in rat brain. *Neuroimmunomodulation* **4**, 84-90.

Bretaud, S., Allen, C., Ingham, P. W., and Bandmann, O. (2007). p53-dependent neuronal cell death in a DJ-1-deficient zebrafish model of Parkinson's disease. *J Neurochem* **100**, 1626-1635.

Bruce, A. J., Boling, W., Kindy, M. S., Peschon, J., Kraemer, P. J., Carpenter, M. K., Holtsberg, F. W., and Mattson, M. P. (1996). Altered neuronal and microglial responses to excitotoxic and ischemic brain injury in mice lacking TNF receptors. *Nat Med* **2**, 788-794.

Canet-Aviles, R. M., Wilson, M. A., Miller, D. W., Ahmad, R., McLendon, C., Bandyopadhyay, S., Baptista, M. J., Ringe, D., Petsko, G. A., and Cookson, M. R. (2004). The Parkinson's disease protein DJ-1 is neuroprotective due to cysteine-sulfinic acid-driven mitochondrial localization. *Proc Natl Acad Sci U S A* **101**, 9103-9108.

Canet-Avilés, R. M., Wilson, M. A., Miller, D. W., Ahmad, R., McLendon, C., Bandyopadhyay, S., Baptista, M. J., Ringe, D., Petsko, G. A., and Cookson, M. R. (2004). The Parkinson's disease protein DJ-1 is neuroprotective due to cysteine-sulfinic acid-driven mitochondrial localization. *Proc Natl Acad Sci U S A* **101**, 9103-9108.

Carlson, N. G., Bacchi, A., Rogers, S. W., and Gahring, L. C. (1998). Nicotine blocks TNF-alpha-mediated neuroprotection to NMDA by an alpha-bungarotoxin-sensitive pathway. *J Neurobiol* **35**, 29-36.

Carvey, P. M., Chang, Q., Lipton, J. W., and Ling, Z. (2003). Prenatal exposure to the bacteriotoxin lipopolysaccharide leads to long-term losses of dopamine neurons in offspring: a potential, new model of Parkinson's disease. *Front Biosci* **8**, s826-837.

Chadi, G., Tinner, B., Agnati, L. F., and Fuxe, K. (1993). Basic fibroblast growth factor (bFGF, FGF-2) immunoreactivity exists in the noradrenaline, adrenaline and 5-HT nerve cells of the rat brain. *Neurosci Lett* **160**, 171-176.

Chappell, V. L., Le, L. X., LaGrone, L., and Mileski, W. J. (2000). Stat proteins play a role in tumor necrosis factor alpha gene expression. *Shock* **14**, 400-402; discussion 402-403.

Chen, L., Cagniard, B., Mathews, T., Jones, S., Koh, H. C., Ding, Y., Carvey, P. M., Ling, Z., Kang, U. J., and Zhuang, X. (2005). Age-dependent motor deficits and dopaminergic dysfunction in DJ-1 null mice. *J Biol Chem* **280**, 21418-21426.

Cheng, B., Christakos, S., and Mattson, M. P. (1994). Tumor necrosis factors protect neurons against metabolic-excitotoxic insults and promote maintenance of calcium homeostasis. *Neuron* **12**, 139-153.

Choi, J., Sullards, M. C., Olzmann, J. A., Rees, H. D., Weintraub, S. T., Bostwick, D. E., Gearing, M., Levey, A. I., Chin, L. S., and Li, L. (2006). Oxidative damage of DJ-1 is linked to sporadic Parkinson and Alzheimer diseases. *J Biol Chem* **281**, 10816-10824.

Chow, J. C., Young, D. W., Golenbock, D. T., Christ, W. J., and Gusovsky, F. (1999). Toll-like receptor-4 mediates lipopolysaccharide-induced signal transduction. *J Biol Chem* **274**, 10689-10692.

Chung, I. Y., and Benveniste, E. N. (1990). Tumor necrosis factor-alpha production by astrocytes. Induction by lipopolysaccharide, IFN-gamma, and IL-1 beta. *J Immunol* **144**, 2999-3007.

Clements, C. M., McNally, R. S., Conti, B. J., Mak, T. W., and Ting, J. P. (2006). DJ-1, a cancer- and Parkinson's disease-associated protein, stabilizes the antioxidant transcriptional master regulator Nrf2. *Proc Natl Acad Sci U S A* **103**, 15091-15096.

Cookson, M. R. (2003). Crystallizing ideas about Parkinson's disease. *Proc Natl Acad Sci U S A* **100**, 9111-9113.

Cotrina, M. L., Lin, J. H., Lopez-Garcia, J. C., Naus, C. C., and Nedergaard, M. (2000). ATP-mediated glia signaling. *J Neurosci* **20**, 2835-2844.

Das, P. C., McElroy, W. K., and Cooper, R. L. (2001). Alteration of catecholamines in pheochromocytoma (PC12) cells in vitro by the metabolites of chlorotriazine herbicide. *Toxicol Sci* **59**, 127-137.

Das, P. C., McElroy, W. K., and Cooper, R. L. (2003). Potential mechanisms responsible for chlorotriazine-induced alterations in catecholamines in pheochromocytoma (PC12) cells. *Life Sci* **73**, 3123-3138.

Dauer, W., and Przedborski, S. (2003). Parkinson's disease: mechanisms and models. *Neuron* **39**, 889-909.

Davidson, B., Hadar, R., Schlossberg, A., Sternlicht, T., Slipicevic, A., Skrede, M., Risberg, B., Florenes, V. A., Kopolovic, J., and Reich, R. (2008). Expression and clinical role of DJ-1, a negative regulator of PTEN, in ovarian carcinoma. *Hum Pathol* **39**, 87-95.

De Simoni, M. G., and Imeri, L. (1998). Cytokine-neurotransmitter interactions in the brain. *Biol Signals* **7**, 33-44.

Dekker, M. C., Eshuis, S. A., Maguire, R. P., Veenma-van der Duijn, L., Pruim, J., Snijders, P. J., Oostra, B. A., van Duijn, C. M., and Leenders, K. L. (2004). PET neuroimaging and mutations in the DJ-1 gene. *J Neural Transm* **111**, 1575-1581.

Dopp, J. M., Mackenzie-Graham, A., Otero, G. C., and Merrill, J. E. (1997). Differential expression, cytokine modulation, and specific functions of type-1 and type-2 tumor necrosis factor receptors in rat glia. *J Neuroimmunol* **75**, 104-112.

Duffy, S., and MacVicar, B. A. (1995). Adrenergic calcium signaling in astrocyte networks within the hippocampal slice. *J Neurosci* **15**, 5535-5550.

Duffy, S., and MacVicar, B. A. (1996). In vitro ischemia promotes calcium influx and intracellular calcium release in hippocampal astrocytes. *J Neurosci* **16**, 71-81.

Ejima, K., Nanri, H., Araki, M., Koji, T., Shibata, E., Kashimura, M., and Ikeda, M. (2000). Expression of mitochondrial thioredoxin-dependent antioxidant protein, SP-22, in normal human and inflammatory mouse placentae. *Placenta* **21**, 847-852.

Fam, S. R., Gallagher, C. J., and Salter, M. W. (2000). P2Y(1) purinoceptor-mediated Ca(2+) signaling and Ca(2+) wave propagation in dorsal spinal cord astrocytes. *J Neurosci* **20**, 2800-2808.

Fan, J., Ren, H., Jia, N., Fei, E., Zhou, T., Jiang, P., Wu, M., and Wang, G. (2007). DJ-1 decreases Bax expression through repressing p53 transcriptional activity. *J Biol Chem*.

Fan, J., Ren, H., Jia, N., Fei, E., Zhou, T., Jiang, P., Wu, M., and Wang, G. (2008). DJ-1 Decreases Bax Expression through Repressing p53 Transcriptional Activity. *J Biol Chem* **283**, 4022-4030.

Feng, Z., Li, D., Fung, P. C., Pei, Z., Ramsden, D. B., and Ho, S. L. (2003). COX-2-deficient mice are less prone to MPTP-neurotoxicity than wild-type mice. *Neuroreport* **14**, 1927-1929.

Filipov, N. M., Stewart, M. A., Carr, R. L., and Sistrunk, S. C. (2007). Dopaminergic toxicity of the herbicide atrazine in rat striatal slices. *Toxicology* **232**, 68-78.

Filosa, J. A., Bonev, A. D., Straub, S. V., Meredith, A. L., Wilkerson, M. K., Aldrich, R. W., and Nelson, M. T. (2006). Local potassium signaling couples neuronal activity to vasodilation in the brain. *Nat Neurosci* **9**, 1397-1403.

Fontaine, V., Mohand-Said, S., Hanoteau, N., Fuchs, C., Pfizenmaier, K., and Eisel, U. (2002). Neurodegenerative and neuroprotective effects of tumor Necrosis factor (TNF) in retinal ischemia: opposite roles of TNF receptor 1 and TNF receptor 2. *J Neurosci* **22**, RC216.

Francalanci, P., Eymard-Pierre, E., Dionisi-Vici, C., Boldrini, R., Piemonte, F., Virgili, R., Fariello, G., Bosman, C., Santorelli, F. M., Boespflug-Tanguy, O., and Bertini, E. (2001). Fatal infantile leukodystrophy: a severe variant of CACH/VWM syndrome, allelic to chromosome 3q27. *Neurology* **57**, 265-270.

Fujita, M., Hayashi, I., Yamashina, S., Fukamizu, A., Itoman, M., and Majima, M. (2005). Angiotensin type 1a receptor signaling-dependent induction of vascular endothelial growth factor in stroma is relevant to tumor-associated angiogenesis and tumor growth. *Carcinogenesis* **26**, 271-279.

Gao, H. M., Hong, J. S., Zhang, W., and Liu, B. (2002). Distinct role for microglia in rotenone-induced degeneration of dopaminergic neurons. *J Neurosci* **22**, 782-790.

Gemma, C., Catlow, B., Cole, M., Hudson, C., Samec, A., Shah, N., Vila, J., Bachstetter, A., and Bickford, P. C. (2007). Early inhibition of TNFalpha increases 6-hydroxydopamine-induced striatal degeneration. *Brain Res* **1147**, 240-247.

Goldberg, M. S., Pisani, A., Haburcak, M., Vortherms, T. A., Kitada, T., Costa, C., Tong, Y., Martella, G., Tscherter, A., Martins, A., Bernardi, G., Roth, B. L., Pothos, E. N., Calabresi, P., and Shen, J. (2005). Nigrostriatal dopaminergic deficits and hypokinesia caused by inactivation of the familial Parkinsonism-linked gene DJ-1. *Neuron* **45**, 489-496.

Gomez-Isla, T., Irizarry, M. C., Mariash, A., Cheung, B., Soto, O., Schrump, S., Sondel, J., Kotilinek, L., Day, J., Schwarzschild, M. A., Cha, J. H., Newell,

K., Miller, D. W., Ueda, K., Young, A. B., Hyman, B. T., and Ashe, K. H. (2003). Motor dysfunction and gliosis with preserved dopaminergic markers in human alpha-synuclein A30P transgenic mice. *Neurobiol Aging* **24**, 245-258.

Gorell, J. M., Johnson, C. C., Rybicki, B. A., Peterson, E. L., and Richardson, R. J. (1998). The risk of Parkinson's disease with exposure to pesticides, farming, well water, and rural living. *Neurology* **50**, 1346-1350.

Gorner, K., Holtorf, E., Odoy, S., Nuscher, B., Yamamoto, A., Regula, J. T., Beyer, K., Haass, C., and Kahle, P. J. (2004). Differential effects of Parkinson's disease-associated mutations on stability and folding of DJ-1. *J Biol Chem* **279**, 6943-6951.

Goswami, A., Dikshit, P., Mishra, A., Mulherkar, S., Nukina, N., and Jana, N. R. (2006). Oxidative stress promotes mutant huntingtin aggregation and mutant huntingtin-dependent cell death by mimicking proteasomal malfunction. *Biochem Biophys Res Commun* **342**, 184-190.

Grzmil, M., Voigt, S., Thelen, P., Hemmerlein, B., Helmke, K., and Burfeind, P. (2004). Up-regulated expression of the MAT-8 gene in prostate cancer and its siRNA-mediated inhibition of expression induces a decrease in proliferation of human prostate carcinoma cells. *Int J Oncol* **24**, 97-105.

Guthrie, P. B., Knappenberger, J., Segal, M., Bennett, M. V., Charles, A. C., and Kater, S. B. (1999). ATP released from astrocytes mediates glial calcium waves. *J Neurosci* **19**, 520-528.

Haas, R. H., Nasirian, F., Nakano, K., Ward, D., Pay, M., Hill, R., and Shults, C. W. (1995). Low platelet mitochondrial complex I and complex II/III activity in early untreated Parkinson's disease. *Ann Neurol* **37**, 714-722.

Hague, S., Rogaeva, E., Hernandez, D., Gulick, C., Singleton, A., Hanson, M., Johnson, J., Weiser, R., Gallardo, M., Ravina, B., Gwinn-Hardy, K., Crawley, A., St George-Hyslop, P. H., Lang, A. E., Heutink, P., Bonifati, V., and Hardy, J. (2003a). Early-onset Parkinson's disease caused by a compound heterozygous DJ-1 mutation. *Ann Neurol* **54**, 271-274.

Hague, S., Rogaeva, E., Hernandez, D., Gulick, C., Singleton, A., Hanson, M., Johnson, J., Weiser, R., Gallardo, M., Ravina, B., Gwinn-Hardy, K., Crawley, A., St George-Hyslop, P. H., Lang, A. E., Heutink, P., Bonifati, V., Hardy, J., and Singleton, A. (2003b). Early-onset Parkinson's disease caused by a compound heterozygous DJ-1 mutation. *Ann Neurol* **54**, 271-274.

Haydon, P. G., and Carmignoto, G. (2006). Astrocyte control of synaptic transmission and neurovascular coupling. *Physiol Rev* **86**, 1009-1031.

Heikkila, R. E., Hess, A., and Duvoisin, R. C. (1984). Dopaminergic neurotoxicity of 1-methyl-4-phenyl-1,2,5,6-tetrahydropyridine in mice. *Science* **224**, 1451-1453.

Hernan, M. A., Takkouche, B., Caamano-Isorna, F., and Gestal-Otero, J. J. (2002). A meta-analysis of coffee drinking, cigarette smoking, and the risk of Parkinson's disease. *Ann Neurol* **52**, 276-284.

Herrera, A. J., Castano, A., Venero, J. L., Cano, J., and Machado, A. (2000). The single intranigral injection of LPS as a new model for studying the

selective effects of inflammatory reactions on dopaminergic system. *Neurobiol Dis* **7**, 429-447.

Hirotani, T., Lee, P. Y., Kuwata, H., Yamamoto, M., Matsumoto, M., Kawase, I., Akira, S., and Takeda, K. (2005). The nuclear IkappaB protein IkappaBNS selectively inhibits lipopolysaccharide-induced IL-6 production in macrophages of the colonic lamina propria. *J Immunol* **174**, 3650-3657.

Hirsch, E. C., Hunot, S., Damier, P., and Faucheux, B. (1998). Glial cells and inflammation in Parkinson's disease: a role in neurodegeneration? *Ann Neurol* **44**, S115-120.

Hod, Y. (2004). Differential control of apoptosis by DJ-1 in prostate benign and cancer cells. *J Cell Biochem* **92**, 1221-1233.

Hod, Y., Pentyala, S. N., Whyard, T. C., and El-Maghrabi, M. R. (1999). Identification and characterization of a novel protein that regulates RNA-protein interaction. *J Cell Biochem* **72**, 435-444.

Honbou, K., Suzuki, N. N., Horiuchi, M., Niki, T., Taira, T., Ariga, H., and Inagaki, F. (2003). The crystal structure of DJ-1, a protein related to male fertility and Parkinson's disease. *J Biol Chem* **278**, 31380-31384.

Hori, O., Matsumoto, M., Kuwabara, K., Maeda, Y., Ueda, H., Ohtsuki, T., Kinoshita, T., Ogawa, S., Stern, D. M., and Kamada, T. (1996). Exposure of astrocytes to hypoxia/reoxygenation enhances expression of glucose-regulated protein 78 facilitating astrocyte release of the neuroprotective cytokine interleukin 6. *J Neurochem* **66**, 973-979.

Huai, Q., Sun, Y., Wang, H., Chin, L. S., Li, L., Robinson, H., and Ke, H. (2003). Crystal structure of DJ-1/RS and implication on familial Parkinson's disease. *FEBS Lett* **549**, 171-175.

Hudson, T. S., Hartle, D. K., Hursting, S. D., Nunez, N. P., Wang, T. T., Young, H. A., Arany, P., and Green, J. E. (2007). Inhibition of prostate cancer growth by muscadine grape skin extract and resveratrol through distinct mechanisms. *Cancer Res* **67**, 8396-8405.

Hunot, S., Dugas, N., Faucheux, B., Hartmann, A., Tardieu, M., Debre, P., Agid, Y., Dugas, B., and Hirsch, E. C. (1999). FcepsilonRII/CD23 is expressed in Parkinson's disease and induces, in vitro, production of nitric oxide and tumor necrosis factor-alpha in glial cells. *J Neurosci* **19**, 3440-3447.

Hunter, R. L., Dragicevic, N., Seifert, K., Choi, D. Y., Liu, M., Kim, H. C., Cass, W. A., Sullivan, P. G., and Bing, G. (2007). Inflammation induces mitochondrial dysfunction and dopaminergic neurodegeneration in the nigrostriatal system. *J Neurochem* **100**, 1375-1386.

Jarskog, L. F., Xiao, H., Wilkie, M. B., Lauder, J. M., and Gilmore, J. H. (1997). Cytokine regulation of embryonic rat dopamine and serotonin neuronal survival in vitro. *Int J Dev Neurosci* **15**, 711-716.

Javitch, J. A., and Snyder, S. H. (1984). Uptake of MPP(+) by dopamine neurons explains selectivity of parkinsonism-inducing neurotoxin, MPTP. *Eur J Pharmacol* **106**, 455-456.

Jayakumar, A. R., Rama Rao, K. V., Kalaiselvi, P., and Norenberg, M. D. (2004). Combined effects of ammonia and manganese on astrocytes in culture. *Neurochem Res* **29**, 2051-2056.

Junn, E., Taniguchi, H., Jeong, B. S., Zhao, X., Ichijo, H., and Mouradian, M. M. (2005). Interaction of DJ-1 with Daxx inhibits apoptosis signal-regulating kinase 1 activity and cell death. *Proc Natl Acad Sci U S A* **102**, 9691-9696.

Kang, J., Jiang, L., Goldman, S. A., and Nedergaard, M. (1998). Astrocyte-mediated potentiation of inhibitory synaptic transmission. *Nat Neurosci* **1**, 683-692.

Kidd, P. M. (2000). Parkinson's disease as multifactorial oxidative neurodegeneration: implications for integrative management. *Altern Med Rev* **5**, 502-529.

Kim, R. H., Peters, M., Jang, Y., Shi, W., Pintilie, M., Fletcher, G. C., DeLuca, C., Liepa, J., Zhou, L., Snow, B., Binari, R. C., Manoukian, A. S., Bray, M. R., Liu, F. F., Tsao, M. S., and Mak, T. W. (2005a). DJ-1, a novel regulator of the tumor suppressor PTEN. *Cancer Cell* **7**, 263-273.

Kim, R. H., Smith, P. D., Aleyasin, H., Hayley, S., Mount, M. P., Pownall, S., Wakeham, A., You-Ten, A. J., Kalia, S. K., Horne, P., Westaway, D., Lozano, A. M., Anisman, H., Park, D. S., and Mak, T. W. (2005b). Hypersensitivity of DJ-1-deficient mice to 1-methyl-4-phenyl-1,2,3,6-tetrahydropyrindine (MPTP) and oxidative stress. *Proc Natl Acad Sci U S A*.

Kim, R. H., Smith, P. D., Aleyasin, H., Hayley, S., Mount, M. P., Pownall, S., Wakeham, A., You-Ten, A. J., Kalia, S. K., Horne, P., Westaway, D., Lozano, A. M., Anisman, H., Park, D. S., and Mak, T. W. (2005c). Hypersensitivity of DJ-1-deficient mice to 1-methyl-4-phenyl-1,2,3,6-tetrahydropyrindine (MPTP) and oxidative stress. *Proc Natl Acad Sci U S A* **102**, 5215-5220.

Kindt, M. V., Heikkila, R. E., and Nicklas, W. J. (1987). Mitochondrial and metabolic toxicity of 1-methyl-4-(2'-methylphenyl)-1,2,3,6-tetrahydropyridine. *J Pharmacol Exp Ther* **242**, 858-863.

Kinumi, T., Kimata, J., Taira, T., Ariga, H., and Niki, E. (2004). Cysteine-106 of DJ-1 is the most sensitive cysteine residue to hydrogen peroxide-mediated oxidation in vivo in human umbilical vein endothelial cells. *Biochem Biophys Res Commun* **317**, 722-728.

Kitada, T., Asakawa, S., Hattori, N., Matsumine, H., Yamamura, Y., Minoshima, S., Yokochi, M., Mizuno, Y., and Shimizu, N. (1998). Mutations in the parkin gene cause autosomal recessive juvenile parkinsonism. *Nature* **392**, 605-608.

Klinefelter, G. R., Welch, J. E., Perreault, S. D., Moore, H. D., Zucker, R. M., Suarez, J. D., Roberts, N. L., Bobseine, K., and Jeffay, S. (2002). Localization of the sperm protein SP22 and inhibition of fertility in vivo and in vitro. *J Androl* **23**, 48-63.

Kohutnicka, M., Lewandowska, E., Kurkowska-Jastrzebska, I., Czlonkowski, A., and Czlonkowska, A. (1998). Microglial and astrocytic involvement in a murine model of Parkinson's disease induced by 1-methyl-4-phenyl-1,2,3,6-tetrahydropyridine (MPTP). *Immunopharmacology* **39**, 167-180.

Kontakos, N., and Stokes, J. (1999). Monograph series on aging-related diseases: XII. Parkinson's disease--recent developments and new directions. *Chronic Dis Can* **20**, 58-76.

Kotaja, N., Karvonen, U., Janne, O. A., and Palvimo, J. J. (2002). PIAS proteins modulate transcription factors by functioning as SUMO-1 ligases. *Mol Cell Biol* **22**, 5222-5234.

Krieger, C., and Duchen, M. R. (2002). Mitochondria, Ca2+ and neurodegenerative disease. *Eur J Pharmacol* **447**, 177-188.

Krueger, J. M., Fang, J., Taishi, P., Chen, Z., Kushikata, T., and Gardi, J. (1998). Sleep. A physiologic role for IL-1 beta and TNF-alpha. *Ann N Y Acad Sci* **856**, 148-159.

Kumaran, R., Kingsbury, A., Coulter, I., Lashley, T., Williams, D., de Silva, R., Mann, D., Revesz, T., Lees, A., and Bandopadhyay, R. (2007). DJ-1 (PARK7) is associated with 3R and 4R tau neuronal and glial inclusions in neurodegenerative disorders. *Neurobiol Dis* **28**, 122-132.

Kuprash, D. V., Udalova, I. A., Turetskaya, R. L., Kwiatkowski, D., Rice, N. R., and Nedospasov, S. A. (1999). Similarities and differences between human and murine TNF promoters in their response to lipopolysaccharide. *J Immunol* **162**, 4045-4052.

Langston, J. W., Ballard, P., Tetrud, J. W., and Irwin, I. (1983). Chronic Parkinsonism in humans due to a product of meperidine-analog synthesis. *Science* **219**, 979-980.

Le Naour, F., Misek, D. E., Krause, M. C., Deneux, L., Giordano, T. J., Scholl, S., and Hanash, S. M. (2001). Proteomics-based identification of RS/DJ-1 as a novel circulating tumor antigen in breast cancer. *Clin Cancer Res* **7**, 3328-3335.

Lee, F. S., Peters, R. T., Dang, L. C., and Maniatis, T. (1998). MEKK1 activates both IkappaB kinase alpha and IkappaB kinase beta. *Proc Natl Acad Sci U S A* **95**, 9319-9324.

Lee, S. J., Kim, S. J., Kim, I. K., Ko, J., Jeong, C. S., Kim, G. H., Park, C., Kang, S. O., Suh, P. G., Lee, H. S., and Cha, S. S. (2003). Crystal structures of human DJ-1 and Escherichia coli Hsp31, which share an evolutionarily conserved domain. *J Biol Chem* **278**, 44552-44559.

Leroy, E., Boyer, R., Auburger, G., Leube, B., Ulm, G., Mezey, E., Harta, G., Brownstein, M. J., Jonnalagada, S., Chernova, T., Dehejia, A., Lavedan, C., Gasser, T., Steinbach, P. J., Wilkinson, K. D., and Polymeropoulos, M. H. (1998). The ubiquitin pathway in Parkinson's disease. *Nature* **395**, 451-452.

Lev, N., Ickowicz, D., Barhum, Y., Blondheim, N., Melamed, E., and Offen, D. (2006). Experimental encephalomyelitis induces changes in DJ-1: implications for oxidative stress in multiple sclerosis. *Antioxid Redox Signal* **8**, 1987-1995.

Leybaert, L., Paemeleire, K., Strahonja, A., and Sanderson, M. J. (1998). Inositol-trisphosphate-dependent intercellular calcium signaling in and between astrocytes and endothelial cells. *Glia* **24**, 398-407.

Li, A. J., Katafuchi, T., Oda, S., Hori, T., and Oomura, Y. (1997). Interleukin-6 inhibits long-term potentiation in rat hippocampal slices. *Brain Res* **748**, 30-38.

Li, H. M., Niki, T., Taira, T., Iguchi-Ariga, S. M., and Ariga, H. (2005). Association of DJ-1 with chaperones and enhanced association and colocalization with mitochondrial Hsp70 by oxidative stress. *Free Radic Res* **39**, 1091-1099.

Li, N., Sul, J. Y., and Haydon, P. G. (2003). A calcium-induced calcium influx factor, nitric oxide, modulates the refilling of calcium stores in astrocytes. *J Neurosci* **23**, 10302-10310.

Ling, Z., Gayle, D. A., Ma, S. Y., Lipton, J. W., Tong, C. W., Hong, J. S., and Carvey, P. M. (2002). In utero bacterial endotoxin exposure causes loss of tyrosine hydroxylase neurons in the postnatal rat midbrain. *Mov Disord* **17**, 116-124.

Livak, K. J., and Schmittgen, T. D. (2001). Analysis of relative gene expression data using real-time quantitative PCR and the 2(-Delta Delta C(T)) Method. *Methods* **25**, 402-408.

Lu, L., Zhu, J., Zheng, Z., Yan, M., Xu, W., Sun, L., Theze, J., and Liu, X. (1998). Jak-STAT pathway is involved in the induction of TNF-beta gene during stimulation by IL-2. *Eur J Immunol* **28**, 805-810.

Macedo, M. G., Anar, B., Bronner, I. F., Cannella, M., Squitieri, F., Bonifati, V., Hoogeveen, A., Heutink, P., and Rizzu, P. (2003). The DJ-1L166P mutant protein associated with early onset Parkinson's disease is unstable and forms higher-order protein complexes. *Hum Mol Genet* **12**, 2807-2816.

MacKeigan, J. P., Clements, C. M., Lich, J. D., Pope, R. M., Hod, Y., and Ting, J. P. (2003). Proteomic profiling drug-induced apoptosis in non-small cell lung carcinoma: identification of RS/DJ-1 and RhoGDIalpha. *Cancer Res* **63**, 6928-6934.

Maeda, Y., Matsumoto, M., Hori, O., Kuwabara, K., Ogawa, S., Yan, S. D., Ohtsuki, T., Kinoshita, T., Kamada, T., and Stern, D. M. (1994). Hypoxia/reoxygenation-mediated induction of astrocyte interleukin 6: a paracrine mechanism potentially enhancing neuron survival. *J Exp Med* **180**, 2297-2308.

Martinat, C., Shendelman, S., Jonason, A., Leete, T., Beal, M. F., Yang, L., Floss, T., and Abeliovich, A. (2004). Sensitivity to oxidative stress in DJ-1-deficient dopamine neurons: an ES- derived cell model of primary Parkinsonism. *PLoS Biol* **2**, e327.

McMullin, T. S., Andersen, M. E., Nagahara, A., Lund, T. D., Pak, T., Handa, R. J., and Hanneman, W. H. (2004). Evidence that atrazine and diaminochlorotriazine inhibit the estrogen/progesterone induced surge of luteinizing hormone in female Sprague-Dawley rats without changing estrogen receptor action. *Toxicol Sci* **79**, 278-286.

Melle, C., Ernst, G., Escher, N., Hartmann, D., Schimmel, B., Bleul, A., Thieme, H., Kaufmann, R., Felix, K., Friess, H. M., Settmacher, U., Hommann, M., Richter, K. K., Daffner, W., Taubig, H., Manger, T., Claussen, U., and von Eggeling, F. (2007). Protein profiling of microdissected pancreas

carcinoma and identification of HSP27 as a potential serum marker. *Clin Chem* **53**, 629-635.

Meulener, M. C., Graves, C. L., Sampathu, D. M., Armstrong-Gold, C. E., Bonini, N. M., and Giasson, B. I. (2005). DJ-1 is present in a large molecular complex in human brain tissue and interacts with alpha-synuclein. *J Neurochem* **93**, 1524-1532.

Miller, L. G., and Fahey, J. M. (1994). Interleukin-1 modulates GABAergic and glutamatergic function in brain. *Ann N Y Acad Sci* **739**, 292-298.

Mitsumoto, A., and Nakagawa, Y. (2001). DJ-1 is an indicator for endogenous reactive oxygen species elicited by endotoxin. *Free Radic Res* **35**, 885-893.

Mitsumoto, A., Nakagawa, Y., Takeuchi, A., Okawa, K., Iwamatsu, A., and Takanezawa, Y. (2001). Oxidized forms of peroxiredoxins and DJ-1 on two-dimensional gels increased in response to sublethal levels of paraquat. *Free Radic Res* **35**, 301-310.

Mizuno, Y., Ohta, S., Tanaka, M., Takamiya, S., Suzuki, K., Sato, T., Oya, H., Ozawa, T., and Kagawa, Y. (1989). Deficiencies in complex I subunits of the respiratory chain in Parkinson's disease. *Biochem Biophys Res Commun* **163**, 1450-1455.

Mizuno, Y., Saitoh, T., and Sone, N. (1987). Inhibition of mitochondrial NADH-ubiquinone oxidoreductase activity by 1-methyl-4-phenylpyridinium ion. *Biochem Biophys Res Commun* **143**, 294-299.

Mo, J. S., Kim, M. Y., Ann, E. J., Hong, J. A., and Park, H. S. (2008). DJ-1 modulates UV-induced oxidative stress signaling through the suppression of MEKK1 and cell death. *Cell Death Differ.*

Mogi, M., Harada, M., Kondo, T., Riederer, P., Inagaki, H., Minami, M., and Nagatsu, T. (1994a). Interleukin-1 beta, interleukin-6, epidermal growth factor and transforming growth factor-alpha are elevated in the brain from parkinsonian patients. *Neurosci Lett* **180**, 147-150.

Mogi, M., Harada, M., Riederer, P., Narabayashi, H., Fujita, K., and Nagatsu, T. (1994b). Tumor necrosis factor-alpha (TNF-alpha) increases both in the brain and in the cerebrospinal fluid from parkinsonian patients. *Neurosci Lett* **165**, 208-210.

Mogi, M., Togari, A., Tanaka, K., Ogawa, N., Ichinose, H., and Nagatsu, T. (2000). Increase in level of tumor necrosis factor-alpha in 6-hydroxydopamine-lesioned striatum in rats is suppressed by immunosuppressant FK506. *Neurosci Lett* **289**, 165-168.

Moore, D. J., Zhang, L., Troncoso, J., Lee, M. K., Hattori, N., Mizuno, Y., Dawson, T. M., and Dawson, V. L. (2005). Association of DJ-1 and parkin mediated by pathogenic DJ-1 mutations and oxidative stress. *Hum Mol Genet* **14**, 71-84.

Moreno, J. A., Sullivan, K. A., Carbone, D. L., Hanneman, W. H., and Tjalkens, R. B. (2008). Manganese potentiates nuclear factor-kappaB-dependent expression of nitric oxide synthase 2 in astrocytes by activating soluble guanylate cyclase and extracellular responsive kinase signaling pathways. *J Neurosci Res.*

Muller, T., Blum-Degen, D., Przuntek, H., and Kuhn, W. (1998). Interleukin-6 levels in cerebrospinal fluid inversely correlate to severity of Parkinson's disease. *Acta Neurol Scand* **98**, 142-144.

Munoz-Fernandez, M. A., and Fresno, M. (1998). The role of tumour necrosis factor, interleukin 6, interferon-gamma and inducible nitric oxide synthase in the development and pathology of the nervous system. *Prog Neurobiol* **56**, 307-340.

Murphy, S., Simmons, M. L., Agullo, L., Garcia, A., Feinstein, D. L., Galea, E., Reis, D. J., Minc-Golomb, D., and Schwartz, J. P. (1993). Synthesis of nitric oxide in CNS glial cells. *Trends Neurosci* **16**, 323-328.

Nagakubo, D., Taira, T., Kitaura, H., Ikeda, M., Tamai, K., Iguchi-Ariga, S. M., and Ariga, H. (1997). DJ-1, a novel oncogene which transforms mouse NIH3T3 cells in cooperation with ras. *Biochem Biophys Res Commun* **231**, 509-513.

Neumann, M., Muller, V., Gorner, K., Kretzschmar, H. A., Haass, C., and Kahle, P. J. (2004). Pathological properties of the Parkinson's disease-associated protein DJ-1 in alpha-synucleinopathies and tauopathies: relevance for multiple system atrophy and Pick's disease. *Acta Neuropathol (Berl)* **107**, 489-496.

Newman, E. A. (1996). Acid efflux from retinal glial cells generated by sodium bicarbonate cotransport. *J Neurosci* **16**, 159-168.

Niki, T., Takahashi-Niki, K., Taira, T., Iguchi-Ariga, S. M., and Ariga, H. (2003). DJBP: a novel DJ-1-binding protein, negatively regulates the androgen receptor by recruiting histone deacetylase complex, and DJ-1 antagonizes this inhibition by abrogation of this complex. *Mol Cancer Res* **1**, 247-261.

Novotny, V., Prieschl, E. E., Csonga, R., Fabjani, G., and Baumruker, T. (1998). Nrf1 in a complex with fosB, c-jun, junD and ATF2 forms the AP1 component at the TNF alpha promoter in stimulated mast cells. *Nucleic Acids Res* **26**, 5480-5485.

Okada, M., Matsumoto, K., Niki, T., Taira, T., Iguchi-Ariga, S. M., and Ariga, H. (2002). DJ-1, a target protein for an endocrine disrupter, participates in the fertilization in mice. *Biol Pharm Bull* **25**, 853-856.

Olanow, C. W., and Tatton, W. G. (1999). Etiology and pathogenesis of Parkinson's disease. *Annu Rev Neurosci* **22**, 123-144.

Olzmann, J. A., Brown, K., Wilkinson, K. D., Rees, H. D., Huai, Q., Ke, H., Levey, A. I., Li, L., and Chin, L. S. (2004). Familial Parkinson's disease-associated L166P mutation disrupts DJ-1 protein folding and function. *J Biol Chem* **279**, 8506-8515.

Paisan-Ruiz, C., Jain, S., Evans, E. W., Gilks, W. P., Simon, J., van der Brug, M., Lopez de Munain, A., Aparicio, S., Gil, A. M., Khan, N., Johnson, J., Martinez, J. R., Nicholl, D., Carrera, I. M., Pena, A. S., de Silva, R., Lees, A., Marti-Masso, J. F., Perez-Tur, J., Wood, N. W., and Singleton, A. B. (2004). Cloning of the gene containing mutations that cause PARK8-linked Parkinson's disease. *Neuron* **44**, 595-600.

Pan, W., Zadina, J. E., Harlan, R. E., Weber, J. T., Banks, W. A., and Kastin, A. J. (1997). Tumor necrosis factor-alpha: a neuromodulator in the CNS. *Neurosci Biobehav Rev* **21**, 603-613.

Pardo, M., Garcia, A., Thomas, B., Pineiro, A., Akoulitchev, A., Dwek, R. A., and Zitzmann, N. (2006). The characterization of the invasion phenotype of uveal melanoma tumour cells shows the presence of MUC18 and HMG-1 metastasis markers and leads to the identification of DJ-1 as a potential serum biomarker. *Int J Cancer* **119**, 1014-1022.

Parker, W. D., Jr., and Swerdlow, R. H. (1998). Mitochondrial dysfunction in idiopathic Parkinson disease. *Am J Hum Genet* **62**, 758-762.

Pasti, L., Volterra, A., Pozzan, T., and Carmignoto, G. (1997). Intracellular calcium oscillations in astrocytes: a highly plastic, bidirectional form of communication between neurons and astrocytes in situ. *J Neurosci* **17**, 7817-7830.

Pasti, L., Zonta, M., Pozzan, T., Vicini, S., and Carmignoto, G. (2001). Cytosolic calcium oscillations in astrocytes may regulate exocytotic release of glutamate. *J Neurosci* **21**, 477-484.

Pawate, S., Shen, Q., Fan, F., and Bhat, N. R. (2004). Redox regulation of glial inflammatory response to lipopolysaccharide and interferongamma. *J Neurosci Res* **77**, 540-551.

Pellerin, L., Pellegri, G., Bittar, P. G., Charnay, Y., Bouras, C., Martin, J. L., Stella, N., and Magistretti, P. J. (1998). Evidence supporting the existence of an activity-dependent astrocyte-neuron lactate shuttle. *Dev Neurosci* **20**, 291-299.

Perry, S. W., Dewhurst, S., Bellizzi, M. J., and Gelbard, H. A. (2002). Tumor necrosis factor-alpha in normal and diseased brain: Conflicting effects via intraneuronal receptor crosstalk? *J Neurovirol* **8**, 611-624.

Pisani, A., Martella, G., Tscherter, A., Costa, C., Mercuri, N. B., Bernardi, G., Shen, J., and Calabresi, P. (2006). Enhanced sensitivity of DJ-1-deficient dopaminergic neurons to energy metabolism impairment: role of Na+/K+ ATPase. *Neurobiol Dis* **23**, 54-60.

Pitkanen-Arsiola, T., Tillman, J. E., Gu, G., Yuan, J., Roberts, R. L., Wantroba, M., Coetzee, G. A., Cookson, M. S., and Kasper, S. (2006). Androgen and anti-androgen treatment modulates androgen receptor activity and DJ-1 stability. *Prostate* **66**, 1177-1193.

Polymeropoulos, M. H., Lavedan, C., Leroy, E., Ide, S. E., Dehejia, A., Dutra, A., Pike, B., Root, H., Rubenstein, J., Boyer, R., Stenroos, E. S., Chandrasekharappa, S., Athanassiadou, A., Papapetropoulos, T., Johnson, W. G., Lazzarini, A. M., Duvoisin, R. C., Di Iorio, G., Golbe, L. I., and Nussbaum, R. L. (1997). Mutation in the alpha-synuclein gene identified in families with Parkinson's disease. *Science* **276**, 2045-2047.

Porter, J. T., and McCarthy, K. D. (1995). Adenosine receptors modulate [Ca2+]i in hippocampal astrocytes in situ. *J Neurochem* **65**, 1515-1523.

Porter, J. T., and McCarthy, K. D. (1996). Hippocampal astrocytes in situ respond to glutamate released from synaptic terminals. *J Neurosci* **16**, 5073-5081.

Priyadarshi, A., Khuder, S. A., Schaub, E. A., and Priyadarshi, S. S. (2001). Environmental risk factors and Parkinson's disease: a metaanalysis. *Environ Res* **86**, 122-127.

Qin, L., Wu, X., Block, M. L., Liu, Y., Breese, G. R., Hong, J. S., Knapp, D. J., and Crews, F. T. (2007). Systemic LPS causes chronic neuroinflammation and progressive neurodegeneration. *Glia* **55**, 453-462.

Queiroz, G., Meyer, D. K., Meyer, A., Starke, K., and von Kugelgen, I. (1999). A study of the mechanism of the release of ATP from rat cortical astroglial cells evoked by activation of glutamate receptors. *Neuroscience* **91**, 1171-1181.

Quigley, P. M., Korotkov, K., Baneyx, F., and Hol, W. G. (2003). The 1.6-A crystal structure of the class of chaperones represented by Escherichia coli Hsp31 reveals a putative catalytic triad. *Proc Natl Acad Sci U S A* **100**, 3137-3142.

Ramsay, R. R., Salach, J. I., and Singer, T. P. (1986). Uptake of the neurotoxin 1-methyl-4-phenylpyridine (MPP+) by mitochondria and its relation to the inhibition of the mitochondrial oxidation of NAD+-linked substrates by MPP+. *Biochem Biophys Res Commun* **134**, 743-748.

Randriamboavonjy, V., Busse, R., and Fleming, I. (2003). 20-HETE-induced contraction of small coronary arteries depends on the activation of Rho-kinase. *Hypertension* **41**, 801-806.

Ritz, B., and Yu, F. (2000). Parkinson's disease mortality and pesticide exposure in California 1984-1994. *Int J Epidemiol* **29**, 323-329.

Rizzu, P., Hinkle, D. A., Zhukareva, V., Bonifati, V., Severijnen, L. A., Martinez, D., Ravid, R., Kamphorst, W., Eberwine, J. H., Lee, V. M., Trojanowski, J. Q., and Heutink, P. (2004). DJ-1 colocalizes with tau inclusions: a link between parkinsonism and dementia. *Ann Neurol* **55**, 113-118.

Roman, R. J. (2002). P-450 metabolites of arachidonic acid in the control of cardiovascular function. *Physiol Rev* **82**, 131-185.

Sagara, J. I., Miura, K., and Bannai, S. (1993). Maintenance of neuronal glutathione by glial cells. *J Neurochem* **61**, 1672-1676.

Sanderson, M. J., Charles, A. C., Boitano, S., and Dirksen, E. R. (1994). Mechanisms and function of intercellular calcium signaling. *Mol Cell Endocrinol* **98**, 173-187.

Sandor, P. (1999). Nervous control of the cerebrovascular system: doubts and facts. *Neurochem Int* **35**, 237-259.

Sawada, M., Kondo, N., Suzumura, A., and Marunouchi, T. (1989). Production of tumor necrosis factor-alpha by microglia and astrocytes in culture. *Brain Res* **491**, 394-397.

Schapira, A. H., Cooper, J. M., Dexter, D., Jenner, P., Clark, J. B., and Marsden, C. D. (1989). Mitochondrial complex I deficiency in Parkinson's disease. *Lancet* **1**, 1269.

Schousboe, A., Hertz, L., Svenneby, G., and Kvamme, E. (1979). Phosphate activated glutaminase activity and glutamine uptake in primary cultures of astrocytes. *J Neurochem* **32**, 943-950.

Schuler, F., and Casida, J. E. (2001a). Functional coupling of PSST and ND1 subunits in NADH:ubiquinone oxidoreductase established by photoaffinity labeling. *Biochim Biophys Acta* **1506**, 79-87.

Schuler, F., and Casida, J. E. (2001b). The insecticide target in the PSST subunit of complex I. *Pest Manag Sci* **57**, 932-940.

Schumann, R. R., Pfeil, D., Freyer, D., Buerger, W., Lamping, N., Kirschning, C. J., Goebel, U. B., and Weber, J. R. (1998). Lipopolysaccharide and pneumococcal cell wall components activate the mitogen activated protein kinases (MAPK) erk-1, erk-2, and p38 in astrocytes. *Glia* **22**, 295-305.

Schwarzenbach, H., Chakrabarti, G., Paust, H. J., and Mukhopadhyay, A. K. (2004). Gonadotropin-mediated regulation of the murine VEGF expression in MA-10 Leydig cells. *J Androl* **25**, 128-139.

Sekito, A., Koide-Yoshida, S., Niki, T., Taira, T., Iguchi-Ariga, S. M., and Ariga, H. (2006). DJ-1 interacts with HIPK1 and affects H2O2-induced cell death. *Free Radic Res* **40**, 155-165.

Sekito, A., Taira, T., Niki, T., Iguchi-Ariga, S. M., and Ariga, H. (2005). Stimulation of transforming activity of DJ-1 by Abstrakt, a DJ-1-binding protein. *Int J Oncol* **26**, 685-689.

Shang, H., Lang, D., Jean-Marc, B., and Kaelin-Lang, A. (2004). Localization of DJ-1 mRNA in the mouse brain. *Neurosci Lett* **367**, 273-277.

Sharif, S. F., Hariri, R. J., Chang, V. A., Barie, P. S., Wang, R. S., and Ghajar, J. B. (1993). Human astrocyte production of tumour necrosis factor-alpha, interleukin-1 beta, and interleukin-6 following exposure to lipopolysaccharide endotoxin. *Neurol Res* **15**, 109-112.

Shelton, M. K., and McCarthy, K. D. (2000). Hippocampal astrocytes exhibit Ca2+-elevating muscarinic cholinergic and histaminergic receptors in situ. *J Neurochem* **74**, 555-563.

Shendelman, S., Jonason, A., Martinat, C., Leete, T., and Abeliovich, A. (2004). DJ-1 is a redox-dependent molecular chaperone that inhibits alpha-synuclein aggregate formation. *PLoS Biol* **2**, e362.

Sherer, T. B., Betarbet, R., Kim, J. H., and Greenamyre, J. T. (2003a). Selective microglial activation in the rat rotenone model of Parkinson's disease. *Neurosci Lett* **341**, 87-90.

Sherer, T. B., Betarbet, R., Testa, C. M., Seo, B. B., Richardson, J. R., Kim, J. H., Miller, G. W., Yagi, T., Matsuno-Yagi, A., and Greenamyre, J. T. (2003b). Mechanism of toxicity in rotenone models of Parkinson's disease. *J Neurosci* **23**, 10756-10764.

Sherer, T. B., Kim, J. H., Betarbet, R., and Greenamyre, J. T. (2003c). Subcutaneous rotenone exposure causes highly selective dopaminergic degeneration and alpha-synuclein aggregation. *Exp Neurol* **179**, 9-16.

Shi, L., Kishore, R., McMullen, M. R., and Nagy, L. E. (2002a). Chronic ethanol increases lipopolysaccharide-stimulated Egr-1 expression in RAW 264.7 macrophages: contribution to enhanced tumor necrosis factor alpha production. *J Biol Chem* **277**, 14777-14785.

Shi, L., Kishore, R., McMullen, M. R., and Nagy, L. E. (2002b). Lipopolysaccharide stimulation of ERK1/2 increases TNF-alpha production via Egr-1. *Am J Physiol Cell Physiol* **282**, C1205-1211.

Shinbo, Y., Taira, T., Niki, T., Iguchi-Ariga, S. M., and Ariga, H. (2005). DJ-1 restores p53 transcription activity inhibited by Topors/p53BP3. *Int J Oncol* **26**, 641-648.

Shinpo, K., Kikuchi, S., Moriwaka, F., and Tashiro, K. (1999). Protective effects of the TNF-ceramide pathway against glutamate neurotoxicity on cultured mesencephalic neurons. *Brain Res* **819**, 170-173.

Simmons, M. L., and Murphy, S. (1992). Induction of nitric oxide synthase in glial cells. *J Neurochem* **59**, 897-905.

Srisomsap, C., Subhasitanont, P., Otto, A., Mueller, E. C., Punyarit, P., Wittmann-Liebold, B., and Svasti, J. (2002). Detection of cathepsin B up-regulation in neoplastic thyroid tissues by proteomic analysis. *Proteomics* **2**, 706-712.

Sul, J. Y., Orosz, G., Givens, R. S., and Haydon, P. G. (2004). Astrocytic Connectivity in the Hippocampus. *Neuron Glia Biol* **1**, 3-11.

Szabo, C., Salzman, A. L., and Ischiropoulos, H. (1995). Endotoxin triggers the expression of an inducible isoform of nitric oxide synthase and the formation of peroxynitrite in the rat aorta in vivo. *FEBS Lett* **363**, 235-238.

Taira, T., Iguchi-Ariga, S. M., and Ariga, H. (2004a). Co-localization with DJ-1 is essential for the androgen receptor to exert its transcription activity that has been impaired by androgen antagonists. *Biol Pharm Bull* **27**, 574-577.

Taira, T., Saito, Y., Niki, T., Iguchi-Ariga, S. M., Takahashi, K., and Ariga, H. (2004b). DJ-1 has a role in antioxidative stress to prevent cell death. *EMBO Rep* **5**, 213-218.

Taira, T., Saito, Y., Niki, T., Iguchi-Ariga, S. M., Takahashi, K., and Ariga, H. (2004c). DJ-1 has a role in antioxidative stress to prevent cell death. *EMBO Rep* **5**, 430.

Taira, T., Takahashi, K., Kitagawa, R., Iguchi-Ariga, S. M., and Ariga, H. (2001). Molecular cloning of human and mouse DJ-1 genes and identification of Sp1-dependent activation of the human DJ-1 promoter. *Gene* **263**, 285-292.

Takahashi, K., Taira, T., Niki, T., Seino, C., Iguchi-Ariga, S. M., and Ariga, H. (2001). DJ-1 positively regulates the androgen receptor by impairing the binding of PIASx alpha to the receptor. *J Biol Chem* **276**, 37556-37563.

Takahashi-Niki, K., Niki, T., Taira, T., Iguchi-Ariga, S. M., and Ariga, H. (2004). Reduced anti-oxidative stress activities of DJ-1 mutants found in Parkinson's disease patients. *Biochem Biophys Res Commun* **320**, 389-397.

Tao, X., and Tong, L. (2003). Crystal structure of human DJ-1, a protein associated with early onset Parkinson's disease. *J Biol Chem* **278**, 31372-31379.

Thomas, B., and Beal, M. F. (2007). Parkinson's disease. *Hum Mol Genet* **16 Spec No. 2**, R183-194.

Thorsen, P., Jensen, I., Jeume, B., Ebbesen, N., Arpi, M., Bremmelgaard, A., and al., e. (1998). Few microorganisms associated with bacterial vaginosis may constitute the pathogeic core: a population-based microbiologica study among 3596 pregnant women. *Am J Obstet Gynecol* **178**, 580-587.

Tillman, J. E., Yuan, J., Gu, G., Fazli, L., Ghosh, R., Flynt, A. S., Gleave, M., Rennie, P. S., and Kasper, S. (2007). DJ-1 binds androgen receptor directly and mediates its activity in hormonally treated prostate cancer cells. *Cancer Res* **67**, 4630-4637.

Timchalk, C., Dryzga, M. D., Langvardt, P. W., Kastl, P. E., and Osborne, D. W. (1990). Determination of the effect of tridiphane on the pharmacokinetics of [14C]-atrazine following oral administration to male Fischer 344 rats. *Toxicology* **61**, 27-40.

Tomas-Camardiel, M., Herrera, A. J., Venero, J. L., Cruz Sanchez-Hidalgo, M., Cano, J., and Machado, A. (2002). Differential regulation of glutamic acid decarboxylase mRNA and tyrosine hydroxylase mRNA expression in the aged manganese-treated rats. *Brain Res Mol Brain Res* **103**, 116-129.

Ulevitch, R. J., and Tobias, P. S. (1995). Receptor-dependent mechanisms of cell stimulation by bacterial endotoxin. *Annu Rev Immunol* **13**, 437-457.

Valente, E. M., Abou-Sleiman, P. M., Caputo, V., Muqit, M. M., Harvey, K., Gispert, S., Ali, Z., Del Turco, D., Bentivoglio, A. R., Healy, D. G., Albanese, A., Nussbaum, R., Gonzalez-Maldonado, R., Deller, T., Salvi, S., Cortelli, P., Gilks, W. P., Latchman, D. S., Harvey, R. J., Dallapiccola, B., Auburger, G., and Wood, N. W. (2004). Hereditary early-onset Parkinson's disease caused by mutations in PINK1. *Science* **304**, 1158-1160.

Vanacore, N., Nappo, A., Gentile, M., Brustolin, A., Palange, S., Liberati, A., Di Rezze, S., Caldora, G., Gasparini, M., Benedetti, F., Bonifati, V., Forastiere, F., Quercia, A., and Meco, G. (2002). Evaluation of risk of Parkinson's disease in a cohort of licensed pesticide users. *Neurol Sci* **23 Suppl 2**, S119-120.

Venance, L., Stella, N., Glowinski, J., and Giaume, C. (1997). Mechanism involved in initiation and propagation of receptor-induced intercellular calcium signaling in cultured rat astrocytes. *J Neurosci* **17**, 1981-1992.

Vernadakis, A. (1996). Glia-neuron intercommunications and synaptic plasticity. *Prog Neurobiol* **49**, 185-214.

Vitkovic, L., Bockaert, J., and Jacque, C. (2000). "Inflammatory" cytokines: neuromodulators in normal brain? *J Neurochem* **74**, 457-471.

Viviani, B., Bartesaghi, S., Corsini, E., Galli, C. L., and Marinovich, M. (2004). Cytokines role in neurodegenerative events. *Toxicol Lett* **149**, 85-89.

Wagenfeld, A., Gromoll, J., and Cooper, T. G. (1998). Molecular cloning and expression of rat contraception associated protein 1 (CAP1), a protein putatively involved in fertilization. *Biochem Biophys Res Commun* **251**, 545-549.

Waragai, M., Nakai, M., Wei, J., Fujita, M., Mizuno, H., Ho, G., Masliah, E., Akatsu, H., Yokochi, F., and Hashimoto, M. (2007). Plasma levels of DJ-1

as a possible marker for progression of sporadic Parkinson's disease. *Neurosci Lett* **425**, 18-22.

Ware, C. F., VanArsdale, S., and VanArsdale, T. L. (1996). Apoptosis mediated by the TNF-related cytokine and receptor families. *J Cell Biochem* **60**, 47-55.

Welch, J. E., Barbee, R. R., Roberts, N. L., Suarez, J. D., and Klinefelter, G. R. (1998). SP22: a novel fertility protein from a highly conserved gene family. *J Androl* **19**, 385-393.

Whetsell, W. O., Jr. (1996). Current concepts of excitotoxicity. *J Neuropathol Exp Neurol* **55**, 1-13.

Whitton, P. S. (2007). Inflammation as a causative factor in the aetiology of Parkinson's disease. *Br J Pharmacol* **150**, 963-976.

Wiencken, A. E., and Casagrande, V. A. (1999). Endothelial nitric oxide synthetase (eNOS) in astrocytes: another source of nitric oxide in neocortex. *Glia* **26**, 280-290.

Willis, S. A., and Nisen, P. D. (1996). Differential induction of the mitogen-activated protein kinase pathway by bacterial lipopolysaccharide in cultured monocytes and astrocytes. *Biochem J* **313 (Pt 2)**, 519-524.

Wilson, M. A., Collins, J. L., Hod, Y., Ringe, D., and Petsko, G. A. (2003). The 1.1-A resolution crystal structure of DJ-1, the protein mutated in autosomal recessive early onset Parkinson's disease. *Proc Natl Acad Sci U S A* **100**, 9256-9261.

Wszolek, Z. K., Gwinn-Hardy, K., Wszolek, E. K., Muenter, M. D., Pfeiffer, R. F., Rodnitzky, R. L., Uitti, R. J., McComb, R. D., Gasser, T., and Dickson, D. W. (2002a). Neuropathology of two members of a German-American kindred (Family C) with late onset parkinsonism. *Acta Neuropathol* **103**, 344-350.

Wszolek, Z. K., Gwinn-Hardy, K., Wszolek, E. K., Muenter, M. D., Pfeiffer, R. F., Rodnitzky, R. L., Uitti, R. J., McComb, R. D., Gasser, T., and Dickson, D. W. (2002b). Neuropathology of two members of a German-American kindred (Family C) with late onset parkinsonism. *Acta Neuropathol (Berl)* **103**, 344-350.

Wu, D. C., Teismann, P., Tieu, K., Vila, M., Jackson-Lewis, V., Ischiropoulos, H., and Przedborski, S. (2003). NADPH oxidase mediates oxidative stress in the 1-methyl-4-phenyl-1,2,3,6-tetrahydropyridine model of Parkinson's disease. *Proc Natl Acad Sci U S A* **100**, 6145-6150.

Wu, D. C., Tieu, K., Cohen, O., Choi, D. K., Vila, M., Jackson-Lewis, V., Teismann, P., and Przedborski, S. (2002). Glial cell response: A pathogenic factor in Parkinson's disease. *J Neurovirol* **8**, 551-558.

Wu du, C., Tieu, K., Cohen, O., Choi, D. K., Vila, M., Jackson-Lewis, V., Teismann, P., and Przedborski, S. (2002). Glial cell response: A pathogenic factor in Parkinson's disease. *J Neurovirol* **8**, 551-558.

Xu, J., Zhong, N., Wang, H., Elias, J. E., Kim, C. Y., Woldman, I., Pifl, C., Gygi, S. P., Geula, C., and Yankner, B. A. (2005). The Parkinson's disease-associated DJ-1 protein is a transcriptional co-activator that protects against neuronal apoptosis. *Hum Mol Genet* **14**, 1231-1241.

Yamaguchi, H., and Shen, J. (2007). Absence of dopaminergic neuronal degeneration and oxidative damage in aged DJ-1-deficient mice. *Mol Neurodegener* **2**, 10.

Yanagisawa, D., Kitamura, Y., Inden, M., Takata, K., Taniguchi, T., Morikawa, S., Morita, M., Inubushi, T., Tooyama, I., Taira, T., Iguchi-Ariga, S. M., Akaike, A., and Ariga, H. (2007). DJ-1 protects against neurodegeneration caused by focal cerebral ischemia and reperfusion in rats. *J Cereb Blood Flow Metab*.

Yokota, T., Sugawara, K., Ito, K., Takahashi, R., Ariga, H., and Mizusawa, H. (2003). Down regulation of DJ-1 enhances cell death by oxidative stress, ER stress, and proteasome inhibition. *Biochem Biophys Res Commun* **312**, 1342-1348.

Yoshida, K., Sato, Y., Yoshiike, M., Nozawa, S., Ariga, H., and Iwamoto, T. (2003). Immunocytochemical localization of DJ-1 in human male reproductive tissue. *Mol Reprod Dev* **66**, 391-397.

Zhang, L., Shimoji, M., Thomas, B., Moore, D. J., Yu, S. W., Marupudi, N. I., Torp, R., Torgner, I. A., Ottersen, O. P., Dawson, T. M., and Dawson, V. L. (2005). Mitochondrial localization of the Parkinson's disease related protein DJ-1: implications for pathogenesis. *Hum Mol Genet* **14**, 2063-2073.

Zhou, W., Zhu, M., Wilson, M. A., Petsko, G. A., and Fink, A. L. (2006). The oxidation state of DJ-1 regulates its chaperone activity toward alpha-synuclein. *J Mol Biol* **356**, 1036-1048.

Zhu, W., Downey, J. S., Gu, J., Di Padova, F., Gram, H., and Han, J. (2000). Regulation of TNF expression by multiple mitogen-activated protein kinase pathways. *J Immunol* **164**, 6349-6358.